INERTIAL PARAMETER DESIGN OF SPATIAL MECHANISMS

A THESIS SUBMITTED TO

THE GRADUATE SCHOOL OF NATURAL AND APLLIED SCIENCES

OF

THE MIDDLE EAST TECHNICAL UNIVERSITY

BY

FATİH CEMAL CAN

IN PARTIAL FULFILLMENT OF THE REQUIREMENTS FOR THE DEGREE OF

MASTER OF SCIENCE

IN

THE DEPARTMENT OF MECHANICAL ENGINEERING

SEPTEMBER 2003

Approval of the Graduate School of Natural and Applied Sciences

_____

Prof. Dr. Canan ÖZGEN

Director

I certify that this thesis satisfies all the requirements as a thesis for the degree of Master of Science.

_____

Prof. Dr. Kemal İDER

Head of Department

This is to certify that we have read this thesis and that in our opinion it is fully adequate, in scope and quality, as a thesis for the degree of Master of Science.

_____

Prof. Dr. Reşit SOYLU

Supervisor

Examining Committee Members

Prof. Dr. Reşit SOYLU _____

Prof. Dr. Eres SÖYLEMEZ _____

Prof. Dr. Kemal İDER _____

Prof. Dr. Tuna BALKAN _____

Prof. Dr. Yavuz YAMAN _____

ABSTRACT

INERTIAL PARAMETER DESIGN OF SPATIAL MECHANISMS

Can, Fatih Cemal
M.S., Department of Mechanical Engineering
Supervisor: Prof. Dr. Reşit Soylu
September 2003, 115 pages

In this thesis, the inertial parameters of a spatial mechanism are used in order to optimize various aspects of the dynamic behaviour of the mechanism (such as minimizing actuator torque/ force fluctuations, shaking force/moment balancing, etc.) while the effects of loads are considered as well. Here, inertial parameters refer to the mass, 6 elements of the inertia tensor and coordinates of the center of mass of the links.

The concept of Force Fluctuation Number (FFN) is utilized to optimize the dynamic behaviour of the mechanism. By using the FFN concept, one obtains a number of linear equations to be satisfied by the optimal inertial parameters. In general, the number of such equations is less than the number of the inertial parameters. Therefore, some of the inertial parameters may be selected freely in order to satisfy other design constraints.

Using MATHEMATICA, a program has been developed to obtain the linear equations to be satisfied by the optimal inertial parameters. The developed program includes a kinematic and force analysis module, which can be used

independently for a complete kinematic and dynamic analysis of any one degree of freedom, single loop, spatial mechanism. The different closures of the mechanism may be identified by using the developed package and these analyses can be performed on any selected closure of the mechanism.

Keywords: Spatial mechanism, optimal inertial parameters, balancing, kinematic analysis, force analysis, closure identification.

ÖZ

UZAYSAL MEKANİZMALARDA ATALET PARAMETRELERİNİN TASARIMI

Can, Fatih Cemal
Yüksek Lisans, Makina Mühendisliği Bölümü
Tez Yöneticisi: Prof. Dr. Reşit Soylu
Eylül 2003, 115 sayfa

Bu tezde, mekanizmanın dinamik davranışlarının optimizasyonu için (örneğin, tahrik torkundaki/kuvvetindeki dalgalanmaların minimum seviyeye indirilmesi, sallanma kuvvetini/momentini dengeleme gibi…) yükün etkileri de göz önüne alınarak, uzaysal bir mekanizmanın atalet parametreleri kullanılmaktadır. Burada, atalet parametreleri olarak kütle, atalet matrisinin 6 elamanı ve linklerin ağırlık merkezleri nitelenmektedir.

Mekanizmanın dinamik davranışlarının optimizasyonu için Force Fluctuation Number (FFN) kavramından yararlanılmıştır. Bu kavram kullanılarak optimal atalet parametrelerinin sağlaması gereken doğrusal denklemler elde edilmektedir. Genelde bu denklemlerin sayısı serbest seçilebilen atalet parametrelerinin sayısından azdır. Bundan dolayı atalet parametrelerinin bazıları dizayn kısıtlamalarını sağlaması için serbestçe seçilebilir.

MATHEMATICA kullanılarak, kısıtlamaları sağlayacak optimum atalet parametrelerini elde etmek için bir program geliştirilmiştir. Program bağımsız olarakda kullanılabilen bir serbestlik dereceli, bir çevrimli uzaysal mekanizmaların kinematik ve kuvvet analizi modüllerini de içermektedir. Geliştirilen program

kullanılarak farklı kapanımlar belirlenebilir ve bu analizler seçilen herhangi bir kapanımda yapılabilir.

Anahtar kelimeler: Uzaysal mekanizma, optimal atalet parametreleri, dengeleme, kinematik analiz, kuvvet analizi, kapanım belirlenmesi.

ACKNOWLEDGMENTS

I would like to thank Prof. Dr. Reşit Soylu, my thesis supervisor, for his guidance, support and advice.

I would like also to thank my friends Erdinç İyiay and Emre Selvi.

TABLE OF CONTENTS

LIST OF TABLES

TABLE

LIST OF FIGURES

FIGURES

LIST OF SYMBOLS

F	degree of freedom
N	number of link in the mechanism
G	group number
N_p	number of prismatic joint
$\mathbf{S_i}$	unit vector of link i
$\mathbf{a_{ij}}$	common normal of link i
a_{ij}	link lengths of link i
S_{ii}	joint offset of link i
θ_i	angle of rotation of link i
$[B_i]$	body fixed frame of link i
$[B_N]$	inertial frame of the N-link mechanism
$\mathbf{r}$	translational loop closure vector
$\mathbf{r_h}$	translational loop closure vector expressed in $[B_h]$ reference frame
$r_{h,x}$	x component of translational loop closure vector expressed in $[B_h]$ reference frame
$r_{h,y}$	y component of translational loop closure vector expressed in $[B_h]$ reference frame
$r_{h,z}$	z component of translational loop closure vector expressed in $[B_h]$ reference frame
t_k	half-angle laws for θ_k
ω_i	relative angular velocity of link i with respect to link i-1
v_i	relative linear velocity of link i with respect to link i-1
$\dot{\omega}_i$	relative angular acceleration of link i with respect to link i-1
$\dot{v}_i$	relative linear acceleration of link i with respect to link i-1
$\tilde{\$}_{j,h}$	unit screw coordinates of the j'th revolute joint axis expressed in the $[B_h]$ reference frame
$\tilde{\$}^P_{j,h}$	unit screw coordinates of the j'th prismatic joint axis expressed in the $[B_h]$ reference frame
$\mathbf{0}$	6×1 zero column vector
$\mathbf{F_{h,i}}$	reaction force applied on link i by link h

$\mathbf{F_{j,i}}$	reaction force applied on link i by link j
$\mathbf{F_{in,i}}$	inertia force acting on link i
m_i	mass of link i
$\mathbf{g}$	gravitational acceleration
$\mathbf{F_{ext,i}}$	resultant of External forces applied to link i (applied at O_i)
$\mathbf{M_{h,i}}$	reaction moment applied on link i by link h
$\mathbf{M_{j,i}}$	reaction moment applied on link i by link j
$\mathbf{c_i}$	center of mass position of link i
$(\mathbf{T_{in}})_{o_i}$	inertia moment of link i plus the moments of inertia forces about O_i
$\mathbf{a_{c,i}}$	mass center acceleration of link i
$\left[\bar{I}_i\right]$	centroidal inertia matrix of link i with respect to body fixed frame $[B_i]$
$\boldsymbol{\alpha_i}$	absolute angular acceleration of link i
$\boldsymbol{\Omega_i}$	absolute angular velocity of link i
$\mathbf{a_{o,i}}$	absolute linear acceleration of O_i
$\mathbf{r_{o,i}}$	Distance between two origins O_i and O_{i-1}
MX_i	mass times x coordinate of center of mass of link i in the body fixed coordinate system
MY_i	mass times y coordinate of center of mass of link i in the body fixed coordinate system
MZ_i	mass times z coordinate of center of mass of link i in the body fixed coordinate system
R	interval, in the time-space, over which FFN is defined
V	length of R
F_i	any linear combination of the F_r's and F_a's where F_r denotes any component of any generalized joint reaction and F_a denotes the generalized actuator force
F_{id}	desired value of F_i which could be any specified constant (including zero) or $\bar{F}_i$, where $\bar{F}_i$ is the average value of F_i over R
nf	number of F_i's that appear in the definition of FFN
$\mathbf{I_t}$	the vector of inertial parameters of the mechanism
$\mathbf{I_f}$	vector of inertial parameters that affect FFN
k	number of inertial parameters that affect FFN
$[A]$	$k \times k$ coefficient matrix
$\mathbf{I_d}$	vector of inertial parameter design variables
$[D]$	$m \times m$ coefficient matrix
$\mathbf{b}$	$m \times 1$ right hand side vector

CHAPTER I

INTRODUCTION

Unbalanced mechanisms running at high speeds generate variable shaking forces and shaking moments on their foundations. The shaking forces and moments are unwanted in a machine because they cause serious problems (i.e. noise, vibrations, unnecessary wear). Hence, balancing the shaking forces and moments in high-speed mechanisms is a very important design objective. Besides balancing of shaking forces and the shaking moments, minimization of the generalized actuator force (input torque of force) fluctuations and joint reaction fluctuations are also important to have a machine working properly and smoothly.

A machine may rest on the ground under its own weight, or may be rigidly connected to the ground via bolts. Forces transmitted to the frame from the machine excite vibrations and these forces are detrimental if they are cyclic in nature. Forces transmitted to the frame due to the inertial effects of moving members of the machine are cyclic and they are the primary contributors to vibration excitation. Since inertial effects depend on masses and mass distribution of moving members, forces that excite vibrations can be controlled by providing a suitable mass distribution.

There exist many studies about balancing of the machines in the literature. In these studies, generally, balancing of the machines is realized by using counterweights, additional links, cams, springs… etc.

By connecting a counterweight to the input link, Arekelian and Dahan[1] presents a solution of the shaking force and shaking moment balancing of planar and spatial linkages. Furthermore, the conditions for balancing are formulated by the minimization of the root-mean-square value of the shaking moment in Arekelian and Dahan's study. The suggested method is illustrated via RSSR spatial mechanism.

By using three rotary counterweights arranged on the perpendicular planes, Chiou and Tsai [2] examined the partial force and moment balancing of the spatial mechanisms. As an example, balancing of the 7 link 7-R spatial linkage is given in this study.

A method of partial force balancing of the RCCC linkage is developed in the study of Chen [3]. In order to obtain partial balancing, three counterweights are attached to moving links of the RCCC linkage. Therefore, the RMS (Root Mean Square) norm of the shaking force of the RCCC linkage is reduced by half.

In the study of Yu [4], the complete balancing of the shaking force and shaking moment of spatial linkages is examined by using additional groups connected with counterweights. Balancing equations for the complete shaking force and shaking moment of the RSPC and RRCRC mechanisms are given.

The study of Wawrzecki [5] presents the balancing of the spatial mechanism of an overlock sewing machine at the stage of design.

The main aim of this thesis is to determine the optimal inertial parameters of a spatial mechanism in order to obtain:

- Minimum Shaking Force and Moment Fluctuations
- Minimum Generalized Force(input torque or force) Fluctuations
- Minimum Joint Reaction Fluctuations

The concept of Force Fluctuation Number, which has been introduced by Tursun[10], is used to reach the above objectives. This number is an average, quantitative indicator of the aforementioned fluctuations (over a given time interval) for a specified input motion (in terms of time) of the mechanism. FFN can be conveniently computed, in closed form, in terms of inertial parameters. Furthermore, it can be analytically minimized to yield a set of linear equations to be satisfied by the inertial parameters.

The computation of FFN needs the position, velocity, acceleration and dynamic force analysis of the mechanism. Therefore, a package has been developed using the symbolic manipulation code MATHEMATICA. This package can be used independently for complete kinematic and dynamic analysis of any one degree-of-freedom, single loop spatial mechanism. In the kinematic and dynamic force analysis, all links are considered to be rigid. Furthermore, friction at the joints has been neglected.

The Outline of the thesis is as follows:

Chapter II is related to the methods used for the kinematic and dynamic force analysis.

In Chapter III the concept of FFN is presented. The methods used for the computation and optimization of FFN are also discussed in the same chapter.

Chapter IV involves four case studies, the results of which are obtained by using the developed package.

Finally, in Chapter V, the conclusions are presented.

CHAPTER II

KINEMATIC AND FORCE ANALYSIS

2.1 Kinematic Analysis

In the kinematic analysis of spatial mechanisms, all relative joint variables and their time derivatives are desired to be determined when F position variables, F velocity variables, etc. are specified. Here, F denotes the degree of freedom of the mechanism. The process of finding these variables is somewhat similar to the inverse kinematics problem in robotics. In the inverse kinematics, the joint variables of the robot are to be found when the position of the end effector is given.

In this study, single loop, single degree of freedom spatial mechanisms are investigated. The 3D representations of three most commonly used joints used in spatial mechanisms are given in Figure 2.1.

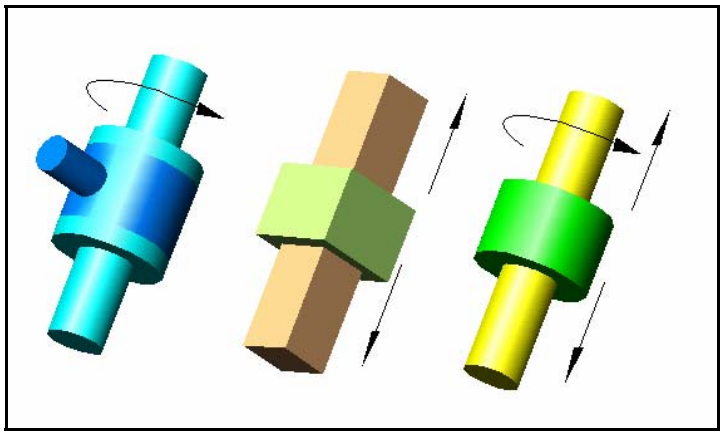

Figure 2.1 Revolute(R), prismatic (P), cylindrical (C) joints respectively

2.1.1 Position Analysis

In this study, the position analysis of a single loop, single degree of freedom mechanism is performed using two steps. In the first step, two of the six unknown joint variables, that appear in the closure equations of the mechanism, are eliminated systematically using the algorithm developed in Soylu-Akbulut[6]. As a result, one obtains four nonlinear equations in 4 of the unknown joint variables. In the second step, these equations are solved as efficiently as possible, for the 4 unknown joint variables using the tools provided in the symbolic manipulation package, MATHEMATICA. The solution procedure depends upon the group number, G, of the mechanism, which is defined to be $G = 4\text{-}N_p$, where N_p the number of Prismatic joints in the mechanism. The solution procedure also takes into account, implicitly, the special dimensions of the mechanism, if any, so that the execution time for the position analysis of the mechanism is as minimum as possible.

2.1.1.1 Determination of the 4 non-linear equations

This section closely follows Soylu-Akbulut[6] and provides some background information that is necessary for the algorithm used in the step 1. Interested readers may see Duffy[7] and Soylu[13] for further information.

Consider the N link spatial mechanism shown in Figure 2.2. The directions of the joint axes are labelled sequentially with the unit vectors $\mathbf{S_i}$ (i=1,2,…,N). The unit vector along the common normal of the two successive joint axes $\mathbf{S_i}$ and $\mathbf{S_j}$ is labelled with $\mathbf{a_{ij}}(ij = 12,\ 23,\ldots,\ N1)$. The length of the common normal between the two successive joint axes $\mathbf{S_i}$ and $\mathbf{S_j}$, on the other hand, is labeled with a_{ij} (link lengths) and the mutual perpendicular distance between the successive common normals $\mathbf{a_{ij}}$ and $\mathbf{a_{jk}}$ is labeled with S_{jj} (joint offsets). The twist angle α_{ij}, is measured from $\mathbf{S_i}$ to $\mathbf{S_j}$ around $\mathbf{a_{ij}}$ and θ_i is measured from $\mathbf{a_{hi}}$ to $\mathbf{a_{ij}}$ around $\mathbf{S_i}$, both in the right and sense. It should be noted that if the ith joint is a revolute(prismatic)

joint, then θ_i (S_{ii}) serves as the joint variable. In this study, the frame [B_N] is the inertial frame of the mechanism since link N is the fixed link.

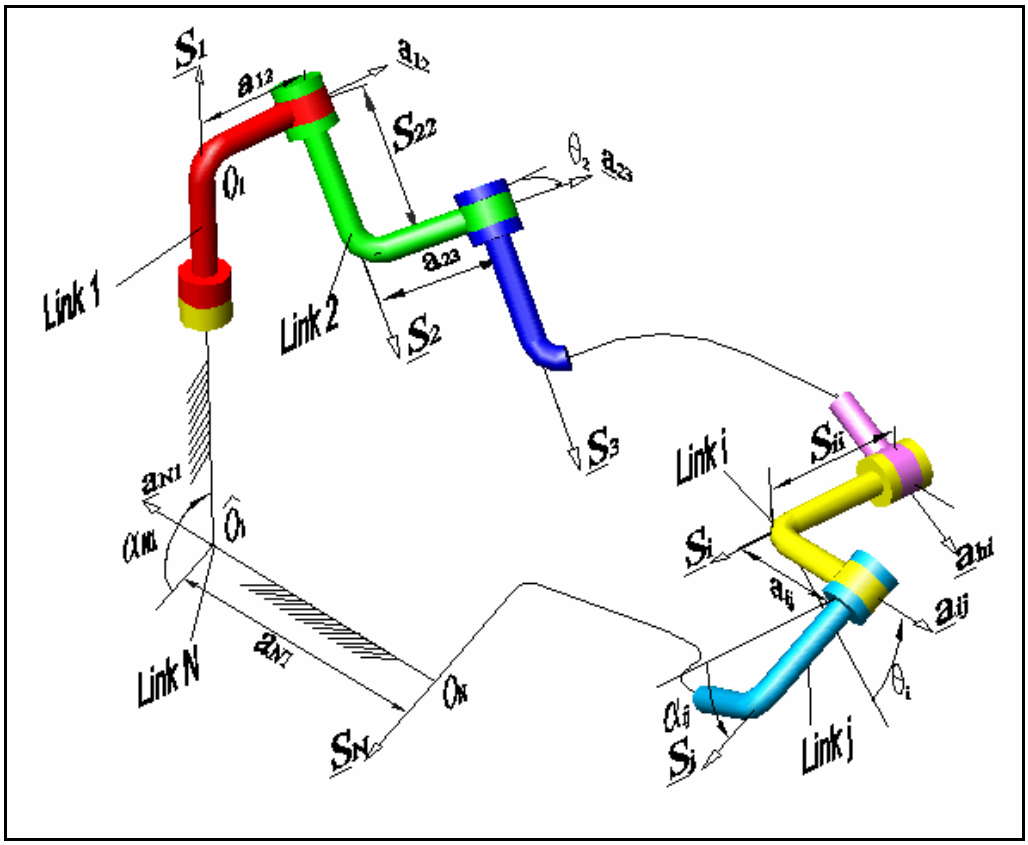

Figure 2.2 N-link spatial mechanism

Now, for notational simplicity, let N=7 and let h, i, j, k, l, m, n denote cyclically increasing sequence of the positive integers 1, 2, 3, 4, 5, 6, 7. Here, cyclically increasing implies that n is followed by h in the sequence. Consider now the frame [B_i] attached to link i. The x and z axes of this frame are parallel to $\mathbf{a_{ij}}$ and $\mathbf{S_i}$ respectively. The y axis is parallel to $\mathbf{b_{ij}} \equiv \mathbf{S_i} \times \mathbf{a_{ij}}$. The origin, O_i, of [B_i] is located at the point of intersection of the lines on which $\mathbf{S_i}$ and $\mathbf{a_{ij}}$ lie. Therefore, the frame [B_i] can be represented by 3 × 3 rotation matrix [$\mathbf{a_{ij}}$ $\mathbf{b_{ij}}$ $\mathbf{S_i}$].

The rotation matrices, [M…]s, which relate any two of the seven frames[B_1], [B_2],…, [B_7], can be found in terms of the notation firstly introduced

by Duffy[7], and later extended by Lipkin and Duffy [8]. These matrices are defined [8] by $[M_i]=[B_h]^{\mathrm{T}}[B_i]$, $[M_{ij}]=[B_h]^{\mathrm{T}}[B_j],\ldots,[M_{ijklmn}]=[B_h]^{\mathrm{T}}[B_n]$ where

$$\left[M_i\right]\equiv\begin{bmatrix} P_i & U_i & 0_i \\ Q_i & V_i & -s_{hi} \\ R_i & W_i & c_{hi} \end{bmatrix} \tag{2.1}$$

$$\left[M_{ij}\right]=\left[M_i\right]\left[M_j\right]\equiv\begin{bmatrix} P_{ij} & U_{ij} & X_i \\ Q_{ij} & V_{ij} & Y_i \\ R_{ij} & W_{ij} & Z_i \end{bmatrix} \tag{2.2}$$

$$\vdots \qquad\qquad \vdots$$

$$\left[M_{ij\ldots mn}\right]=\left[M_i\right]\left[M_j\right]\cdots\left[M_m\right]\left[M_n\right]\equiv\begin{bmatrix} P_{ijklmn} & U_{ijklmn} & X_{ijklm} \\ Q_{ijklmn} & V_{ijklmn} & Y_{ijklm} \\ R_{ijklmn} & W_{ijklmn} & Z_{ijklm} \end{bmatrix} \tag{2.3}$$

and $c_{hi}=\cos(\alpha_{hi})$, $s_{hi}=\sin(\alpha_{hi})$. The recursive definitions of the elements of the Duffy-Lipkin (DL) notation, i.e. *P*, *Q*, *R*, *U*, *V*, *W*, *X*, *Y* and *Z* terms, are given in Appendix A.

Consider, now, the rotation matrix $\left[M_{ijklmnh}\right]$ which is by definition equal to $\left[B_h\right]^{\mathrm{T}}\left[B_h\right]$, which in turn is equal to the identity matrix. On the other hand, $\left[M_{ijklmnh}\right]$ can also be expressed as $\left[M_{ijkl}\right]\left[M_{mnh}\right]$. Therefore it follows that $\left[M_{ijkl}\right]=\left[M_{mnh}\right]^{\mathrm{T}}$, which, upon substituting the elements of the matrices yields

$$\begin{bmatrix} P_{ijkl} & U_{ijkl} & X_{ijk} \\ Q_{ijkl} & V_{ijkl} & Y_{ijk} \\ R_{ijkl} & W_{ijkl} & Z_{ijk} \end{bmatrix}=\begin{bmatrix} P_{mnh} & Q_{mnh} & R_{mnh} \\ U_{mnh} & V_{mnh} & W_{mnh} \\ X_{mn} & Y_{mn} & Z_{mn} \end{bmatrix} \tag{2.4}$$

After equating the elements of the two matrices, one obtains:

$$P_{ijkl}=P_{mnh}\quad Q_{ijkl}=U_{mnh}\quad V_{ijkl}=V_{mnh}$$
$$R_{ijkl}=X_{mn}\quad W_{ijkl}=Y_{mn}\quad Z_{ijk}=Z_{mn} \tag{2.5}$$

which will be called the *PP*, *QU*, *VV*, *RX*, *WY* and *ZZ* laws, respectively. These laws represent the so-called orientational loop closure equations of the mechanism and at most three of these laws will be independent. Furthermore, for a 7 link mechanism, the *PP*, *QU* and *VV* laws involve all 7 θs, the RX and WY laws involve 6 θs and ZZ laws involves only 5 θs. Here, it has been noted that subscripts of a DL term indicates the θs involved in that term. For instance, X_{671} is a function of θ_6, θ_7 and θ_1 only. The special cases of the aforementioned six laws where a *P*, *Q*, *U* or *V* term contains seven subscripts; an *R*, *X*, *W* or *Y* term contains six subscripts, a *Z* term contains five subscripts can be similarly obtained to yield $P_{hijklmn}=1$, $Q_{hijklmn}=0$, $U_{hijklmn}=0$, $V_{hijklmn}=1$, $R_{hijklm}=0$, $X_{hijklm}=0$, $W_{hijklm}=0$ and $Z_{hijkl}=c_{mn}$. Some illustrative examples for these laws are $P_{345}=P_{6712}$, $Q_{23456}=U_{71}$, $R_{71234}=X_5$, $W_1=Y_{23456}$, $Z_{45}=Z_{712}$ and $Z_{12345}=c_{67}$ for a 7-link mechanism.

When the Δ operator (defined in Appendix A) is applied to the DL terms, the duals of these terms are obtained. Using this operator on the six laws given by equation (2.6), the following so called mutual moment laws are obtained.

$$P_{0ijkl}=P_{0mnh} \quad Q_{0ijkl}=U_{0mnh} \quad V_{0ijkl}=V_{0mnh}$$
$$R_{0ijkl}=X_{0mn} \quad W_{0ijkl}=Y_{0mn} \quad Z_{0ijk}=Z_{0mn} \tag{2.6}$$

Here, a zero placed in front of the subscripts denotes the dual of a DL term. P_{0123}, for instance, is the dual of P_{123} and $\Delta(P_{123})$.

The mutual moment laws are associated with the translational vector loop closure equation of the mechanism, and thus at most three of them can be independent. The translational loop closure equation can be represented (see Figure 2.2) as:

$$\mathbf{r} \equiv S_{hh}\mathbf{S_h} + S_{ii}\mathbf{S_i} + \cdots + S_{nn}\mathbf{S_n} + a_{ij}\mathbf{a_{ij}} + \cdots + a_{nh}\mathbf{a_{nh}} = \mathbf{0} \tag{2.7}$$

The vector **r**, which should be equal to the zero vector for the mechanism to close, can indeed be represented as in any one of the fames. Suppose, now, that one would like to express in $[B_h]$.

Firstly, it is noted that $\left[M_{ij\ldots m}\right]$ is a rotation matrix such that $\mathbf{v_h} = \left[M_{ij\ldots m}\right]\mathbf{v_m}$, where $\mathbf{v_h}$ and $\mathbf{v_m}$ represent the coordinates of the vector **v** expressed in the frames $\left[B_h\right]$ and $\left[B_m\right]$, respectively. It then follows that the x, y, z components of $\mathbf{r_h}$ (i.e. r expressed in $\left[B_h\right]$) are:

$$r_{h,x} = a_{hi} + a_{ij}P_i + a_{jk}P_{ij} + \cdots + a_{nh}P_{ij\ldots n} + S_{jj}X_i + S_{kk}X_{ij} + \cdots + S_{mm}X_{ij\ldots l} + S_{nn}c_{nh} \tag{2.8}$$

$$r_{h,y} = a_{ij}Q_i + a_{jk}Q_{ij} + \cdots + a_{nh}Q_{ij\ldots n} - S_{ii}s_{hi} + S_{jj}Y_i + S_{kk}Y_{ij} + \cdots + S_{nn}Y_{ij\ldots m} \tag{2.9}$$

$$r_{h,z} = a_{ij}R_i + a_{jk}R_{ij} + \cdots + a_{mn}R_{ij\ldots m} + S_{hh} + S_{ii}c_{hi} + S_{jj}Z_i + S_{kk}Z_{ij} + \cdots + S_{mm}Y_{ij\ldots l} + S_{nn}c_{nh} \tag{2.10}$$

where $\mathbf{r_h} = (r_{h,x}, r_{h,y}, r_{h,z})^{\mathrm{T}}$.

It should be noted that, all of aforementioned discussions were related to DL terms with ascending subscripts. Similarly, one can determine recursive definitions for the DL terms with descending subscripts (see Appendix A) and extend the six laws to the case of DL terms with descending subscripts.

Using RX and WY laws, one can drive the so called half-angle laws [7]. These laws can be employed to uniquely determine any θ in terms of any other 5 θs (for a 7 link mechanism with 1 degree of freedom joints). For instance, the six alternative expressions for $t_k \equiv \tan(\theta_k / 2)$ are given by

$$
\begin{aligned}
t_k &= X_{lmnhi}/(Y_{lmnhi}+s_{jk}) = (X_{lmnh}-\overline{X}_j)/(Y_{lmnh}-\overline{Y}_j) \\
&= (X_{lmn}-X_{ji})/(Y_{lmn}-Y_{ji}) = (X_{lm}-X_{jih})/(Y_{lm}-Y_{jih}) \\
&= (X_l-X_{jihn})/(Y_l-Y_{jihn}) = X_{jihnm}/(Y_{jihnm}+s_{kl})
\end{aligned}
\tag{2.11}
$$

It should be noted that all of the discussions in this section have been based on 7 link mechanisms with one degree of freedom joints. These concepts can be very easily extended to the case of *N*-link mechanism $(N \le 7)$ with multi degree of freedom joints.

Using the concepts discussed in this section, the complete position analysis of any 1 degree of freedom, single loop spatial mechanism can be performed by using the following systematic algorithm. Here, recall that *h*, *i*, *j*, *k*, *l*, *m*, *n* stand for any cyclically increasing sequence of the integers 1, 2, 3, 4, 5, 6, 7 for a 7-link mechanism.

1. Choose any two rotational joint variables (other than the input and "output" joint variables), for instance, θ_i and θ_m. Here, "output" refers to a joint variable, which will be solved firstly.

2. Write the ZZ law which excludes these two variables, i.e. $Z_{nh} = Z_{jkl}$.

3. Write the corresponding mutual moment ZZ law, i.e. $Z_{0nh} = Z_{0jkl}$.

4. Write the z component of the translational loop closure equation expressed in the frame$\left[B_i\right]$, i.e. $r_{i,z} = 0$, and eliminate θ_m by applying appropriate RX and ZZ laws to the DL terms, which involve θ_m.

5. Write the z component of the translational loop closure equation expressed in the frame$\left[B_m\right]$, i.e. $r_{m,z} = 0$, and eliminate θ_i by applying appropriate RX and ZZ laws to the DL terms, which involve θ_i.

6. Solve four unknown joint variables from the four equations obtained in steps 2-5. (Note that the number of real and distinct solutions yields the number of closures of the mechanism).

7. Using the half-angle laws, determine the remaining two rotational variables selected in step 1, i.e. θ_i and θ_m, uniquely.

2.1.1.2 Solution of the 4 non-linear equations

Step 6 of the algorithm given in the previous section involves solution of the 4 unknown joint variables from four equations obtained in steps 2-5. In Soylu-Akbulut[6], these equations are solved by using the method of successive eliminations. In this study, however, a different approach, which is more suitable for MATHEMATICA, is taken. The approach used to solve the nonlinear equations is dependent upon the group number of the mechanism. This approach, which assumes that the input is a rotational joint variable is explained in the following paragraphs.

Group 1: A group 1 mechanism has three translational and three rotational unknown joint variables. Therefore, the four nonlinear equations will involve three translational and one rotational unknown joint variable.

- The unknown rotational joint variable is directly obtained from the ZZ law written in step 2 of the algorithm because this law involves only one unknown, namely the rotational joint variable.
- After solving the unknown rotational joint variable and substuting it into the three equations obtained in steps 3-5, the three translational joint variables are obtained by solving the resulting 3 linear equations.

Group 2: A group 2 mechanism has two translational and four rotational unknown joint variables. Therefore, the four nonlinear equations will involve two translational and two rotational unknown joint variables.

- The two unknown translational joint variables are eliminated linearly from the four nonlinear equations. This elimination leads to two nonlinear equations involving the two unknown joint variables.
- Let θ_{u1} and θ_{u2} denote the two unknown rotational joint variables. Firstly, the two nonlinear equations are transformed into 2 algebraic equations in t_{u1} and t_{u2} via the half-tangent identities

$$\sin(\theta_{u1}) = \frac{2t_{u1}}{1+t_{u1}^2} \tag{2.12}$$

$$\cos(\theta_{u1}) = \frac{1-t_{u1}^2}{1+t_{u1}^2} \tag{2.13}$$

$$\cos(\theta_{u2}) = \frac{1-t_{u2}^2}{1+t_{u2}^2} \tag{2.14}$$

$$\sin(\theta_{u2}) = \frac{2t_{u2}}{1+t_{u2}^2} \tag{2.15}$$

where, $t_{u1} \overset{\Delta}{=} \tan(\theta_{u1}/2)$ and $t_{u2} \overset{\Delta}{=} \tan(\theta_{u2}/2)$. Secondly, t_{u2} is eliminated from the resulting two equations by equating the resultant of the equations to zero. Finally, all solutions of the resulting polynomial equations in t_{u1} are obtained via the algebraic equation solver, NSOLVE, leading to the solutions for θ_{u1}. The common roots of the 2 algebraic equations in t_{u2}, then, lead to the solutions for θ_{u2}.

Group 3: A group 3 mechanism has one translational and five rotational unknown rotational unknown joint variables. Therefore, the four nonlinear equations will involve one translational and three rotational joint variables.

- Let θ_{u1}, θ_{u2} and θ_{u3} denote the unknown rotational joint variables and S_{u11} denote the unknown translational joint variable. Consider, now, the 3 equations.

$$s_i^2 + c_i^2 = 1 \qquad i = 1,2,3 \tag{2.16}$$

where $s_i = \sin(\theta_{ui})$ and $c_i = \cos(\theta_{ui})$ for $i = 1,2,3$. Clearly, equations given by (2.16) and the 4 equations obtained in steps 2-5 of the algorithm constitute 7 algebraic equations in the 7 unknowns $s_1, c_1, s_2, c_2, s_3, c_3$ and S_{u11}. These 7 equations can then be solved via NSOLVE to lead to all solutions for all of the unknown joint variables, namely θ_{u1}, θ_{u2}, θ_{u3} and S_{u11}.

Group 4: A group 4 mechanism has 6 unknown rotational joint variables. Hence, the 4 nonlinear equations will involve 4 rotational joint variables.

- The solution procedure is very similar to that of group 3 mechanisms. The only difference is that one has 4 equations of the form of (2.16) leading to 8 algebraic equations in the 8 unknowns $s_1, c_1, s_2, c_2, s_3, c_3, s_4, c_4$.

It should be noted that there are many different alternatives for solving the 4 nonlinear equations obtained from the algorithm described in the previous section. For instance, one could apply the solution procedure described for group 3 mechanisms for all of the groups. For each groups different solution methods have been implemented on the computer and it has been found that the solution procedures described in the previous paragraphs are the optimal ones (as far as the execution time is concerned) for each group.

It has been observed that the choice of θ_i and θ_m in the first step of the algorithm effects the execution time of the position analysis extensively for group3 and group 4 mechanisms. Therefore, the developed package firstly performs complete position analysis for all possible θ_i, θ_m combinations at an arbitrary value of the input joint variable (taken to be 21°). The execution times for each θ_i, θ_m combination are then compared automatically to determine the "best" θ_i, θ_m combination, which is then used for the "full cycle" position analysis. For example, consider a 7-R mechanism having general dimensions. The best combination (θ_1, θ_4) , which is found by the package, spends 2.7 seconds at 21° for a complete position analysis. On the other hand, the worst combination (θ_2, θ_6) spends 156 seconds at 21° for a complete position analysis .Therefore, the special dimensions of $\alpha_{ij} = 0°$ *or* $90°$, offsets being zero are implicitly taken into account to render the position analysis as efficient as possible.

In table 2.1, typical execution times are given for full cycle, complete position analysis of different types of mechanisms via the developed package. It should be noted that the package has been run on a 533 MHz Intel Pentium PC

with 256 MB of RAM. Here, "full cycle" implies that position analysis has been performed for 360 different θ_{input} values. "Complete", on the other hand, implies that all unknown joint variables are solved. Furthermore, it should be noted that all solutions (corresponding to all closures of the mechanism) for the unknown joint variables are determined via the developed package.

Table 2.1 Typical Execution times for position analysis of different mechanisms

Mechanism	Execution Time (seconds)	# of links, N	Group, G
CCCR	15	4	1
CRPRC	27	5	1
RPRPRPR	139	7	1
RCRCR	46	5	2
RRPRPRR	260	7	2
RCRRRR	6117	6	3
RRRRRRR	36000	7	4

It is clear from Table 2.1 that the larger the number of links (N) and/or the group number (G) is, the larger the execution time will be.

2.1.2 Velocity Analysis

Consider the N-link spatial mechanism shown in Figure 2.2. Using screw coordinates, the velocity loop equation for this mechanism, expressed in reference frame $[B_h]$ can be written as (see Soylu[13]).

$$\omega_1\tilde{\$}_{1,h} + v_1\tilde{\$}^{P}_{1,h} + \omega_2\tilde{\$}_{2,h} + v_2\tilde{\$}^{P}_{2,h} + \cdots + \omega_N\tilde{\$}_{N,h} + v_N\tilde{\$}^{P}_{N,h} = \mathbf{0} \tag{2.17}$$

where,

$\omega_j = \dot{\theta}_j$: Relative angular velocity of link j with respect to link (j-1).

$v_j = \dot{S}_j$: Relative linear velocity of link j with respect to link (j-1).

$\tilde{\$}_{j,h}$: Unit screw coordinates of the j'th revolute joint axis expressed in the $[B_h]$ reference frame.

$\tilde{\$}^{P}_{j,h}$: Unit screw coordinates of the j'th prismatic joint axis expressed in the $[B_h]$ reference frame.

$\mathbf{0}$: 6×1 zero column vector.

Here, it should be noted that if joint j is a revolute joint, then v_j is zero. Similarly, if joint j is a prismatic joint, then ω_j is zero. The unit screw coordinates $\tilde{\$}_{j,h}$ and $\tilde{\$}^{P}_{j,h}$ for the joints …e, f,..., j, k,…, on the other hand, can be expressed (Soylu[13]) in terms of the DL notation as given by the following two equation sets.

$$
\begin{aligned}
&\vdots \qquad\qquad\qquad \vdots \\
&\tilde{\$}_{e,h} = \left[X_{hgf}, -X^{*}_{hgf}, Z_{gf}, X_{ohgf}, -X^{*}_{ohgf}, Z_{ogf} \right]^{T} \\
&\tilde{\$}_{f,h} = \left[X_{hg}, -X^{*}_{hg}, \overline{Z}_{g}, X_{ohg}, -X^{*}_{ohg}, \overline{Z}_{og} \right]^{T} \\
&\tilde{\$}_{g,h} = \left[s_{gh}s_{h}, s_{gh}c_{h}, c_{gh}, a_{gh}c_{gh}s_{h} + S_{hh}s_{gh}c_{h}, a_{gh}c_{gh}c_{h} - S_{hh}s_{gh}s_{h}, -a_{gh}s_{gh} \right]^{T} \\
&\tilde{\$}_{h,h} = \left[0,0,1,0,0,0 \right]^{T} \\
&\tilde{\$}_{i,h} = \left[0, -s_{hi}, c_{hi}, 0, -a_{hi}c_{hi}, -a_{hi}s_{hi} \right]^{T} \\
&\tilde{\$}_{j,h} = \left[X_{i}, Y_{i}, Z_{i}, X_{oi}, Y_{oi}, Z_{oi} \right]^{T} \\
&\tilde{\$}_{k,h} = \left[X_{ij}, Y_{ij}, Z_{ij}, X_{oij}, Y_{oij}, Z_{oij} \right]^{T} \\
&\vdots \qquad\qquad\qquad \vdots
\end{aligned}
\tag{2.18}
$$

$$
\begin{aligned}
&\vdots \qquad\qquad\qquad \vdots \\
&\tilde{\$}^{P}_{e,h} = \left[0,0,0, X_{hgf}, -X^{*}_{hgf}, Z_{gf} \right]^{T} \\
&\tilde{\$}^{P}_{f,h} = \left[0,0,0, X_{hg}, -X^{*}_{hg}, \overline{Z}_{g} \right]^{T} \\
&\tilde{\$}^{P}_{g,h} = \left[0,0,0, s_{gh}s_{h}, s_{gh}c_{h}, c_{gh} \right]^{T} \\
&\tilde{\$}^{P}_{h,h} = \left[0,0,0,0,0,1 \right]^{T} \\
&\tilde{\$}^{P}_{i,h} = \left[0,0,0,0, -s_{hi}, c_{hi} \right]^{T} \\
&\tilde{\$}^{P}_{j,h} = \left[0,0,0, X_{i}, Y_{i}, Z_{i} \right]^{T}
\end{aligned}
$$

$$\tilde{\$}^{P}_{k,h} = \begin{bmatrix} 0,0,0,X_{ij},Y_{ij},Z_{ij} \end{bmatrix}^{T} \\ \vdots \qquad\qquad \vdots \tag{2.19}$$

From equations (2.18) and (2.19), it is clear that the screw coordinates are functions of dimensions and joint variables of the mechanism. If the position of the mechanism is known at a certain instant (i.e. position analysis has already been performed), then the screw coordinates will be fully known. At that instant, if any one of the relative velocities (i.e., ω_j or v_j's) is specified, then the velocity loop equation (2.17) will be equivalent to 6 linear equations in 6 unknown relative velocities (i.e. ω_j or v_j's). Therefore, the velocity analysis boils down to solving 6 linear equations in 6 unknowns which can be realized via the Solve command of MATHEMATICA.

It should be noted that the velocity loop equations given by (2.17) can be formulated in any one of the frames $[B_1],[B_2],\ldots,[B_N]$, i.e., h can be arbitrarily selected to be 1, 2, …, N. The optimal choice of h, such that the screw coordinates given by equations (2.18) and (2.19) are as simple as possible, is given in Soylu and Duffy[9] depending on the the type of the mechanism. The results indicate, most of time, that h=3 or 4 is the optimal choice. In this study, equation (2.17) is used with h, which is formulated by equation (2.20), to minimize the execution time associated with the velocity analysis.

$$h = \begin{cases} \text{if N is even} & N/2 \\ \text{else} & (N+1)/2 \end{cases} \tag{2.20}$$

where, N is link number of the mechanism.

It should be noted that acceleration analysis is also based upon the velocity loop equation (see next section) used. Therefore, a good choice of h leads to an efficient acceleration analysis as well.

2.1.3 Acceleration Analysis

Time derivative of the velocity loop closure equation (2.17) yields the following acceleration loop equation given by

$$\dot{\omega}_1\tilde{\$}_{1,h} + \omega_1\dot{\tilde{\$}}_{1,h} + \dot{v}_1\tilde{\$}^{P}_{1,h} + v_1\dot{\tilde{\$}}^{P}_{1,h} + \cdots + \dot{\omega}_N\tilde{\$}_{N,h} + \omega_N\dot{\tilde{\$}}_{N,h} + \dot{v}_N\tilde{\$}^{P}_{N,h} + v_N\dot{\tilde{\$}}^{P}_{N,h} = \mathbf{0} \qquad (2.21)$$

where,

$\dot{\omega}_j = \ddot{\theta}_j$: Relative angular acceleration of link j with respect to link (j-1).

$\dot{v}_j = \ddot{S}_{jj}$: Relative linear acceleration of link j with respect to link (j-1).

In equation (2.21), the time derivatives of the unit screw coordinates are obtained via the differentiation tools of MATHEMATICA. If the position and velocity state of the mechanism is known at a certain instant (i.e. position and velocity analysis have already been performed), then all of the screw coordinates and their time derivatives; and all of the relative velocities will be fully known. At that instant, if any one of the relative accelerations (i.e., $\dot{\omega}_j$ or $\dot{v}_j$'s) is specified, then the acceleration loop equation (2.21) will be equivalent to 6 linear equations in 6 unknown relative accelerations (i.e., $\dot{\omega}_j$ or $\dot{v}_j$'s). Therefore, the acceleration analysis boils down to solving 6 linear equations in 6 unknowns which can be realized via the Solve command of MATHEMATICA.

2.2 Force Analysis

In order to perform the force analysis of the mechanism, D'Alembert's principle is employed and the dynamic equilibrium of each of the moving links is considered.

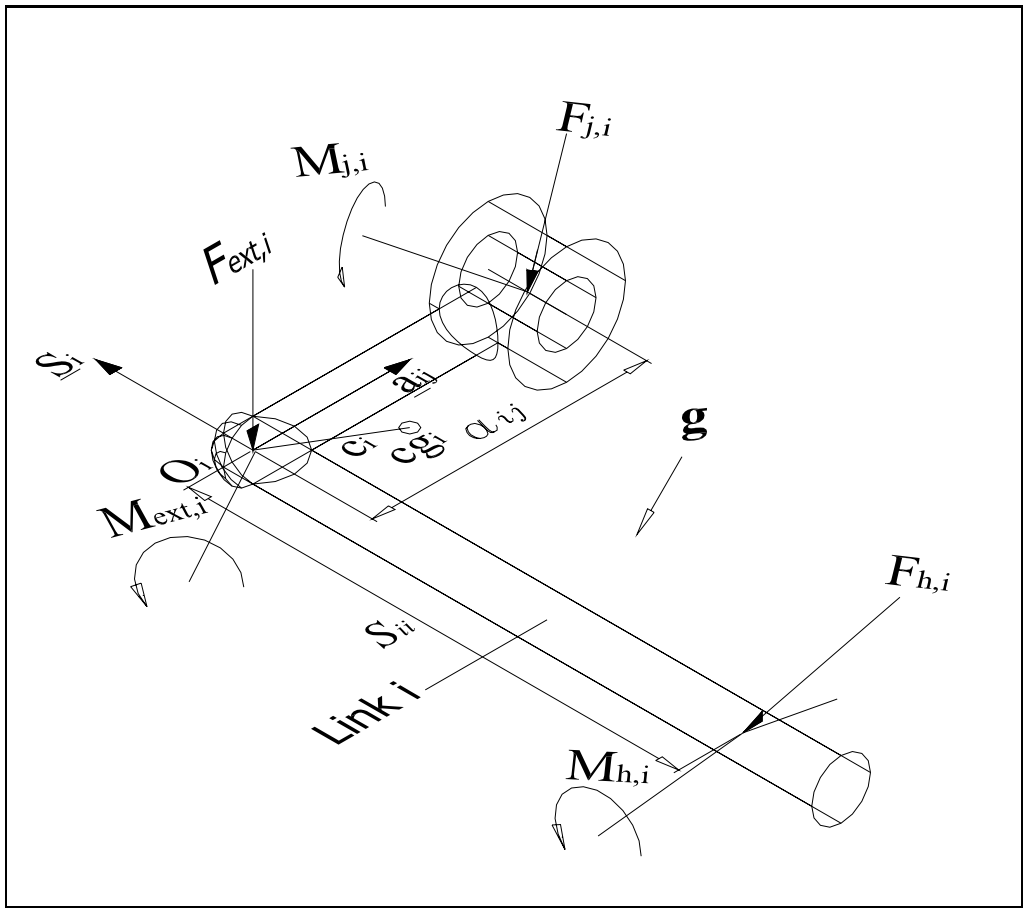

Figure 2.3 Free body diagram of link i.

Free body diagram of link i is shown in Figure 2.3. Note that h, i, j denote cyclically increasing sequence of the positive integers.

Magnitude and direction of the gravitational acceleration can be determined by the user in the developed package. Here, the direction of **g** a unit vector in the inertial frame$\left[B_N\right]$. (e.g. $\mathbf{g} = \{9.81, \{0, 0, -1\}\}$)

The two dynamic equilibrium equations for link i are given by the following two equations.

Force equilibrium:

$$\sum \mathbf{F_i} = \mathbf{F_{in,i}} + \mathbf{F_{h,i}} + \mathbf{F_{j,i}} + m_i\,\mathbf{g} + \mathbf{F_{ext,i}} = \mathbf{0} \qquad i = 1, \ldots, N-1 \tag{2.22}$$

where

$\mathbf{F_{h,i}}$: Reaction force applied on link i by link h

$\mathbf{F_{j,i}}$: Reaction force applied on link i by link j

$\mathbf{F_{in,i}}$: Inertia force acting on link i

m_i : mass of link i

$\mathbf{g}$: Gravitational acceleration

$\mathbf{F_{ext,i}}$: Resultant of External forces applied to link i (applied at O_i)

Moment equilibrium:

Moment equilibrium about O_i of link i can be represented as given below.

$$\sum \mathbf{M_{o_i}} =$$
$$(\mathbf{T_{in}})_{o_i} + \mathbf{M_{h,i}} + \mathbf{M_{j,i}} - S_{ii}\mathbf{S_i} \times \mathbf{F_{h,i}} + a_{ij}\mathbf{a_{ij}} \times \mathbf{F_{j,i}} + \mathbf{c_i} \times (m_i\,\mathbf{g}) + \mathbf{M_{ext,i}} = \mathbf{0}$$
$$i = 1, \ldots, N-1 \tag{2.23}$$

where

$\mathbf{M_{h,i}}$: Reaction moment applied on link i by link h

$\mathbf{M_{j,i}}$: Reaction moment applied on link i by link j

$\mathbf{M_{ext,i}}$: Resultant of external moments applied to link i.

$\mathbf{c_i}$: Center of mass position of link i.

$(\mathbf{T_{in}})_{o_i}$: Inertia moment of link i plus the moments of inertia forces about O_i.

The expression for $\mathbf{F_{in,i}}$ and $(\mathbf{T_{in}})_{o_i}$ will now be derived in the next section.

2.2.1 Equivalent Inertia Force System

Consider the inertia force system shown in Figure 2.4.

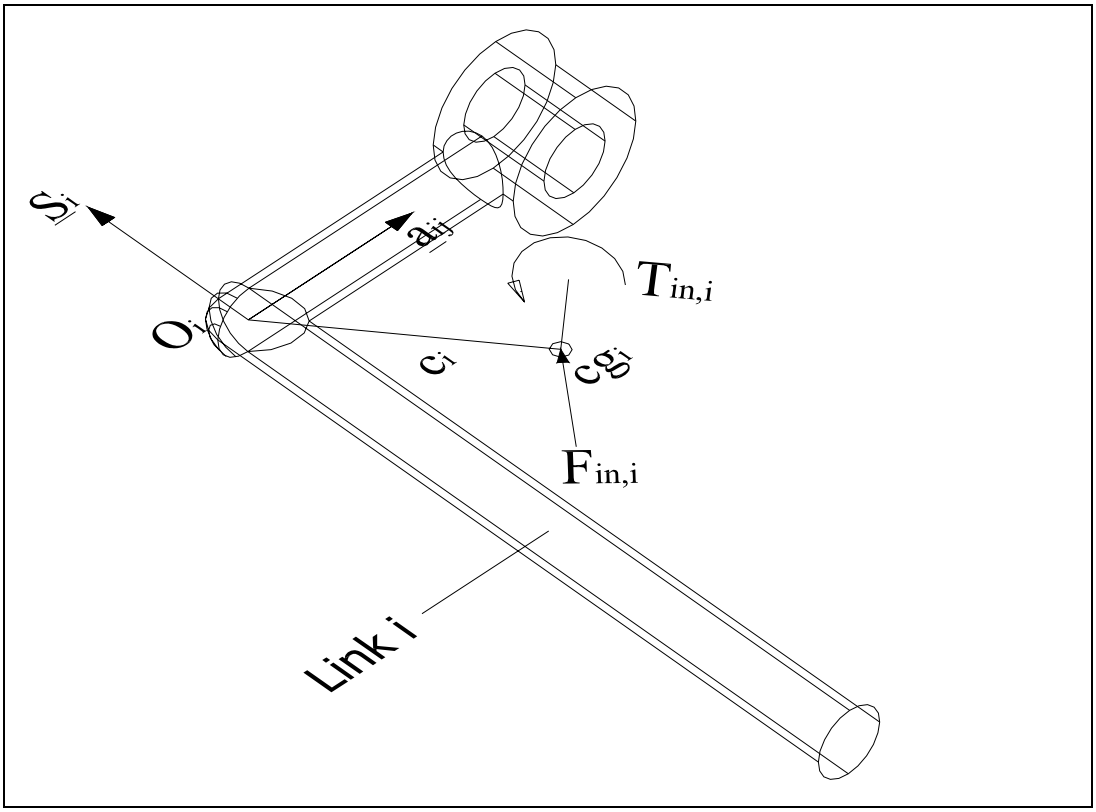

Figure 2.4 Inertia force system acting on cg_i

The inertia forces and the inertia torque are given by,

$$\mathbf{F}_{\mathbf{in,i}} = -m_i \mathbf{a}_{\mathbf{c,i}} \tag{2.24}$$

$$\mathbf{T}_{\mathbf{in,i}} = -\left[\bar{\mathrm{I}}_{\mathrm{i}}\right]\boldsymbol{\alpha}_{\mathbf{i}} - \boldsymbol{\Omega}_{\mathbf{i}} \times \left[\bar{\mathrm{I}}_{\mathrm{i}}\right]\boldsymbol{\Omega}_{\mathbf{i}} \tag{2.25}$$

respectively, where

$\mathbf{a}_{\mathbf{c,i}}$: mass center acceleration of link i

$\left[\bar{\mathrm{I}}_{\mathrm{i}}\right]$: Centroidal inertia matrix of link i with respect to body fixed frame $\left[B_i\right]$

$\boldsymbol{\alpha}_\mathbf{i}$: Absolute angular acceleration of link i (components of $\boldsymbol{\alpha}_\mathbf{i}$ are $\alpha_{x,i}, \alpha_{y,i}, \alpha_{z,i}$ in body fixed frame $[B_i]$)

$\boldsymbol{\Omega}_\mathbf{i}$: Absolute angular velocity of link i (components of $\boldsymbol{\Omega}_\mathbf{i}$ are $\Omega_{x,i}, \Omega_{y,i}, \Omega_{z,i}$ in body fixed frame $[B_i]$)

Now, let the inertia force system shown in Figure 2.4 be equivalent to the inertia force system shown in Figure 2.5. It is clear that the force systems shown in Figures 2.4 and 2.5 will be equivalent if and only if the moments about O_i are the same for both systems, i.e.,

$$\mathbf{T}_{\mathbf{in,i}} + \mathbf{c}_\mathbf{i} \times \mathbf{F}_{\mathbf{in,i}} = \left(\mathbf{T}_{\mathbf{in}}\right)_{o_i} \tag{2.26}$$

where

$\mathbf{c}_\mathbf{i} = \begin{bmatrix} x_i \\ y_i \\ z_i \end{bmatrix}$: position vector of center of mass with respect to O_i

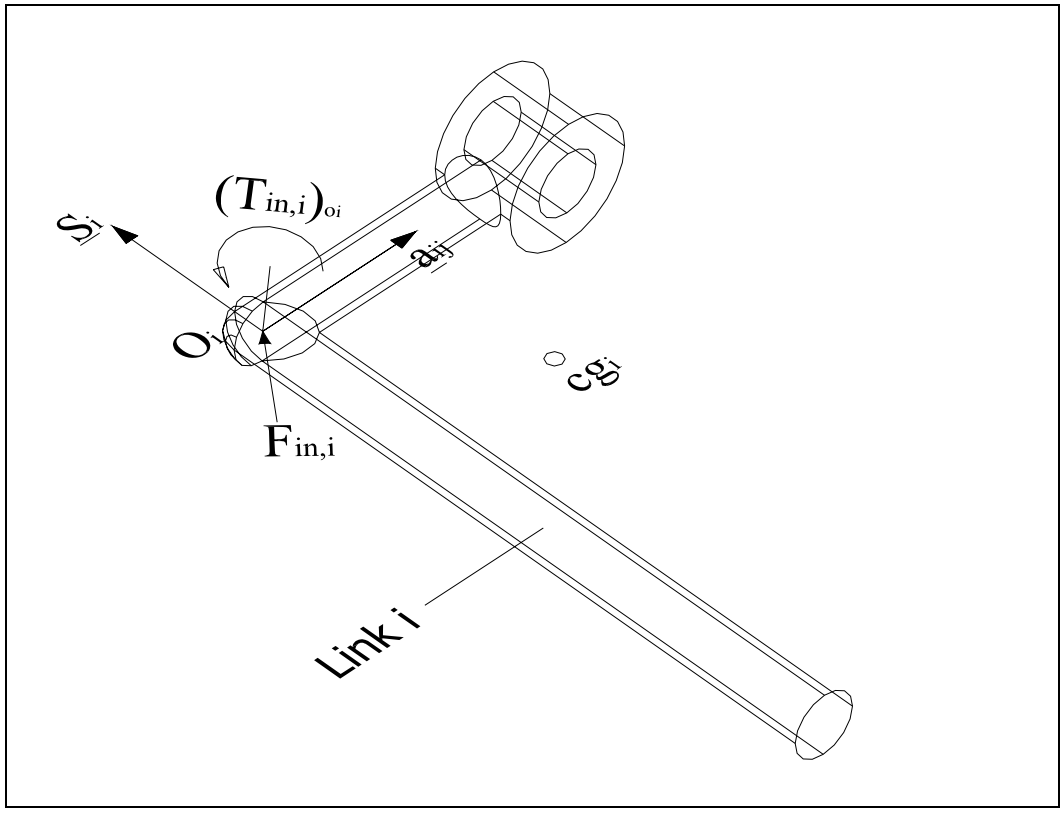

Figure 2.5 Inertia force system acting at O_i

It is clear from simple kinematics that

$$\mathbf{a_{c,i}} = \mathbf{a_{o,i}} + \boldsymbol{\alpha}_\mathbf{i} \times \mathbf{c_i} + \boldsymbol{\Omega}_\mathbf{i} \times (\boldsymbol{\Omega}_\mathbf{i} \times \mathbf{c_i}) \tag{2.27}$$

where

$\mathbf{a_{o,i}}$: Absolute linear acceleration of O_i (components of $\mathbf{a_{o,i}}$ are $a_{ox,i}, a_{oy,i}, a_{oz,i}$ in body fixed frame $[B_i]$)

Let, now, the inertia matrix of link i with respect to $[B_i]$ be given by:

$$[\mathrm{I_i}] = \begin{bmatrix} XX_i & -XY_i & -XZ_i \\ -XY_i & YY_i & -YZ_i \\ -XZ_i & -YZ_i & ZZ_i \end{bmatrix} \tag{2.28}$$

Using the parallel axis theorem, the centroidal inertia matrix $[\bar{\mathrm{I}}_\mathrm{i}]$ and $[\mathrm{I_i}]$ are related by the equation.

$$[\bar{\mathrm{I}}_\mathrm{i}] = [\mathrm{I_i}] - m_i \mathbf{c_i} \mathbf{c_i}^\mathrm{T} \tag{2.29}$$

Using equations (2.24)-(2.29) one can obtain (after a fair amount of algebraic manipulations) $\mathbf{F_{in,i}}$ and $(\mathbf{T_{in}})_{o_i}$ to be

$$\mathbf{F_{in,i}} = \begin{bmatrix} -a_{ox,i} m_i + MX_i(\Omega_{y,i}^2 + \Omega_{z,i}^2) + MY_i(-\Omega_{x,i}\Omega_{y,i} + \alpha_{z,i}) + MZ_i(-\Omega_{x,i}\Omega_{z,i} - \alpha_{y,i}) \\ -a_{oy,i} m_i + MX_i(-\Omega_{x,i}\Omega_{y,i} - \alpha_{z,i}) + MY_i(\Omega_{x,i}^2 + \Omega_{z,i}^2) + MZ_i(-\Omega_{y,i}\Omega_{z,i} + \alpha_{x,i}) \\ -a_{oz,i} m_i + MX_i(-\Omega_{x,i}\Omega_{z,i} + \alpha_{y,i}) + MY_i(-\Omega_{y,i}\Omega_{z,i} - \alpha_{x,i}) + MZ_i(\Omega_{x,i}^2 + \Omega_{y,i}^2) \end{bmatrix} \tag{2.30}^*$$

$$(\mathbf{T_{in,i}})_{o_i} = \begin{bmatrix} -a_{oz,i} MY_i + a_{oy,i} MZ_i + YY_i \Omega_{y,i}\Omega_{z,i} - ZZ_i \Omega_{y,i}\Omega_{z,i} + YZ_i(\Omega_{y,i}^2 - \Omega_{z,i}^2) \\ -XX_i \alpha_{x,i} + XY_i(-\Omega_{x,i}\Omega_{z,i} + \alpha_{y,i}) + XZ_i(\Omega_{x,i}\Omega_{y,i} + \alpha_{z,i}) \\ \hline a_{oz,i} MX_i - a_{ox,i} MZ_i - XX_i \Omega_{x,i}\Omega_{z,i} + ZZ_i \Omega_{x,i}\Omega_{z,i} + XZ_i(-\Omega_{x,i}^2 + \Omega_{z,i}^2) \\ -YY_i \alpha_{y,i} + XY_i(\Omega_{y,i}\Omega_{z,i} + \alpha_{x,i}) + YZ_i(-\Omega_{x,i}\Omega_{y,i} + \alpha_{z,i}) \\ \hline -a_{oy,i} MX_i + a_{ox,i} MY_i + XX_i \Omega_{x,i}\Omega_{y,i} - YY_i \Omega_{x,i}\Omega_{y,i} + XY_i(\Omega_{x,i}^2 - \Omega_{y,i}^2) \\ -ZZ_i \alpha_{z,i} + XZ_i(-\Omega_{y,i}\Omega_{z,i} + \alpha_{x,i}) + YZ_i(\Omega_{x,i}\Omega_{z,i} + \alpha_{y,i}) \end{bmatrix} \tag{2.31}^*$$

Note that if an equation number is marked with an asterisk, this means that the marked equation has a Mathematica output in Appendix B (throughout the study).

Note that $\mathbf{F_{in,i}}$ and $\left(\mathbf{T_{in}}\right)_{o_i}$ given by equations (2.30) and (2.31) are expressed in the body fixed frame [B_i]. Before substituting them into (2.22) and (2.23), they should be represented in the inertial frame which is always taken to be $\left[B_N\right]$. This is because equations (2.22) and (2.23) are expressed in $\left[B_N\right]$ in the computer implementation.

It is clear that, in order to determine $\mathbf{F_{in,i}}$ and $\left(\mathbf{T_{in}}\right)_{o_i}$ via equations (2.30) and (2.31), one needs to determine the angular velocity, the angular acceleration of link i, as well as the absolute acceleration of O_i. The following recursive equations yield the aforementioned quantities in terms of the relative joint velocities and accelerations.

Absolute velocities and accelerations:

Absolute angular velocity:

$$\mathbf{\Omega_i} = \mathbf{\Omega_{i-1}} + \dot{\theta}_i \mathbf{S_i} \qquad i = 1, \ldots, N-1 \tag{2.32}$$

$\mathbf{\Omega_i}$: Absolute angular velocity of link i

$\mathbf{\Omega_{i-1}}$: Absolute angular velocity of link (i-1)

Absolute angular acceleration:

$$\boldsymbol{\alpha}_\mathbf{i} = \boldsymbol{\alpha}_{\mathbf{i-1}} + \ddot{\theta}_i \mathbf{S_i} + \dot{\theta}_i \mathbf{\Omega_{i-1}} \times \mathbf{S_i} \quad i = 1, \ldots, N-1 \tag{2.33}$$

$\boldsymbol{\alpha}_\mathbf{i}$: Absolute angular acceleration of link i

$\boldsymbol{\alpha}_\mathbf{i-1}$: Absolute angular acceleration of link (i-1)

Absolute linear acceleration of the origin:

$$\mathbf{a_{o,i}} = \mathbf{a_{o,i-1}} + \ddot{S}_{ii}\mathbf{S_i} + 2\dot{S}_{ii}\,\mathbf{\Omega_i} \times \mathbf{S_i} + \boldsymbol{\alpha}_\mathbf{i} \times \mathbf{r_{o,i}} + \mathbf{\Omega_i} \times (\mathbf{\Omega_i} \times \mathbf{r_{o,i}}) \quad i = 1, \ldots, N-1 \tag{2.34}$$

$\mathbf{a_{o,i}}$: Absolute linear acceleration of the origin of link i

$\mathbf{a}_{\mathbf{o,i-1}}$: Absolute linear acceleration of the origin of link (i-1)

$\mathbf{r}_{\mathbf{o,i}}$: Distance between two origins given by $\mathbf{r}_{\mathbf{o,i}} = S_{ii}\mathbf{S}_{\mathbf{i}} + a_{hi}\mathbf{a}_{\mathbf{hi}}$

2.2.2 Determination of the joint reactions and the actuator force

After performing position, velocity and acceleration analysis, the two dynamic equilibrium equations (2.22) and (2.23) are written for each moving link. Therefore, one obtains a set of linear equations involving the joint reactions and the actuator torque (or force). This equation system is solved via the LinearSolve command of MATHEMATICA to yield the joint reactions and the actuator torque. It should be noted that the formulations of $\mathbf{F}_{\mathbf{in,i}}$ and $\left(\mathbf{T}_{\mathbf{in}}\right)_{o_i}$ as given by equations (2.30) and (2.31) indicate clearly that joint forces and the actuator torque will be linear in the inertial parameters of the links, [namely, $m_i, MX_i, MY_i, MZ_i, XX_i, YY_i, ZZ_i, XY_i, YZ_i$, XZ_i for $i = 1,\ldots,N-1$]. This facilities the minimization of the FFN (see Chapter 3) extensively.

CHAPTER III

FORCE FLUCTUATION NUMBER

The concept of Force Fluctuation Number has been introduced in Tursun [10]. Therefore, sections 3.1 and 3.2.1 are mostly excerpted from Tursun [10] with necessary modifications for application to spatial mechanisms.

3.1 Computation of the Force Fluctuation Number

Consider a one degree of freedom mechanism with the generalized coordinate q having a specified input motion (i.e. $q(t)$ is known, where t denotes time). Now, let the Force Fluctuation Number be defined by

$$FFN = \sqrt{\int_R \left[\sum_{i=1}^{i=nf} \left(F_i - F_{id} \right)^2 \right] dt / V} \tag{3.1}$$

where,

R: Interval, in the time-space, over which FFN is defined

V: Length of R

F_i: Any linear combination of the F_r's and F_a's where F_r denotes any component of any generalized joint reaction and F_a denotes the generalized actuator force.

F_{id}: Desired value of F_i which could be any specified constant (including zero) or $\overline{F}_i$, where $\overline{F}_i$ is the average value of F_i over R.

nf: Number of F_i's that appear in the definition of FFN.

Clearly, FFN will be zero if and only if $F_i=F_{id}$=constant for all i. Furthermore, the smaller FFN is, the smaller the fluctuations of the F_i's (from their desired values) will be over the interval R, for the given input motion $q(t)$. By selecting the definitions of the F_i's appropriately, one can get different average quantitative indicators from FFN, representing different dynamic behaviors of the mechanism. For instance, if nf=1, $F_i = T_q$, $F_{id} = \overline{T}_q$ and $q(t) = \omega.t$ where ω is constant, then FFN becomes equivalent to the Torque Fluctuation Number. (Soylu-M.Çetin[11])

The input motion given by q(t) may be adjusted conveniently so that the user can consider the mechanism either in the steady state motion, or during the acceleration phase.

In order to compute FFN, it is necessary to determine the reaction forces and moments (F_i) that appear in the definition of FFN. These forces are found by using the developed package, which uses the methods described in Chapter 2. Note that this package may provide any F_i in terms of $\mathbf{I_t}$. Here, $\mathbf{I_t}$ is the vector of inertial parameters of the mechanism given by

$$\mathbf{I_t} = \begin{bmatrix} m_1, MX_1, MY_1, MZ_1, XX_1, YY_1, ZZ_1, XY_1, YZ_1, XZ_1; \ldots \\ ; m_{N-1}, MX_{N-1}, MY_{N-1}, MZ_{N-1}, XX_{N-1}, YY_{N-1}, ZZ_{N-1}, XY_{N-1}, YZ_{N-1}, XZ_{N-1} \end{bmatrix} \quad (3.2)$$

where,

m_i :mass of link i

$MX_i \overset{\Delta}{=} m_i x_i$

$MY_i \overset{\Delta}{=} m_i y_i$

$MZ_i \overset{\Delta}{=} m_i z_i$

x_i, y_i, z_i : Coordinates of center of mass of link i with respect to the body fixed frame $[B_i]$.

XX_i, YY_i, ZZ_i, XY_i, YZ_i, XZ_i : Elements of moment of inertia matrix with respect to the body fixed frame $[B_i]$. (i.e. elements of $[\mathrm{I_i}]$)

The position analysis of a mechanism does not yield a closed form solution in general. Therefore, it is not possible to solve an F_i, in closed form , in terms of time. On the other hand, if time is specified numerically, the package will yield any F_i in terms of $\mathbf{I_t}$ only. Therefore, symbo-numeric integration is employed to obtain FFN, in closed form, in terms of $\mathbf{I_t}$ only. Here, symbo-numeric integration refers to the implementation of a numerical integration algorithm using symbolic manipulation package. The numerical integration algorithm used in this study is the Gaussian Quadrature method, where the number of Gaussian Quadrature points may be selected by the user.

The F_i forces obtained via the force analysis algorithm described in section 2.2.2 are linear in the elements of the $\mathbf{I_t}$ vector. Therefore, FFN will be quadratic in the elements of $\mathbf{I_f}$, where

$\mathbf{I_f}$: k×1 vector of inertial parameters that affect FFN

k: number of inertial parameters that affect FFN

If some elements of the $\mathbf{I_f}$ vector is specified and/or there exists external forces/moments other than the actuator force, then FFN will contain constant terms and terms which are linear (with respect to the elements of $\mathbf{I_f}$), as well.

3.2 Minimization of FFN

3.2.1 Minimization of FFN by designing inertial parameters

Minimization of FFN is necessary in order to obtain the desired design objective, which depends on the specific definition of FFN used. Indeed, the optimal inertial parameters should be physically meaningful; therefore they must satisfy certain constraints. These constraints (on the inertial parameters of the mechanism) can be obtained as follows.

- All masses must be greater than zero.

$$m_i > 0 \quad i = 1,2,\ldots,N-1 \tag{3.3}$$

- The principal moments of inertia of $[I_i]$, which are the eigenvalues of $[I_i]$, must be greater than zero, which implies the following constraints.

$$\begin{aligned} &XX_i > 0 \\ &(XX_i)(YY_i) - (XY_i)^2 > 0 \\ &(XX_i)(YY_i)(ZZ_i) - (XX_i)(YZ_i)^2 - (XY_i)^2(ZZ_i) \\ &-2(XY_i)(XZ_i)(YZ_i) - (XZ_i)^2(YY_i) > 0 \end{aligned} \qquad i = 1,2,\ldots,N-1 \tag{3.4}$$

- Using the parallel axis theorem one obtains:

$$\begin{aligned} &XX_i - m_i(y_i^2 + z_i^2) > 0 \\ &YY_i - m_i(x_i^2 + z_i^2) > 0 \\ &ZZ_i - m_i(x_i^2 + y_i^2) > 0 \end{aligned} \qquad i = 1,2,\ldots,N-1 \tag{3.5}$$

where the left hand sides correspond to the principal moments of inertia of link i in the frame $\left[B_{c_i}\right]$. Here, $\left[B_{c_i}\right]$ is the reference frame whose origin is at center of mass of link i and whose axes are parallel to these of $\left[B_i\right]$.

Equation (3.5) can be written as:

$$\begin{aligned} &\frac{m_i XX_i - (MY_i^2 + MZ_i^2)}{m_i} > 0 \\ &\frac{m_i YY_i - (MX_i^2 + MZ_i^2)}{m_i} > 0 \\ &\frac{m_i ZZ_i - (MX_i^2 + MY_i^2)}{m_i} > 0 \end{aligned} \qquad i = 1,2,\ldots,N-1 \tag{3.6}$$

in terms of the elements of $\mathbf{I_t}$. Considering constraint (3.3), the inequalities given by equation (3.6) simplify to:

$$
\begin{aligned}
&m_i XX_i - (MY_i^2 + MZ_i^2) > 0 \\
&m_i YY_i - (MX_i^2 + MZ_i^2) > 0 \qquad i = 1,2,\ldots,N-1 \\
&m_i ZZ_i - (MX_i^2 + MY_i^2) > 0
\end{aligned} \tag{3.7}
$$

Therefore, an optimal $\mathbf{I_t}$ vector will lead to a physically realizable mechanism if and only if (3.3), (3.4) and (3.7) are satisfied.

If there are no external forces and/or torques acting on the mechanism and if all elements of $\mathbf{I_f}$ are available as design variables, then FFN contains only quadratic terms. Therefore, the equation that yields the critical $\mathbf{I_f}$ vector, i.e.

$$
\frac{d(FFN)}{d\,\mathbf{I_f}} = \mathbf{0} \tag{3.8}
$$

leads to the homogenous linear equation system

$$
[A]\mathbf{I_f} = \mathbf{0} \tag{3.9}
$$

where $[A]$ is the $k \times k$ coefficient matrix (known). Most of the time, $\mathbf{I_f}$ contains an inertial parameter that must be strictly positive (i.e., an m_i or $[I_i]$ term). This implies that a necessary, but not sufficient, condition for a physically realizable mechanism is

$$
Det[A] = 0 \tag{3.10}
$$

where *Det* denotes the determinant operator. In other words, the critical $\mathbf{I_f}$ vector, $\mathbf{I_f^*}$, that correspond to a physically realizable mechanism lies in the nullspace of $[A]$. In the developed package, the NULLSPACE command of MATHEMATICA is conveniently used to obtain $\mathbf{I_f^*}$.

In the computer implementation, $Det[A]$ may deviate from zero slightly (although it should be zero) due to the round off errors and the errors introduced

by the symbo-numeric integration used to compute FFN. In such a case, the NullSpace of $[A]$ would be the empty set. One remedy for this situation may be increasing the tolerance value of the NullSpace command slightly and thus obtain the correct $\mathbf{I}_\mathbf{f}^*$ vector.

If there are external forces and/or torques acting on the mechanism, or if some elements of $\mathbf{I}_\mathbf{f}$ are not available as design variables, then (3.8) yields the non-homogenous linear equation system

$$[D]\mathbf{I}_\mathbf{d} = \mathbf{b} \tag{3.11}$$

$\mathbf{I}_\mathbf{d}$: $m \times 1$ vector of design variables (i.e., those elements of $\mathbf{I}_\mathbf{f}$ that are available for design)

m : number of elements of $\mathbf{I}_\mathbf{d}$

$[D]$: $m \times m$ coefficient matrix (known)

$\mathbf{b}$: $m \times 1$ right hand side vector (known)

Due to the round off and integration errors, as explained before, it is advantageous to solve (3.11) by using the NullSpace command. In order to transform (3.11) to a homogenous equation, one firstly defines

$$\mathbf{I}'_\mathbf{d} \overset{\Delta}{=} \begin{bmatrix} \mathbf{I}_\mathbf{d} \\ \cdots \\ c \end{bmatrix} \tag{3.12}$$

where c is an artificially introduced unknown. Therefore, (3.11) can be written as

$$[D']\mathbf{I}'_\mathbf{d} \overset{\Delta}{=} \mathbf{0} \tag{3.13}$$

where $[D'] \overset{\Delta}{=} [D \vdots -\mathbf{b}]$ is an $m \times (m+1)$ coefficient matrix. One may solve $\mathbf{I}'_\mathbf{d}$ from (3.13) by the NullSpace command (note that the NullSpace command works on

rectangular matrices as well). The solution for $\mathbf{I_d}$ (which yields the critical point of FFN, $\mathbf{I_d^*}$) is then determined by noting that the artificial unknown *c* must have the value 1 in reality.

Once $\mathbf{I_f^*}$ (or $\mathbf{I_d^*}$) is determined, one has to check whether it corresponds to a minimum (rather than maximum) and also ensure that the links are physically realizable (i.e., equations (3.3), (3.4) and (3.7) are satisfied).

3.2.2 Minimization of FFN by using counterweights

In order to minimize FFN by designing the inertial parameters of the mechanism, the mechanism must be at the design stage such that all inertial parameters of the mechanism are available for design. If the mechanism already exists, then the dynamic performance of the mechanism can be enhanced via addition of suitable counterweights, which are considered to be point masses in this study. This enhancement can be realized as explained in the following paragraphs.

Let $m_{bi}, x_{bi}, y_{bi}, z_{bi}$ denote the counterweight to be added to link i, and its coordinates with respect to the $[B_i]$ reference frame. Furthermore, let the inertial parameters of the existing N-link mechanism, the mechanism with the counterweights and the counterweights themselves be denoted by

$$m_{oi}, MX_{oi}, MY_{oi}, MY_{oi}, XX_{oi}, YY_{oi}, ZZ_{oi}, XY_{oi}, YZ_{oi}, XZ_{oi} \quad i = 1, \ldots, N-1 \qquad (3.14)$$

$$m_{ti}, MX_{ti}, MY_{ti}, MY_{ti}, XX_{ti}, YY_{ti}, ZZ_{ti}, XY_{ti}, YZ_{ti}, XZ_{ti} \quad i = 1, \ldots, N-1 \qquad (3.15)$$

$$m_{bi}, MX_{bi}, MY_{bi}, MY_{bi} \quad i = 1, \ldots, N-1 \qquad (3.16)$$

respectively.

The inertial parameters $m_{ti}, MX_{ti}, MY_{ti}, MY_{ti}, XX_{ti}, YY_{ti}, ZZ_{ti}, XY_{ti}, YZ_{ti}, XZ_{ti}$ can be expressed in terms of $m_{oi}, MX_{oi}, MY_{oi}, MY_{oi}, XX_{oi}, YY_{oi}, ZZ_{oi}, XY_{oi}, YZ_{oi}, XZ_{oi}$ and $m_{bi}, MX_{bi}, MY_{bi}, MY_{bi}$ as described below.

The total mass of the resulting mechanism given by

$$m_{ti} = m_{oi} + m_{bi} \quad i = 1, \ldots, N-1 \tag{3.17}$$

The coordinates of the center of mass of the resulting mechanism will be:

$$\begin{aligned} x_{ti} &= \frac{m_{oi}x_{oi} + m_{bi}x_{bi}}{m_{ti}} \\ y_{ti} &= \frac{m_{oi}y_{oi} + m_{bi}y_{bi}}{m_{ti}} \quad i = 1, \ldots, N-1 \\ z_{ti} &= \frac{m_{oi}z_{oi} + m_{bi}z_{bi}}{m_{ti}} \end{aligned} \tag{3.18}$$

which leads to

$$\begin{aligned} MX_{ti} &= MX_{oi} + MX_{bi} \\ MY_{ti} &= MY_{oi} + MY_{bi} \quad i = 1, \ldots, N-1 \\ MZ_{ti} &= MZ_{oi} + MZ_{bi} \end{aligned} \tag{3.19}$$

The inertia matrices of the original and the resulting mechanism, on the other hand, are related to each other via the equation.

$$\begin{bmatrix} XX_{ti} & -XY_{ti} & -XZ_{ti} \\ -XY_{ti} & YY_{ti} & -YZ_{ti} \\ -XZ_{ti} & -YZ_{ti} & ZZ_{ti} \end{bmatrix} = \begin{bmatrix} XX_{oi} & -XY_{oi} & -XZ_{oi} \\ -XY_{oi} & YY_{oi} & -YZ_{oi} \\ -XZ_{oi} & -YZ_{oi} & ZZ_{oi} \end{bmatrix} + \begin{bmatrix} m_{bi}(y_{bi}^{\,2} + z_{bi}^{\,2}) & -m_{bi}x_{bi}y_{bi} & -m_{bi}x_{bi}z_{bi} \\ -m_{bi}x_{bi}y_{bi} & m_{bi}(x_{bi}^{\,2} + z_{bi}^{\,2}) & -m_{bi}y_{bi}z_{bi} \\ -m_{bi}x_{bi}z_{bi} & -m_{bi}y_{bi}z_{bi} & m_{bi}(x_{bi}^{\,2} + y_{bi}^{\,2}) \end{bmatrix} \quad i = 1, \ldots, N-1 \tag{3.20}$$

which leads to

$$
\begin{aligned}
XX_{ti} &= XX_{oi} + m_{bi}(y_{bi}{}^2 + z_{bi}{}^2) \\
YY_{ti} &= YY_{oi} + m_{bi}(x_{bi}{}^2 + z_{bi}{}^2) \\
ZZ_{ti} &= ZZ_{oi} + m_{bi}(x_{bi}{}^2 + y_{bi}{}^2) \\
-XY_{ti} &= -XY_{oi} - m_{bi}x_{bi}y_{bi} \\
-XZ_{ti} &= -XZ_{oi} - m_{bi}x_{bi}z_{bi} \\
-YZ_{ti} &= -YZ_{oi} - m_{bi}y_{bi}z_{bi}
\end{aligned}
\qquad i = 1, \ldots, N-1 \qquad (3.21)
$$

which is equivalent to

$$
\begin{aligned}
XX_{ti} &= \frac{m_{bi}XX_{oi} + MY_{bi}^2 + MZ_{bi}^2}{m_{bi}} \\
YY_{ti} &= \frac{m_{bi}YY_{oi} + MX_{bi}^2 + MZ_{bi}^2}{m_{bi}} \\
ZZ_{ti} &= \frac{m_{bi}ZZ_{oi} + MX_{bi}^2 + MY_{bi}^2}{m_{bi}} \\
XY_{ti} &= \frac{m_{bi}XY_{oi} + MX_{bi}MY_{bi}}{m_{bi}} \\
XZ_{ti} &= \frac{m_{bi}XZ_{oi} + MX_{bi}MZ_{bi}}{m_{bi}} \\
YZ_{ti} &= \frac{m_{bi}YZ_{oi} + MY_{bi}MZ_{bi}}{m_{bi}}
\end{aligned}
\qquad i = 1, \ldots, N-1 \qquad (3.22)
$$

Using the developed package, FFN^2 can be obtained in terms of the total inertial parameters. If one substitutes equations (3.17), (3.19) and (3.22) into FFN^2, FFN^2 will be a function of the inertial parameters of the counterweights m_{bi}, MX_{bi}, MY_{bi}, MZ_{bi} for $i = 1, \ldots, N-1$. The constrained, numerical optimization function, NMinimize, of Mathematica can then be used to find the optimal counterweight masses and their locations. Practical constraints on m_{bi}, MX_{bi}, MY_{bi}, MZ_{bi} can be considered during this minimization.

It should be noted that it is also possible to add more than one counterweight to each link. Equation (3.17), (3.19) and (3.22) can be trivially extended for this situation.

CHAPTER IV

CASE STUDIES

4.1 Analysis of a CCCR Mechanism

4.1.1 Kinematic Analysis

The dimensions of a $C_1C_2C_3R_4$ mechanism shown in Figure 4.1 are given in Table 4.1. This mechanism is same as the mechanism in page 179 of Duffy [7].

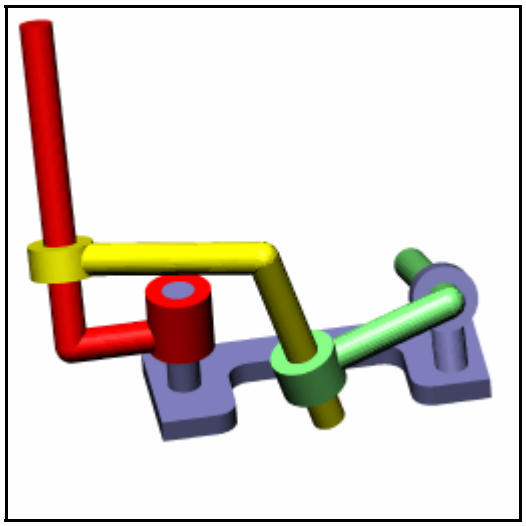

Figure 4.1 3-D model of a CCCR mechanism

Table 4.1 CCCR mechanism dimensions

	Link 1 (green)	Link 2 (yellow)	Link 3 (red)	Link 4 (blue)
Link lengths	a_{12}= 0.07 m	a_{23}=0.1 m	a_{34}=0.05 m	a_{41}=0.12 m
Twist angles	α_{12}= 60°	α_{23}= 30°	α_{34}= 20°	α_{41}= 65°
Offsets	S_{11}= variable	S_{22}=variable	S_{33}=variable	S_{44}=0 m

In figure 4.2, a schematic drawing of a CCCR mechanism is shown. The three dimensional drawing of the mechanism in Figure 4.1 is more appealing than this drawing. But note that a CCCR mechanism has only four links and its 3D model is not very difficult to draw. If a spatial mechanism with more links is considered, the schematic representation of the mechanism as in Figure 4.2 will be more convenient than the 3D model of the mechanism since the 3D model will become very complicated.

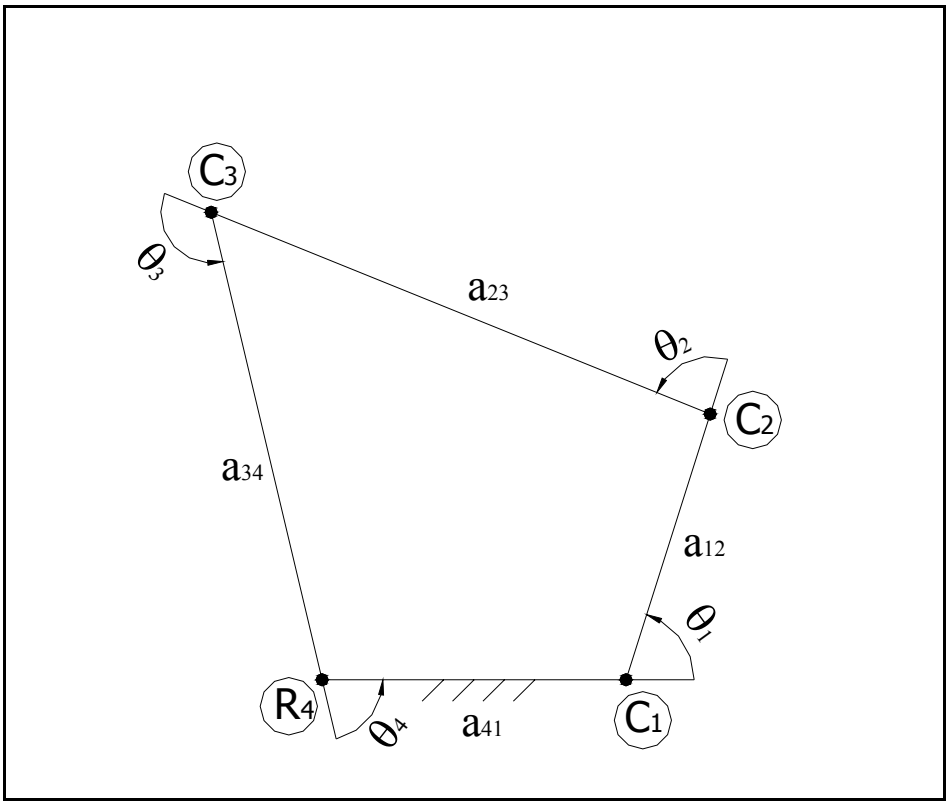

Figure 4.2 CCCR Mechanism

Clearly, this is a group 1 mechanism, since there are three prismatic joint variables, S_{11}, S_{22} and S_{33} (note that a cylindrical joint is kinematically equivalent to a revolute and a prismatic joint whose rotation and sliding axes are coincident). The remaining four joint variables are θ_1, θ_2, θ_3 and θ_4.. Let θ_4 be the input joint variable and θ_2 be the output joint variable. The complete position analysis of this

mechanism can be performed by following the steps of the algorithm explained in section 2.1.1.1.

1. The two rotational variables to be excluded should be θ_1 and θ_3.
2. The ZZ law which excludes θ_1 and θ_3 is

$$Z_2 = Z_4 \tag{4.1}$$

3. The corresponding mutual moment law is

$$Z_{02} = Z_{04} \tag{4.2}$$

4. Using equation (2.10) with h=1, one obtains

$$r_{1,z} \equiv a_{23}R_2 + a_{34}R_{23} + a_{41}R_{234} + S_{11} + S_{22}\cos(\alpha_{12}) + S_{33}Z_2 + S_{44}Z_{23} = 0 \tag{4.3}$$

5. Using equation (2.10) with h=3, one obtains

$$r_{3,z} \equiv a_{12}R_{41} + a_{23}R_{412} + a_{41}R_4 + S_{11}Z_4 + S_{22}Z_{41} + S_{33} + S_{44}\cos(\alpha_{34}) = 0 \tag{4.4}$$

6. The four joint variables θ_2, S_{11}, S_{22} and S_{33} are to be solved by using equations (4.1)-(4.4). Since the mechanism belongs to group 1, firstly, the rotational joint variable θ_2 can be solved using equation (4.1). Then the remaining three joint variables can be obtained by solving a linear equation system.
7. Using the half-angle laws, determine θ_1 and θ_3.

Let the input motion of the mechanism be given by:

$$\theta_4(t) = 2\pi \times \mathrm{t} \tag{4.5}$$

where t denotes time.

The six unknown joint variables θ_1, θ_2, θ_3, S_{11}, S_{22} and S_{33} have been found by using the developed package. The graphs of the unknown position variables (versus the input, θ_4) are shown in Figures 4.3-4.8. The relative angular velocity $\dot{\theta}_2$ (versus θ_4) is shown in Figure 4.9. The relative angular accelerations $\ddot{\theta}_2$ and $\ddot{\theta}_1$ (versus θ_4) are shown in Figure 4.10-4.11.

In all graphs, the units for the rotational joint variables are degrees. The units for the translational joint variables are meters. The units of the relative angular velocities are rad/sec and the relative angular accelerations are rad/sec^2. In the following graphs, the position analysis has been performed of 360 points (i.e., 1° increments have been used for θ_4). Therefore, the graphs look like a continuous curve although they are not.

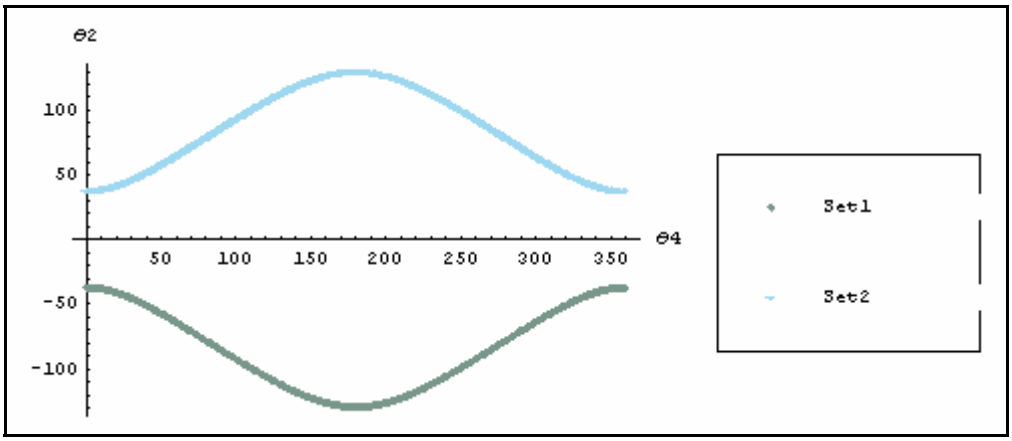

Figure 4.3 θ_2 versus θ_4 graph (Set1 is closure1)

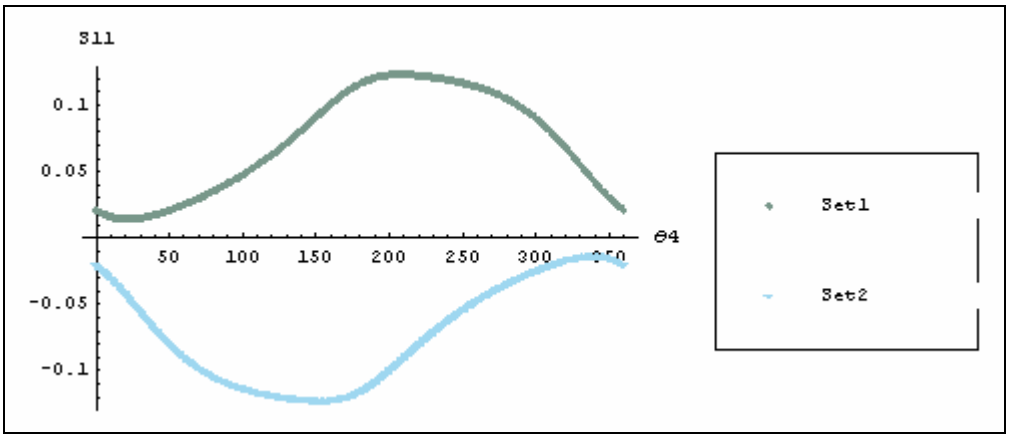

Figure 4.4 S_{11} versus θ_4 graph

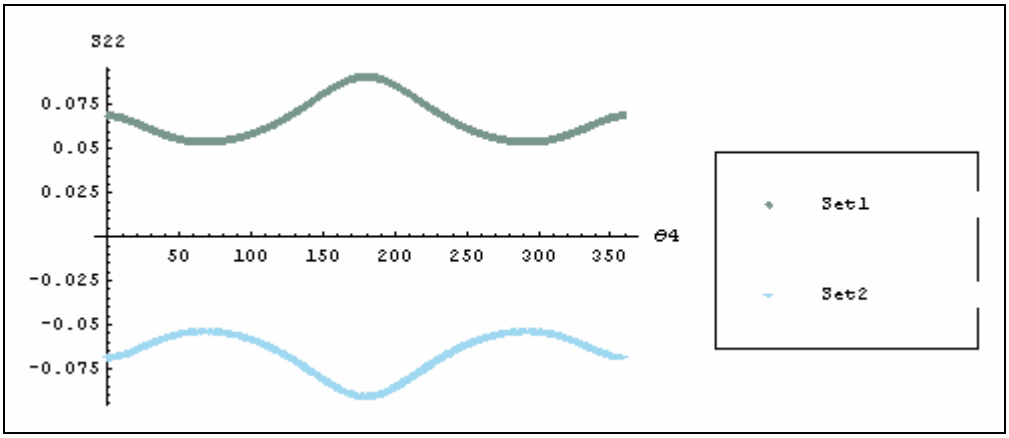

Figure 4.5 S_{22} versus θ_4 graph

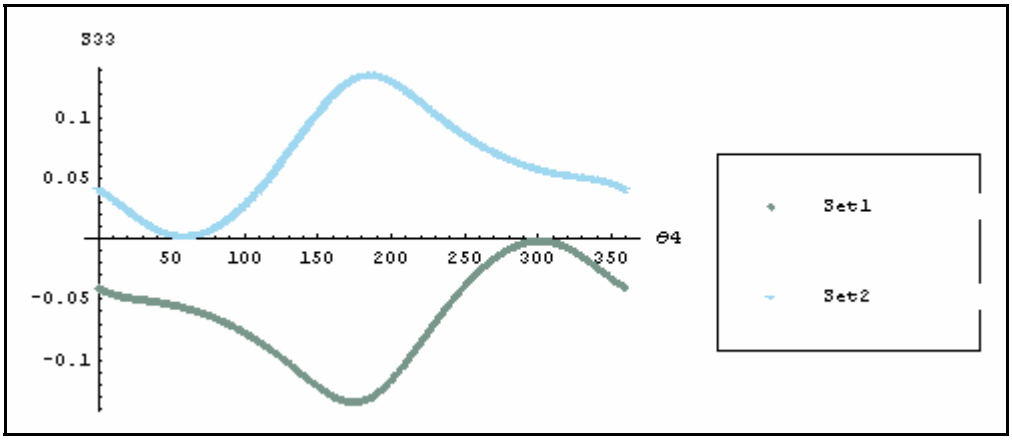

Figure 4.6 S_{33} versus θ_4 graph

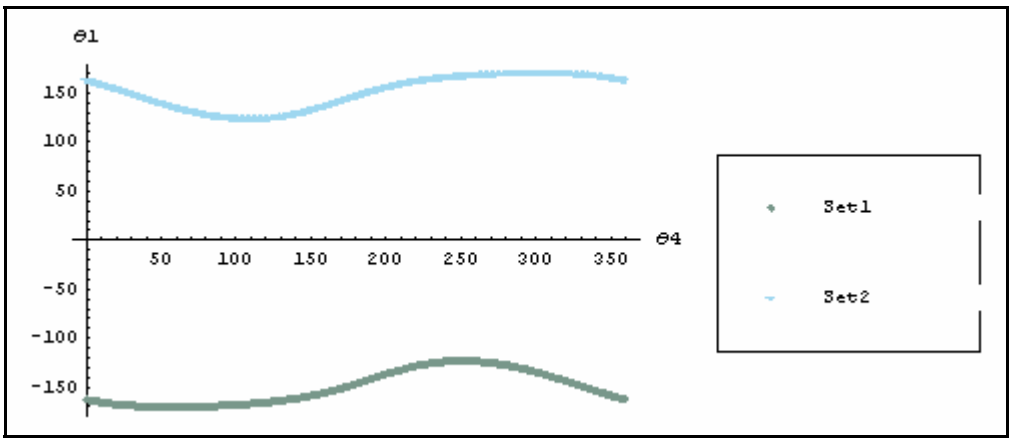

Figure 4.7 θ_1 versus θ_4 graph

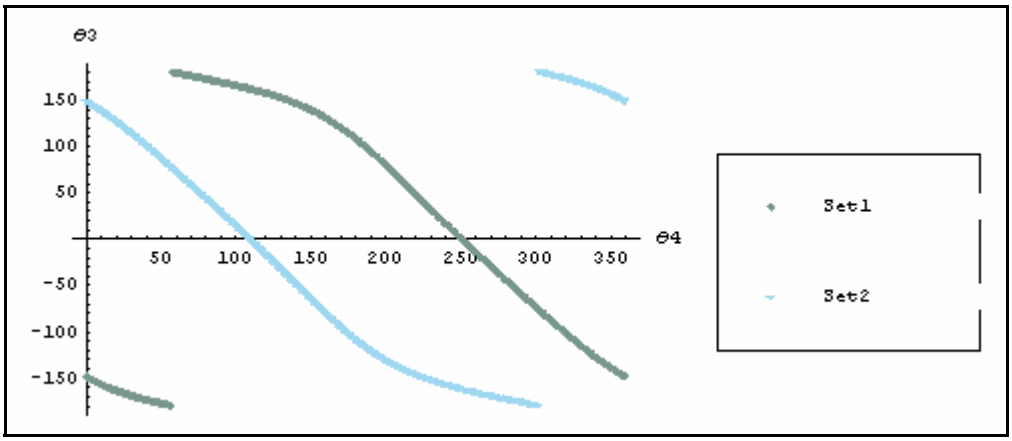

Figure 4.8 θ_3 versus θ_4 graph

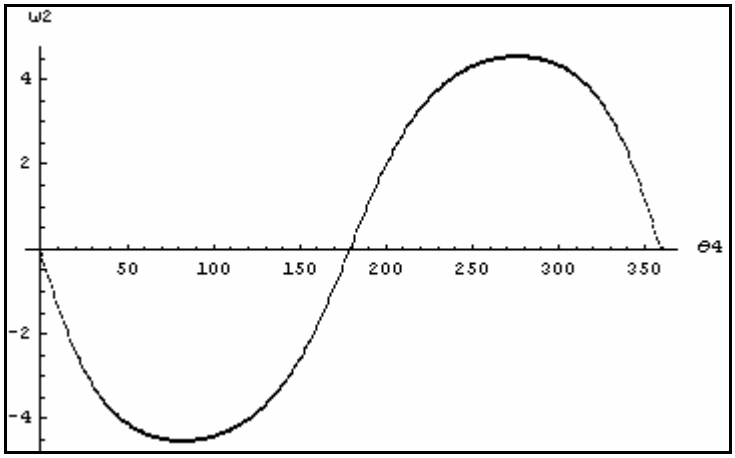

Figure 4.9 $\dot{\theta}_2(\omega_2)$ versus θ_4 graph on closure 1

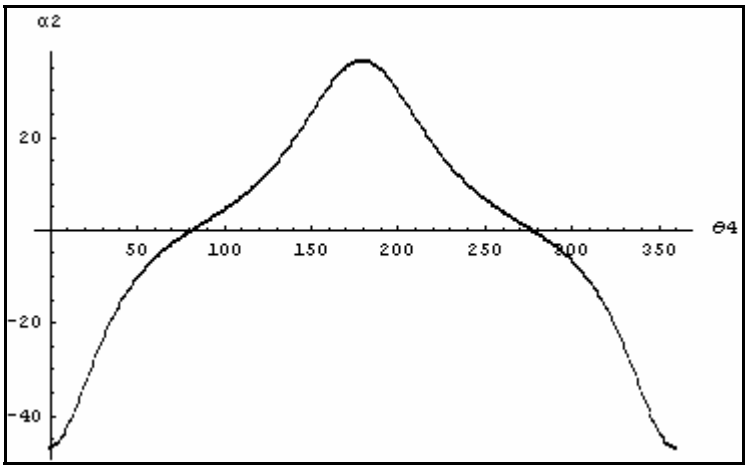

Figure 4.10 $\ddot{\theta}_2(\alpha_2)$ versus θ_4 graph on closure 1

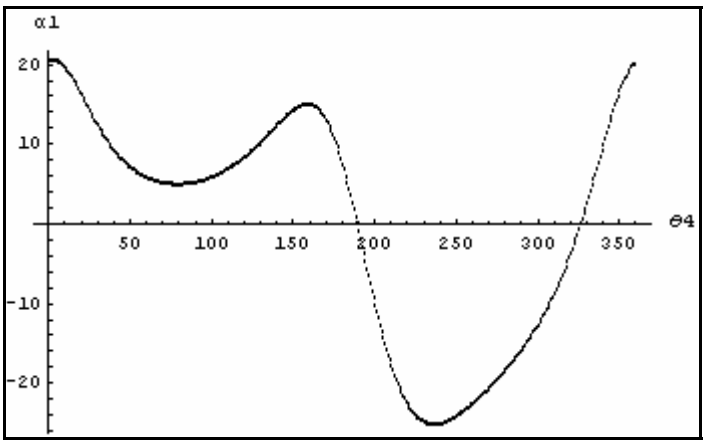

Figure 4.11 $\ddot{\theta}_1(\alpha_1)$ versus θ_4 graph on closure 1

The angular velocities and the angular accelerations of the mechanism can be obtained in closed form by using the *getoutput* function of the developed package (see Appendix C). For example, the following angular acceleration $\ddot{\theta}_1(\alpha_1)$ has been computed via the developed package in terms of the angular velocities, the position variables and the input angular acceleration. Note that closure 1 has been selected to find α_1.

$$\alpha_1 = 0.39493\csc(\theta_2)(-\omega_3\omega_4\cos(\theta_3) + (-\alpha_4 + \omega_2\omega_4\cot(\theta_2))\sin(\theta_3)) \qquad (4.6)^*$$

4.1.2 Closure Identification

For a CCCR mechanism, all of the position analysis plots are shown in Figures 4.3-4.8. It can be easily deduced from these plots that there are two closures of the mechanism. This mechanism is one of the simplest cases. Therefore, the method of closure identification will be explained in the analysis of a RPRRCR mechanism, which is more complicated than the analysis of a CCCR mechanism.

In Figure 4.12 and Figure 4.13, 3D views of the mechanism are shown for the two closures when θ_4=113° (see Figures 4.3-4.8 for the two closures). The numerical values of the position variables for the first (the green one) and the second (the blue one) closures are given by,

$$\left\{\begin{array}{l}\theta_1 = -166.626°,\ \theta_2 = -101.352°,\ \theta_3 = 160.41° \\ S_{11} = 0.0571\,\text{m},\ S_{22} = 0.0629\,\text{m}, S_{33} = -0.0875\,\text{m}\end{array}\right\} \tag{4.7}$$

and

$$\left\{\begin{array}{l}\theta_1 = 123.426°,\ \theta_2 = 101.352°,\ \theta_3 = -5.839° \\ S_{11} = -0.117\,\text{m},\ S_{22} = -0.0629\,\text{m}, S_{33} = 0.0433\,\text{m}\end{array}\right\} \tag{4.8}$$

respectively.

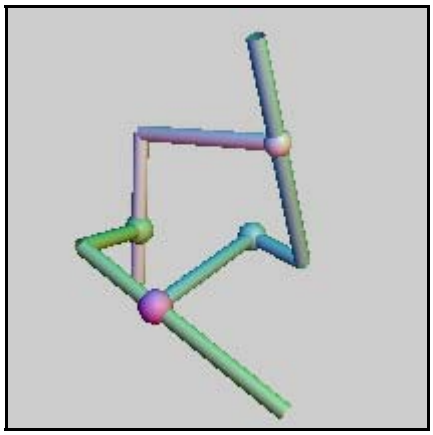

Figure 4.12 CCCR mechanism at θ_4=113° (Closure1)

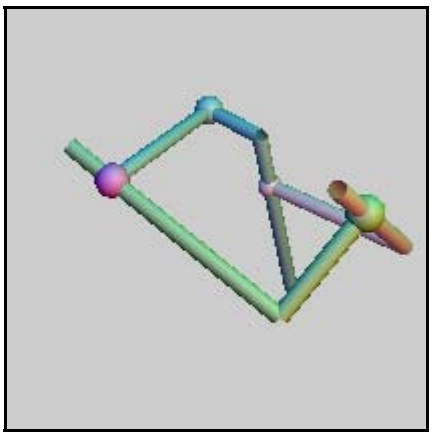

Figure 4.13 CCCR mechanism at θ_4=113° (Closure2)

4.1.3 Dynamic Analysis

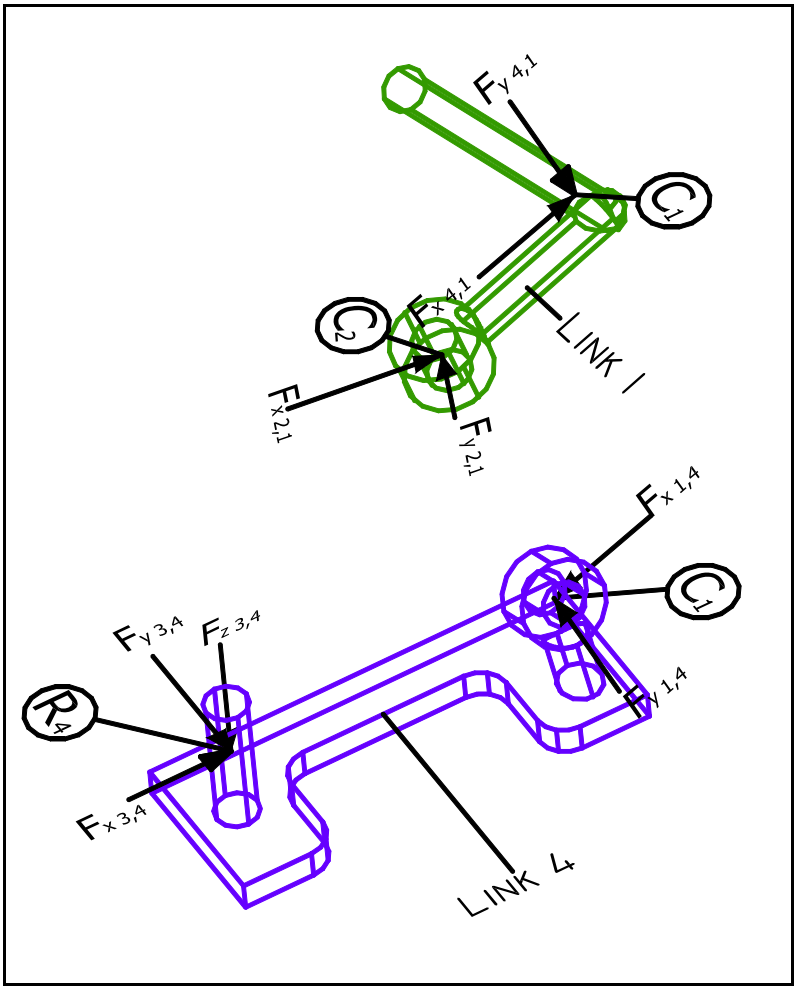

Figure 4.14 Reaction forces on link 1 and link 4

The components of the reaction forces acting on each link are shown in Figures 4.14 and 4.15. Here, Link 4 is the ground and its body fixed frame, $[B_4]$, is the inertial frame. As seen from the figures, the components of the reaction forces are not in the same frame system. Note that the reaction force acting on the *i*th joint is expressed in the *i*th frame system for $i = 1, 2, \ldots, N$ (i.e. components of $F_{2,1}$ expressed in $[B_2]$). This is the convention used throughout the study.

This mechanism has 9 unknown reaction forces. Each cylindrical and revolute joint has two and three unknown reaction forces respectively. Since the mechanism has 3 moving links, 9 force equilibrium equations can be written for the moving links of the mechanism. Therefore, 9 unknown reaction forces can be found by solving these force equilibrium equations. This implies that the reaction forces do not involve elements of the inertia matrix (i.e. XX_1, YY_2) because none of the moment equilibrium equations is used to solve these forces.

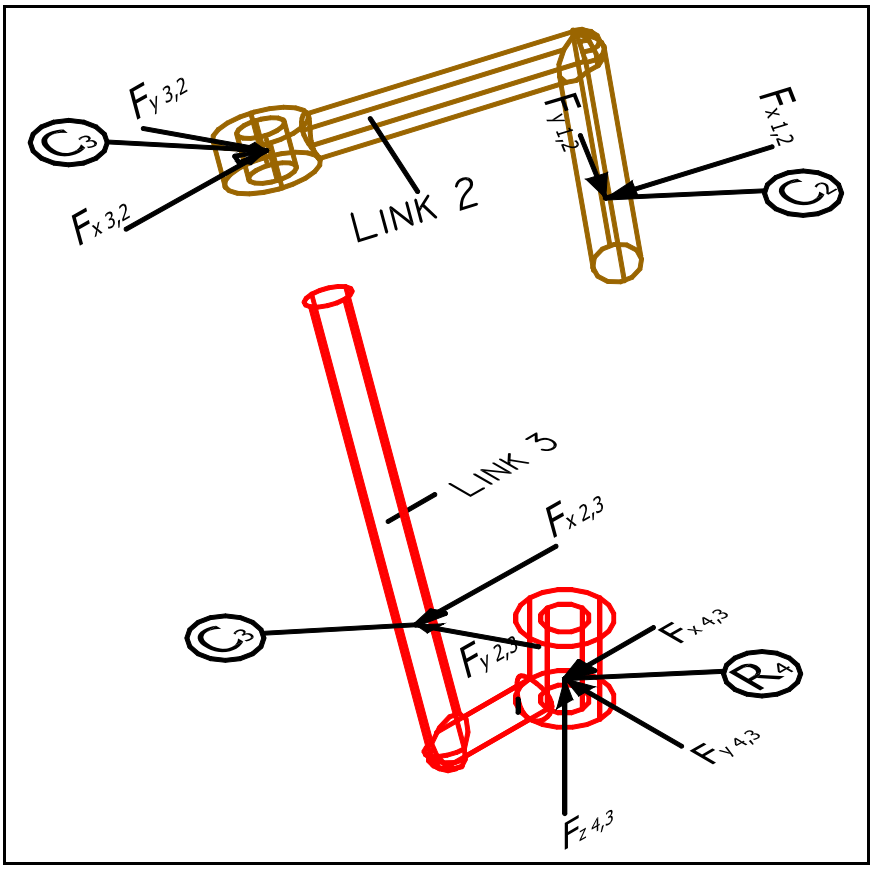

Figure 4.15 Reaction forces on link 2 and link 3

Consider the same CCCR mechanism shown in Figure 4.1 and same input motion, i.e., $\theta_4(t) = 2\pi \times \mathrm{t}$. Using the approach described in Appendix D (the links are considered to be steel), the inertial parameters of the links are found to be as follows.

$m_1 = 0.367$ kg,

$m_2 = 0.319$ kg,

$m_3 = 0.381$ kg

$MX_1 = 0.00792$ kg.m

$MY_1 = 0$

$MZ_1 = -0.0156$ kg.m

$MX_2 = 0.0112$ kg.m

$MY_2 = 0$

$MZ_2 = -0.00693$ kg.m

$MX_3 = 0.00709$ kg.m

$MY_3 = -0.00032$ kg.m

$MZ_3 = 0.0164$ kg.m

$$[I_1] = \begin{bmatrix} 0.00157 & 0 & 0 \\ 0 & 0.00206 & 0.00000133 \\ 0 & 0.00000133 & 0.000501 \end{bmatrix} \text{ kg.m}^2$$

$$[I_2] = \begin{bmatrix} 0.000473 & 0 & 0 \\ 0 & 0.00138 & 0.00000139 \\ 0 & 0.00000139 & 0.00921 \end{bmatrix} \text{ kg.m}^2$$

$$[I_3] = \begin{bmatrix} 0.00159 & 0.00016 & -0.000439 \\ 0.00016 & 0.00192 & 0.00000133 \\ -0.000439 & 0.00000133 & 0.000356 \end{bmatrix} \text{ kg.m}^2 \qquad (4.9)$$

In order to check the results of dynamic analysis obtained via the developed program, Visual Nastran, a simulation program, has been used. Firstly, the 3D model of the mechanism is drawn in Autocad. Then, this model is imported to Visual Nastran (see Figure 4.1). The actuator torque, one of the simulation results of Visual Nastran, for the inertial parameters given by equation (4.9) is shown in Figure 4.16. The actuator torque obtained by using the same inertial parameters via the developed package is shown in Figure 4.17. Because the two graphs are the same, one can conclude that the position, velocity, acceleration and force analysis obtained via the developed package are correct. Note that in this example, gravitational acceleration has been neglected.

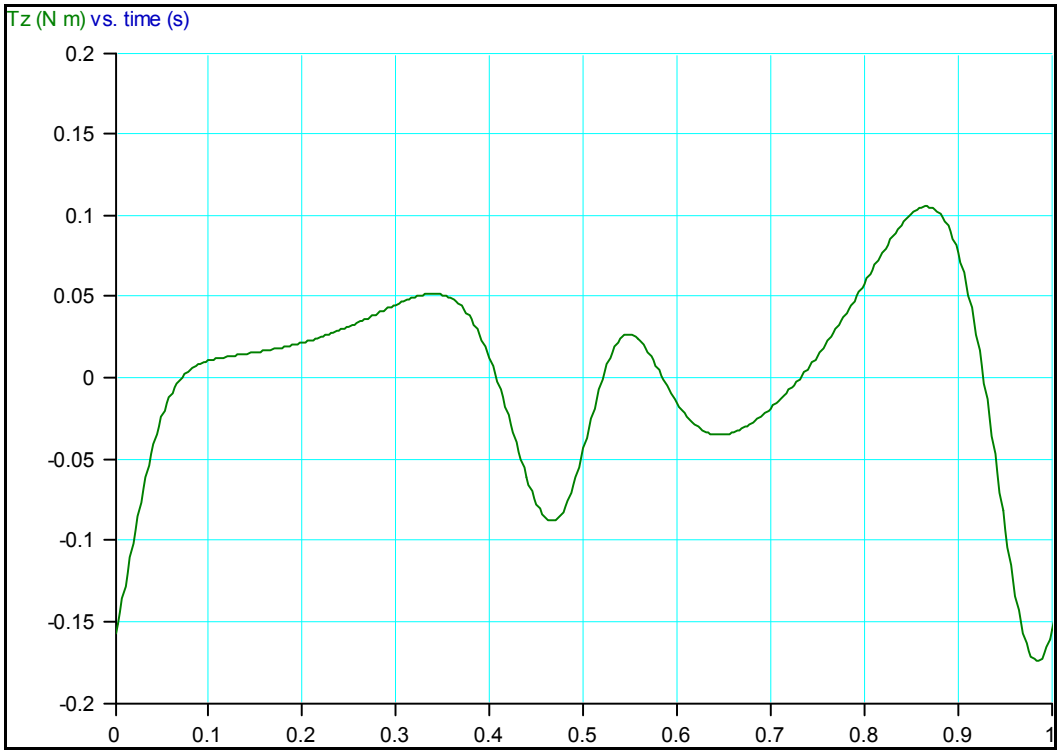

Figure 4.16 Actuator torque graph (Visual Nastran)

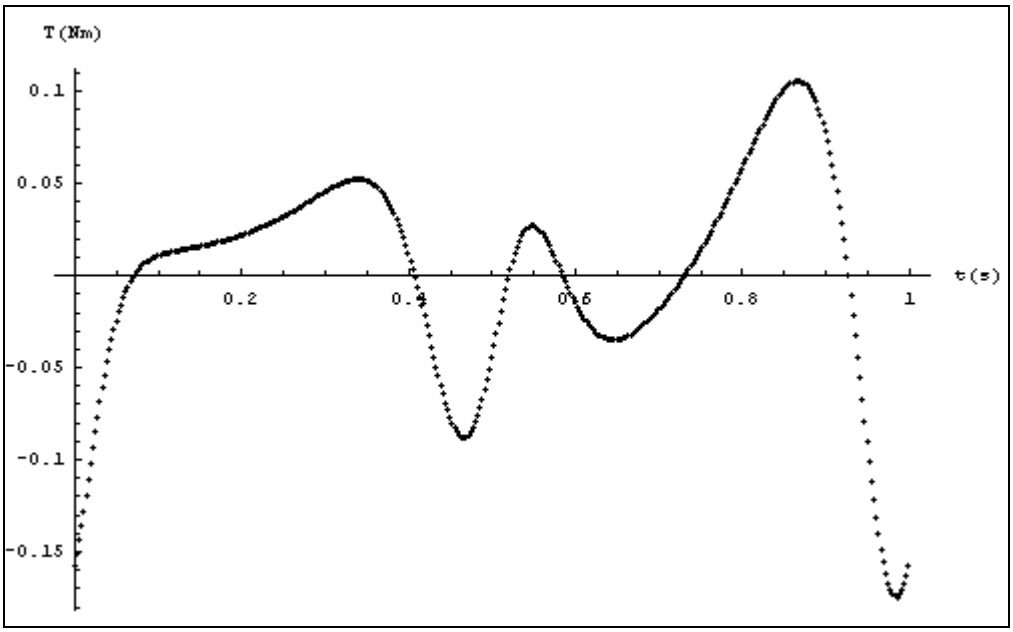

Figure 4.17 Actuator torque graph on closure 1 (Using the developed program)

4.1.4 Shaking Force Balancing of a CCCR Mechanism

If one takes into account only the shaking forces in the X_4 axis direction (i.e. the first axis of $[B_4]$ frame), FFN should be formulated as

$$FFN^2 = \int_R \left[(F_{x1,4} + F_{x3,4}) - (F_{x1,4} + F_{x3,4})_d \right]^2 dt \tag{4.10}$$

Here, the desired value of FFN $(F_{x1,4} + F_{x3,4})_d$ is specified to be zero. The first closure of the mechanism is selected. The gravitational acceleration is neglected and the input motion is given by

$$\theta_4(t) = 2\pi \times \mathrm{t} \tag{4.11}$$

50 Gaussian Quadrature points have been used to find FFN^2.

One can obtain FFN^2 as in equation (4.12) by taking $R = \{t : 0 \le t \le 1\}$ and using the developed package.

$$
\begin{aligned}
FFN^2 &= 2.934\times10^{-16}\,m_1^{\,2} + 1.29512\,m_2^{\,2} + 1.94818\,m_3^{\,2} + 5.17692\,m_3\,MX_1 \\
&+ 100.695\,MX_1^{\,2} + 43.8095\,m_3\,MX_2 - 118.553\,MX_1\,MX_2 + 384.853\,MX_2^{\,2} \\
&- 77.9273\,m_3\,MX_3 - 103.538\,MX_1\,MX_3 - 876.191\,MX_2\,MX_3 + 779.273\,MX_3^{\,2} \\
&+ 8.89279\,m_3\,MY_1 + 174.068\,MX_1\,MY_1 - 21.6443\,MX_2\,MY_1 - 177.856\,MX_3\,MY_1 \\
&+ 132.857\,MY_1^{\,2} - 13.3392\,m_3\,MY_2 - 48.7083\,MX_1\,MY_2 - 124.472\,MX_2\,MY_2 \\
&+ 266.784\,MX_3\,MY_2 - 52.5357\,MY_1\,MY_2 + 144.504\,MY_2^{\,2} + 8.44028\times10^{-9}\,m_3\,MY_3 \\
&- 291.774\,MX_1\,MY_3 + 215.593\,MX_2\,MY_3 + 2.61404\times10^{-9}\,MX_3\,MY_3 \\
&- 475.363\,MY_1\,MY_3 - 288.767\,MY_2\,MY_3 + 688.115\,MY_3^{\,2} - 7.70138\,m_3\,MZ_2 \\
&- 150.747\,MX_1\,MZ_2 + 18.7445\,MX_2\,MZ_2 + 154.028\,MX_3\,MZ_2 - 230.115\,MY_1\,MZ_2 \\
&+ 45.4972\,MY_2\,MZ_2 + 411.676\,MY_3\,MZ_2 + 99.6425\,MZ_2^{\,2} + m_1(-1.43847\times10^{-8}\,m_2 \\
&- 4.23788\times10^{-10}\,m_3 - 3.42426\times10^{-8}\,MX_1 + 2.96461\times10^{-8}\,MX_2 \\
&+ 8.47577\times10^{-9}\,MX_3 + 6.02451\times10^{-8}\,MY_1 - 3.15558\times10^{-8}\,MY_2 \\
&- 8.07925\times10^{-8}\,MY_3 - 5.21737\times10^{-8}\,MZ_2 - 2.94061\times10^{-8}\,MZ_3) \\
&+ 3.07201\times10^{-9}\,m_3\,MZ_3 - 106.197\,MX_1\,MZ_3 + 78.4696\,MX_2\,MZ_3 \\
&+ 9.51379\times10^{-10}\,MX_3MZ_3 - 173.018\,MY_1\,MZ_3 - 105.103\,MY_2\,MZ_3 \\
&+ 500.907\,MY_3\,MZ_3 + 149.838\,MZ_2\,MZ_3 + 91.1576\,MZ_3^{\,2} + m_2(-0.545522\,m_3 \\
&+ 11.812\,MX_1 - 12.206\,MX_2 + 10.9104\,MX_3 - 0.94384\,MY_1 - 2.02377\,MY_2 \\
&+ 4.72496\,MY_3 + 0.817389\,MZ_2 + 1.71975\,MZ_3)
\end{aligned}
\tag{4.12}^{*}
$$

The inertial parameters that affect *FFN*, the minimum value of FFN^2 and the optimal $\mathbf{I}_\mathbf{f}^*$ vector can be obtained via the developed package as

$$
\mathbf{I}_\mathbf{f} = \{m_1, m_2, m_3, MX_1, MY_1, MX_2, MY_2, MZ_2, MX_3, MY_3, MZ_3\} \tag{4.13}
$$

$$
\begin{aligned}
FFN_*^2 &= 2.33058\times10^{-11}c_1^{\,2} - 9.9476\times10^{-14}c_1c_2 - 8.52651\times10^{-14}c_2^{\,2} \\
&-6.21725\times10^{-15}c_2c_3 + 1.11022\times10^{-15}c_3^{\,2} - 5.55112\times10^{-17}c_1c_4 \\
&+1.38778\times10^{-17}c_2c_4 + 8.67362\times10^{-19}c_3c_4 + 2.14889\times10^{-16}c_4^{\,2}
\end{aligned}
\tag{4.14}
$$

$$\mathbf{I}_\mathbf{f}^* = \left\{ \begin{array}{l} m_1 \to -0.000233489\,c_1 - 0.000693356\,c_2 + 0.0000286613\,c_3 + c_4 \\ m_2 \to 3.568\times10^{-6}\,c_1 - 1.942\times10^{-9}\,c_2 + 8.270\times10^{-10}\,c_3 + 1.433\times10^{-8}\,c_4 \\ m_3 \to -0.000188898\,c_1 - 0.0392707\,c_2 + 0.99798\,c_3 - 0.0000558787\,c_4 \\ MX_1 \to -1.123\times10^{-6}\,c_1 + 7.220\times10^{-10}\,c_2 - 2.945\times10^{-10}\,c_3 - 1.879\times10^{-9}\,c_4 \\ MY_1 \to -0.739632\,c_1 + 0.000402135\,c_2 - 0.000115291\,c_3 - 0.000129322\,c_4 \\ MX_2 \to 9.902\times10^{-8}\,c_1 - 3.782\times10^{-11}\,c_2 + 1.792\times10^{-12}\,c_3 - 7.406\times10^{-10}\,c_4 \\ MY_2 \to -0.11259\,c_1 + 0.0000886416\,c_2 - 4.161\times10^{-6}\,c_3 + 0.0000400131\,c_4 \\ MZ_2 \to -0.659402\,c_1 + 0.000310814\,c_2 - 0.000125919\,c_3 - 0.000218633\,c_4 \\ MX_3 \to -9.328\times10^{-6}\,c_1 - 0.00196354\,c_2 + 0.049899\,c_3 - 2.794\times10^{-6}\,c_4 \\ MY_3 \to -0.0721971\,c_1 + 0.341813\,c_2 + 0.0134455\,c_3 + 0.000262331\,c_4 \\ MZ_3 \to -0.02682\,c_1 - 0.938945\,c_2 - 0.0369496\,c_3 - 0.000640724\,c_4 \end{array} \right\} \tag{4.15}^*$$

respectively. Here, c_1, c_2, c_3, c_4 are arbitrary constants. For instance, assume that $c_1 = 1$, $c_2 = 3$, $c_3 = 4$, $c_4 = 2$. Using this assumption, $\mathbf{I}_\mathbf{f}^*$ becomes

$$\mathbf{I}_\mathbf{f}^* = \left\{ \begin{array}{l} m_1 \to 1.9978 \\ m_2 \to 3.595\times10^{-6} \\ m_3 \to 3.87381 \\ MX_1 \to -1.12584\times10^{-6} \\ MY_1 \to -0.739145 \\ MX_2 \to 9.74401\times10^{-8} \\ MY_2 \to -0.112261 \\ MZ_2 \to -0.659051 \\ MX_3 \to 0.19369 \\ MY_3 \to 1.0075 \\ MZ_3 \to -2.99273 \end{array} \right\} \tag{4.16}$$

which satisfies the physical realizability conditions given by

$$m_1 > 0$$

$$m_3 > 0 \tag{4.17}$$

although m_2 is close to zero.

In Figures 4.18 and 4.19, the X_4 components of the shaking forces are shown.

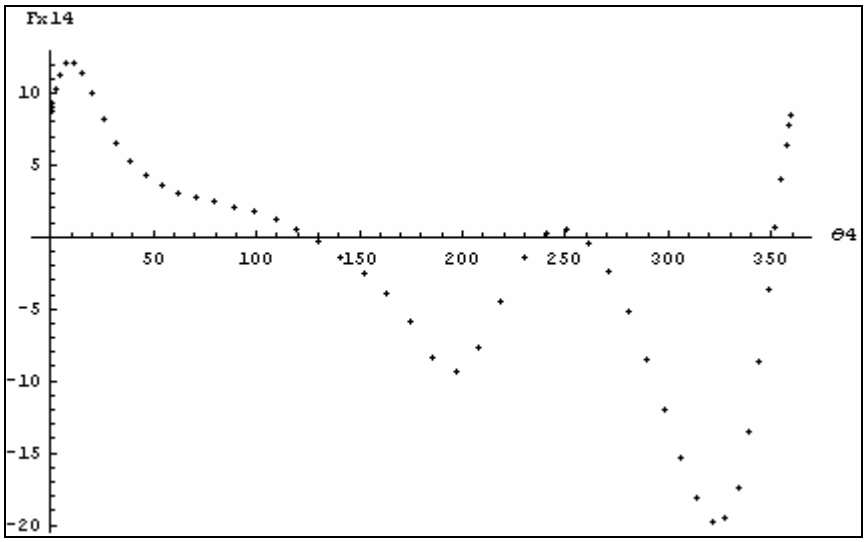

Figure 4.18 $F_{x\,1,4}$ versus θ_4 graph

From these two graphs, it can be concluded that the X_4 component of the shaking force is fully balanced during the whole cycle since $F_{x\,1,4}$ and $F_{x\,3,4}$ have the same magnitudes, but opposite directions. Figure 4.20, on the other hand, depicts the total shaking force in the X_4 direction. Actually, the total shaking force should be identically zero, if there has been no round off errors and if the integral in the definition of FFN has been computed exactly.

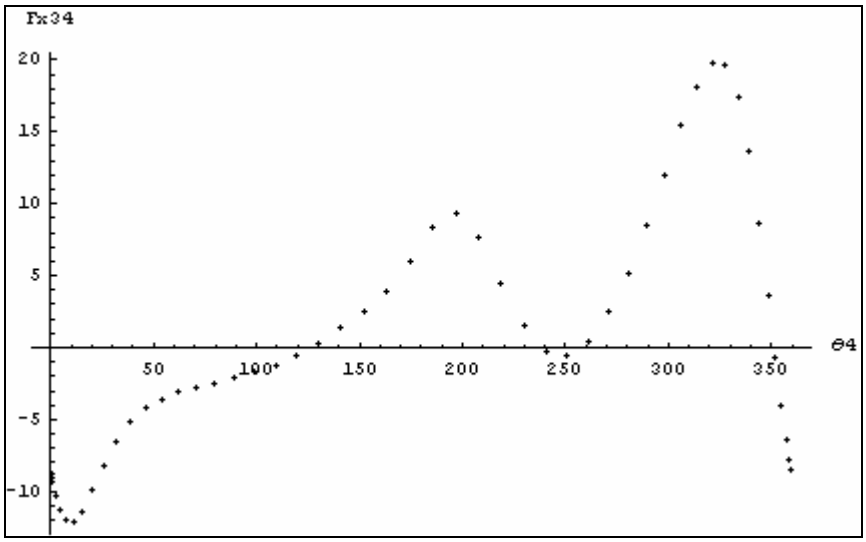

Figure 4.19 $F_{x\,3,4}$ versus θ_4 graph

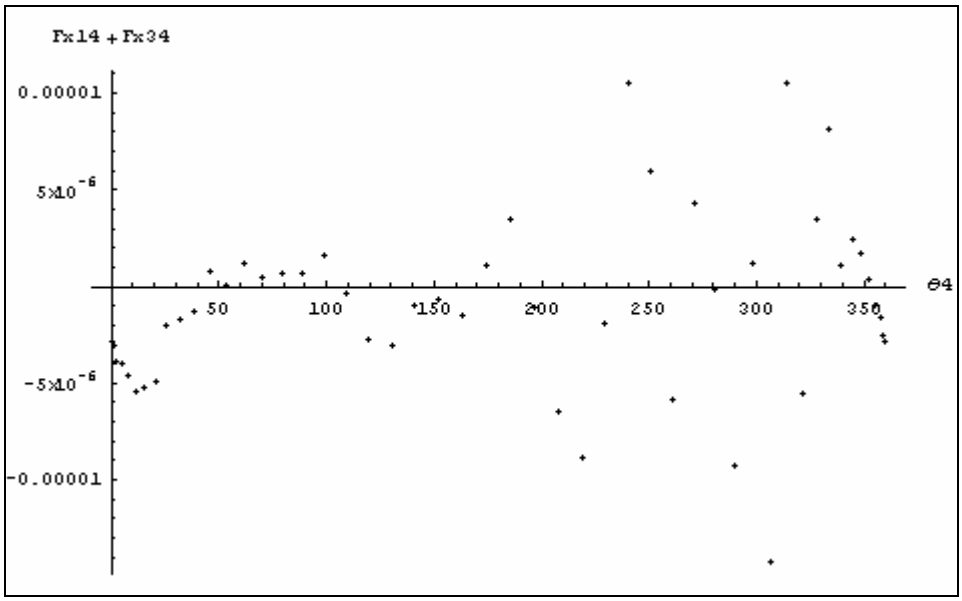

Figure 4.20 ($F_{x\,1,4} + F_{x\,3,4}$) versus θ_4 graph

The Y_4 (i.e. the second axis of $[B_4]$ frame)) components of the shaking force, on the other hand, do not add up to zero, as would be expected, to yield a zero shaking force along the Y_4 direction (see Figures 4.21 - 4.22).

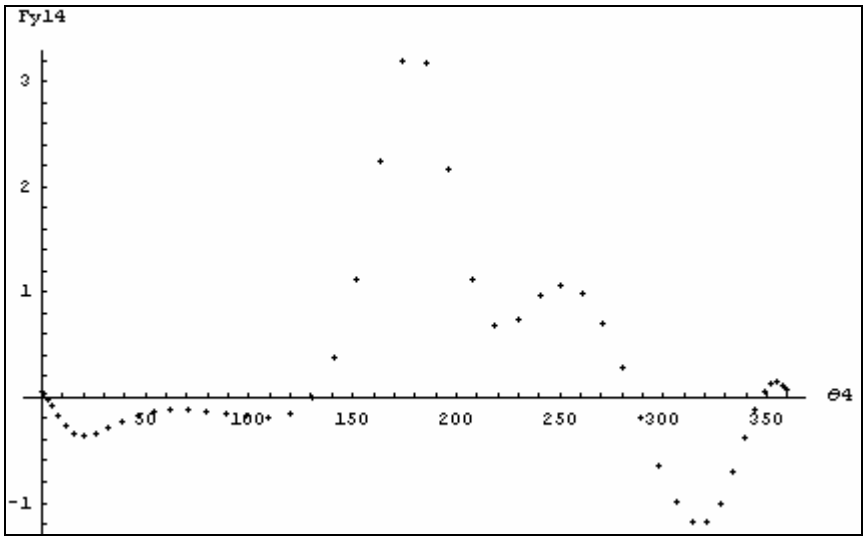

Figure 4.21 $F_{y\,1,4}$ versus θ_4 graph

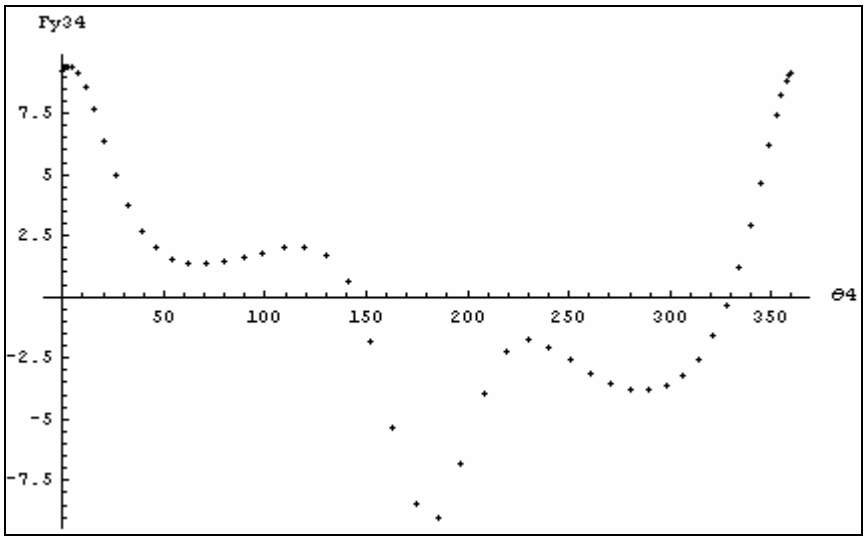

Figure 4.22 $F_{y\,3,4}$ versus θ_4 graph

Let's, now, consider all components of the shaking force in the X_4, Y_4 and Z_4 directions. Therefore, FFN is defined via the equation

$$FFN^2 = \int_R \left\{ \left[(F_{x1,4} + F_{x3,4}) \right]^2 + \left[(F_{y1,4} + F_{y3,4}) \right]^2 + \left[(F_{z1,4} + F_{z3,4}) \right]^2 \right\} dt \qquad (4.18)$$

Using the developed package, one can obtain FFN^2 as:

$$
\begin{aligned}
FFN^2 &= 4.23365\,m_1^{\,2} + 10.5192\,m_2^{\,2} + 3.89636\,m_3^{\,2} + 15.8664\,m_3\,MX_1 \\
&+ 233.551\,MX_1^{\,2} + 47.5989\,m_3\,MX_2 - 166.652\,MX_1\,MX_2 + 855.069\,MX_2^{\,2} \\
&- 155.855\,m_3\,MX_3 - 317.329\,MX_1\,MX_3 - 951.979\,MX_2\,MX_3 \\
&+ 1558.55\,MX_3^{\,2} + 2.33165\,m_3\,MY_1 - 6.24854\times10^{-16}\,MX_1 MY_1 \\
&+ 64.4285\,MX_2\,MY_1 - 46.633\,MX_3\,MY_1 + 233.551\,MY_1^{\,2} - 3.49746\,m_3\,MY_2 \\
&+ 160.977\,MX_1\,MY_2 - 44.7223\,MX_2\,MY_2 + 69.9492\,MX_3\,MY_2 \\
&- 324.687\,MY_1\,MY_2 + 690.797\,MY_2^{\,2} + 8.41721\times10^{-9}\,m_3\,MY_3 \\
&- 221.142\,MX_1\,MY_3 - 71.3235\,MX_2\,MY_3 - 1.40076\times10^{-9}\,MX_3\,MY_3 \\
&- 516.481\,MY_1\,MY_3 - 1228.9\,MY_2\,MY_3 + 1376.23\,MY_3^{\,2} - 2.01926\,m_3\,MZ_2 \\
&+ 0.000569408\,MX_1\,MZ_2 - 55.7962\,MX_2\,MZ_2 + 40.3852\,MX_3\,MZ_2 \\
&- 404.523\,MY_1\,MZ_2 + 281.188\,MY_2\,MZ_2 + 447.285\,MY_3\,MZ_2 + 175.163\,MZ_2^{\,2} \\
&+ 3.06361\times10^{-9}\,m_3\,MZ_3 - 80.4891\,MX_1\,MZ_3 - 25.9596\,MX_2\,MZ_3 \\
&- 5.09843\times10^{-10}\,MX_3\,MZ_3 - 187.984\,MY_1\,MZ_3 - 447.283\,MY_2\,MZ_3 \\
&+ 1001.81\,MY_3\,MZ_3 + 162.798\,MZ_2\,MZ_3 + 182.315\,MZ_3^{\,2} + m_1(8.10757\,m_2 \\
&+ 2.47969\,m_3 - 0.000151995\,MX_1 - 21.1041\,MX_2 - 49.5939\,MX_3 \\
&+ 0.000178817\,MY_1 - 40.6809\,MY_2 + 55.8849\,MY_3 - 0.000177431\,MZ_2 \\
&+ 20.3404\,MZ_3) + m_2(3.03279\,m_3 + 51.8235\,MX_1 - 20.1642\,MX_2 \\
&- 60.6558\,MX_3 - 37.4675\,MY_1 + 4.94832\,MY_2 + 70.4083\,MY_3 + 32.4479\,MZ_2 \\
&+ 25.6265\,MZ_3)
\end{aligned}
\tag{4.19}^{*}
$$

The inertial parameters that affect *FFN*, the minimum value of FFN^2 and the optimal $\mathbf{I}_\mathbf{f}^*$ vector can be obtained by using the developed package as

$$\mathbf{I}_\mathbf{f} = \{m_1, m_2, m_3, MX_1, MY_1, MX_2, MY_2, MZ_2, MX_3, MY_3, MZ_3\} \tag{4.20}$$

$$FFN_*^2 = -7.10543\times10^{-15}\,c_1^{\,2} - 2.84217\times10^{-14}\,c_2^{\,2} \tag{4.21}$$

$$\mathbf{I}_{\mathbf{f}}^{*}=\left\{\begin{array}{l} m_1 \to 2.13863\times10^{-12}\,c_1-3.21998\times10^{-10}\,c_2 \\ m_2 \to 1.74533\times10^{-10}\,c_1+7.35142\times10^{-10}\,c_2 \\ m_3 \to 0.844801\,c_1-0.532746\,c_2 \\ MX_1 \to -8.21086\times10^{-11}\,c_1-2.07009\times10^{-10}\,c_2 \\ MY_1 \to -4.83487\times10^{-6}\,c_1-0.0000233361\,c_2 \\ MX_2 \to 2.291\times10^{-14}\,c_1-1.47065\times10^{-11}\,c_2 \\ MY_2 \to -0.0000109456\,c_1-0.0000326741\,c_2 \\ MZ_2 \to 0.0000133755\,c_1+0.0000296469\,c_2 \\ MX_3 \to 0.04224\,c_1-0.0266373\,c_2 \\ MY_3 \to 0.18243\,c_1+0.289279\,c_2 \\ MZ_3 \to -0.501245\,c_1-0.794852\,c_2 \end{array}\right\} \qquad (4.22)^{*}$$

respectively, where c_1 and c_2 arbitrary constants.

The arbitrary constants c_1 and c_2 can be obtained in terms of m_1 and m_2 by using the first and second element of the $\mathbf{I}_{\mathbf{f}}^{*}$ vector to yield

$$\left\{\begin{array}{l} c_1 \to 1.2725\times10^{10}\,m_1+5.57365\times10^{10}\,m_2 \\ c_2 \to -3.02109\times10^{9}\,m_1+3.70187\times10^{7}\,m_2 \end{array}\right\} \qquad (4.23)$$

If c_1 and c_2 are substituted into the third element of the $\mathbf{I}_{\mathbf{f}}^{*}$ vector, one obtains

$$m_3 = 1.23595\times10^{10}\,m_1+4.6889\times10^{9}\,m_2 \qquad (4.24)$$

From equation (4.24), the first and second elements of $\mathbf{I}_{\mathbf{f}}^{*}$, it appears that m_1 and m_2 should both be zero for the mechanism to be fully shaking force balanced. This, infact, implies that this mechanism could not be fully force balanced by using internal mass redistribution. This conclusion is actually supported by the contour theorem. According to the contour theorem, introduced by Tepper and Lowen [11], "A planar mechanism without axisymetric link groupings can be fully force balanced by internal mass redistribution if and only if, from each link, there is a contour to the ground by way of revolutes only." This criterion is also valid for spatial mechanism. Because a CCCR mechanism has three sliding joints, link 1 and link 2 do not have a contour to the ground by way of revolute joints. Because of this, m_1 and m_2 is nearly zero with respect to m_3, i.e.

mass of link 3, in equation (4.24). Note that link 3 has a contour, or path, to the ground by way of revolute joints.

This mechanism may be partially balanced by using counterweights. Assume that the inertial parameters of the mechanism are the same as those in equation (4.9).

Let's use only a single counterweight on link 3. Equation (4.25) follows from equations (3.17), (3.19), (3.22) in Chapter 3.

$$
\begin{aligned}
m_{t3} &= 0.381 + m_{b3} \text{ kg} \\
MX_{t3} &= 0.00709 + MX_{b3} \text{ kg.m} \\
MY_{t3} &= -0.00032 + MY_{b3} \text{ kg.m} \\
MZ_{t3} &= 0.0164 + MZ_{b3} \text{ kg.m}
\end{aligned}
\tag{4.25}
$$

Using the developed package based upon the definition (4.18), FFN^2 has already been obtained as given by equation (4.19). By simply adding t subscripts, one obtains

$$
\begin{aligned}
FFN^2 &= 4.23365\,{m_{t1}}^2 + 10.5192\,{m_{t2}}^2 + 3.89636\,{m_{t3}}^2 + 15.8664\,m_{t3}\,MX_{t1} \\
&+ 233.551\,{MX_{t1}}^2 + 47.5989\,m_{t3}\,MX_{t2} - 166.652\,MX_{t1}\,MX_{t2} + 855.069\,{MX_{t2}}^2 \\
&- 155.855\,m_{t3}\,MX_{t3} - 317.329\,MX_{t1}\,MX_{t3} - 951.979\,MX_{t2}\,MX_{t3} \\
&+ 1558.55\,{MX_{t3}}^2 + 2.33165\,m_{t3}\,MY_{t1} - 6.24854\times10^{-16}\,MX_{t1}MY_{t1} \\
&+ 64.4285\,MX_{t2}\,MY_{t1} - 46.633\,MX_{t3}\,MY_{t1} + 233.551\,{MY_{t1}}^2 - 3.49746\,m_{t3}\,MY_{t2} \\
&+ 160.977\,MX_{t1}\,MY_{t2} - 44.7223\,MX_{t2}\,MY_{t2} + 69.9492\,MX_{t3}\,MY_{t2} \\
&- 324.687\,MY_{t1}\,MY_{t2} + 690.797\,{MY_{t2}}^2 + 8.41721\times10^{-9}\,m_{t3}\,MY_{t3} \\
&- 221.142\,MX_{t1}\,MY_{t3} - 71.3235\,MX_{t2}\,MY_{t3} - 1.40076\times10^{-9}\,MX_{t3}\,MY_{t3} \\
&- 516.481\,MY_{t1}\,MY_{t3} - 1228.9\,MY_{t2}\,MY_{t3} + 1376.23\,{MY_{t3}}^2 - 2.01926\,m_{t3}\,MZ_{t2} \\
&+ 0.000569408\,MX_{t1}\,MZ_{t2} - 55.7962\,MX_{t2}\,MZ_{t2} + 40.3852\,MX_{t3}\,MZ_{t2} \\
&- 404.523\,MY_{t1}\,MZ_{t2} + 281.188\,MY_{t2}\,MZ_{t2} + 447.285\,MY_{t3}\,MZ_{t2} + 175.163\,{MZ_{t2}}^2 \\
&+ 3.06361\times10^{-9}\,m_{t3}\,MZ_{t3} - 80.4891\,MX_{t1}\,MZ_{t3} - 25.9596\,MX_{t2}\,MZ_{t3} \\
&- 5.09843\times10^{-10}\,MX_{t3}\,MZ_{t3} - 187.984\,MY_{t1}\,MZ_{t3} - 447.283\,MY_{t2}\,MZ_{t3} \\
&+ 1001.81\,MY_{t3}\,MZ_{t3} + 162.798\,MZ_{t2}\,MZ_{t3} + 182.315\,{MZ_{t3}}^2 + m_{t1}(8.10757\,m_{t2} \\
&+ 2.47969\,m_{t3} - 0.000151995\,MX_{t1} - 21.1041\,MX_{t2} - 49.5939\,MX_{t3} \\
&+ 0.000178817\,MY_{t1} - 40.6809\,MY_{t2} + 55.8849\,MY_{t3} - 0.000177431\,MZ_{t2} \\
&+ 20.3404\,MZ_{t3}) + m_{t2}(3.03279\,m_{t3} + 51.8235\,MX_{t1} - 20.1642\,MX_{t2} \\
&- 60.6558\,MX_{t3} - 37.4675\,MY_{t1} + 4.94832\,MY_{t2} + 70.4083\,MY_{t3} + 32.4479\,MZ_{t2} \\
&+ 25.6265\,MZ_{t3})
\end{aligned}
\tag{4.26}
$$

Equation (4.27) can be obtained by substituting equation (4.25) into (4.26).

$$
\begin{aligned}
FFN^2 &= 3.70668 + 4.42202\,m_{b3} + 3.89636\,{m_{b3}}^2 - 88.4403\,MX_{b3} - 155.855\,m_{b3}\,MX_{b3} \\
&+ 1558.55\,{MX_{b3}}^2 + 52.9847\,MY_{b3} + 8.41721\times10^{-9}\,m_{b3}\,MY_{b3} \\
&- 1.40076\times10^{-9}\,MX_{b3}MY_{b3} + 1376.23\,{MY_{b3}}^2 + 19.2848\,MZ_{b3} \\
&+ 3.06361\times10^{-9}\,m_{b3}MZ_{b3} - 5.09843\times10^{-10}\,MX_{b3}MZ_{b3} + 1001.81\,MY_{b3}\,MZ_{b3} \\
&+ 182.315\,{MZ_{b3}}^2
\end{aligned}
\tag{4.27}^*
$$

In order to minimize *FFN*, the NMinimize function of Mathematica can be conveniently used. When this function is used with the constraint $m_{b3} > 0$, the inertial parameters of the counterweight can be obtained as:

$$
\{m_{b3} \to 0.53345, MX_{b3} \to 0.05504, MY_{b3} \to -0.0191, MZ_{b3} \to -0.000391\} \tag{4.28}
$$

The shaking force defined by the equation

$$F_s = \sqrt{\left(F_{x1,4} + F_{x3,4}\right)^2 + \left(F_{y1,4} + F_{y3,4}\right)^2 + \left(F_{z1,4} + F_{z3,4}\right)^2} \tag{4.29}$$

before balancing and after balancing is shown in Figure 4.23. The red curve indicates the shaking force after balancing and the blue curve indicates the shaking force before balancing.

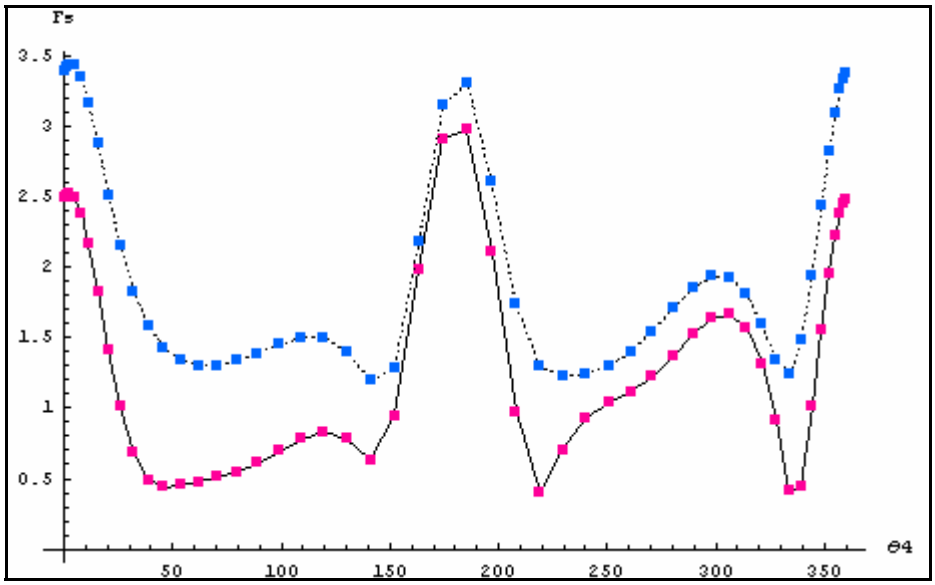

Figure 4.23 Shaking force versus θ_4 graph (one counterweight)

If two counterweights are added to link 1 and link 3 respectively, then the shaking force variations become as shown in Figure 4.24. As in Figure 4.23, the red curve indicates the shaking force after balancing and the blue curve indicates the shaking force before balancing. Clearly, the results are better than the previous case, as expected.

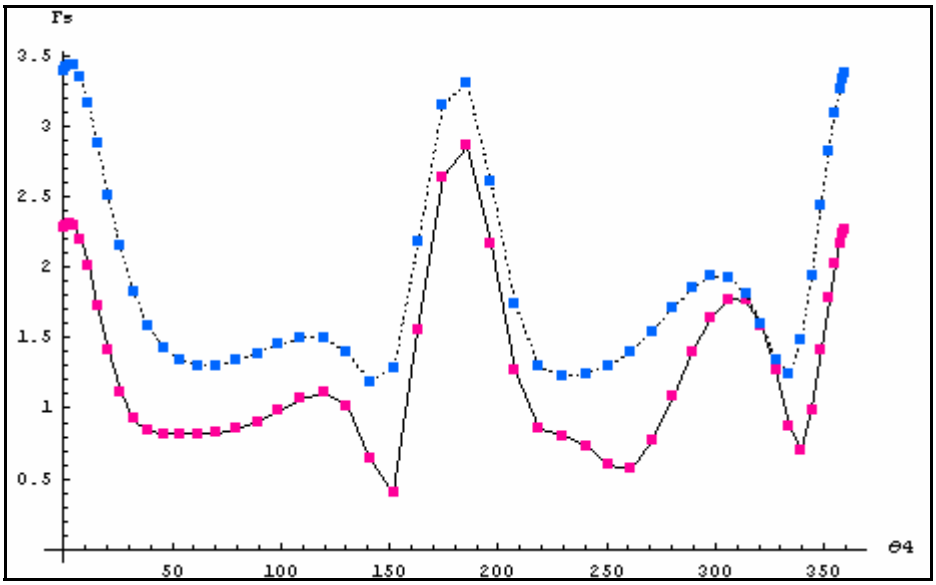

Figure 4.24 Shaking force versus θ_4 graph (two counterweights)

4.2 Analysis of a RPRRCR Mechanism

4.2.1 Position Analysis

Table 4.2 RPRRCR mechanism dimensions (link lengths and offsets are in meters)

	Link 1	Link 2	Link 3	Link 4	Link 5	Link 6
Link Lengths	a_{12}=0.1	a_{23}=0.05	a_{34}=0.4	a_{45}=0.3	a_{56}=0.25	a_{61}=0.32
Twist angles	α_{12}=30°	α_{23}=5°	α_{34}=35°	α_{45}=45°	α_{56}=60°	α_{61}=10°
Offsets	S_{11}=0	variable	S_{33}=0.05	S_{44}=0.25	variable	S_{66}=0.3
Angle of rotation	variable	θ_2=0°	variable	variable	variable	variable

RPRRCR is a group 2 mechanism, the schematic sketch of which is given in Figure 4.25. This mechanism is same as the mechanism in page 292 of Duffy [7]. The dimensions are given in Table 4.2. θ_6 is taken as the input variable. The position analysis of the mechanism has been performed for $0 \leq \theta_6 \leq 2\pi$. All graphs of the position analysis are shown in Figure 4.26-4.31. It is clear that the input link does not make a full rotation because there is no solution for the unknown position variables when $125° \leq \theta_6 \leq 155°$.

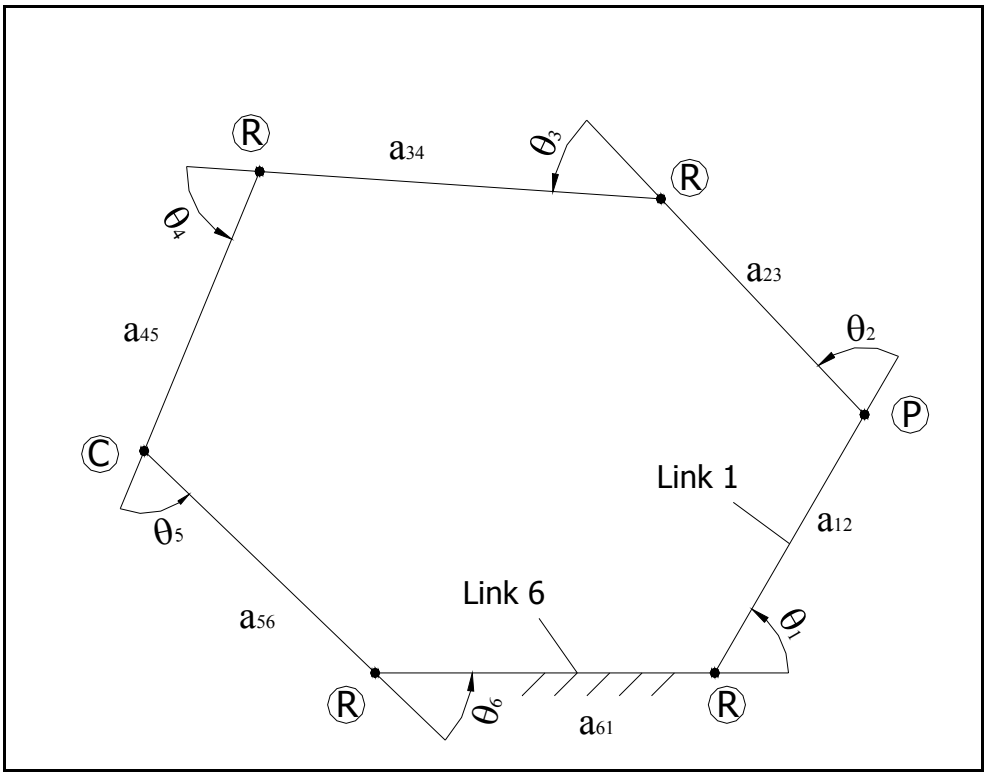

Figure 4.25 RPRRCR mechanism

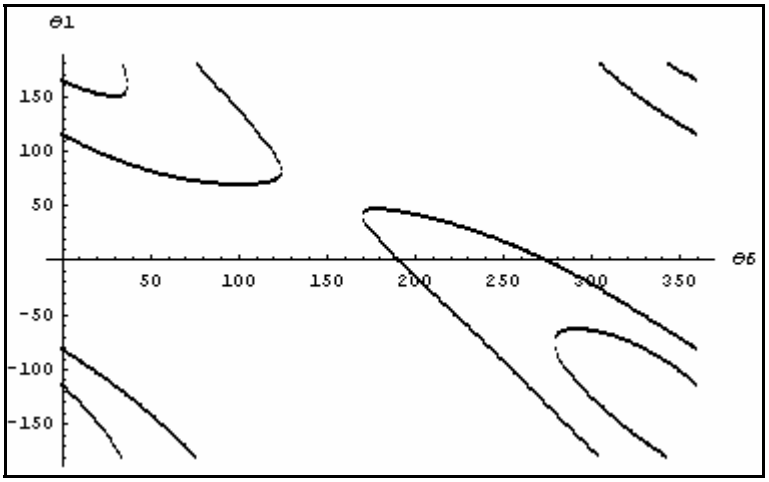

Figure 4.26 θ_1 versus θ_6 graph

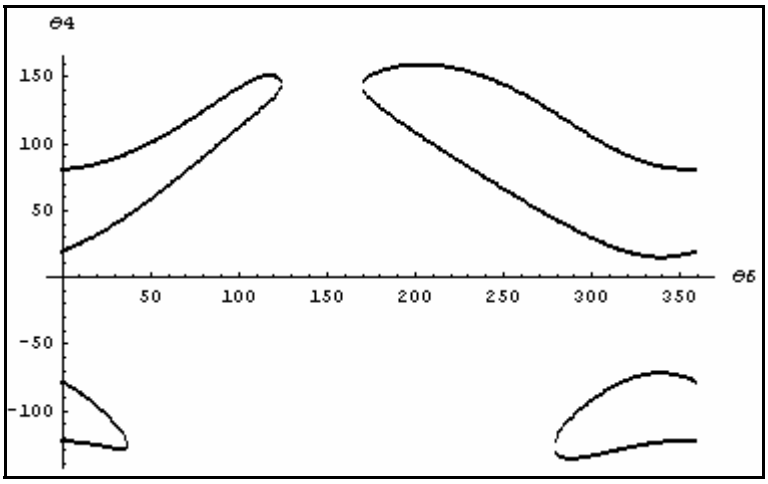

Figure 4.27 θ_4 versus θ_6 graph

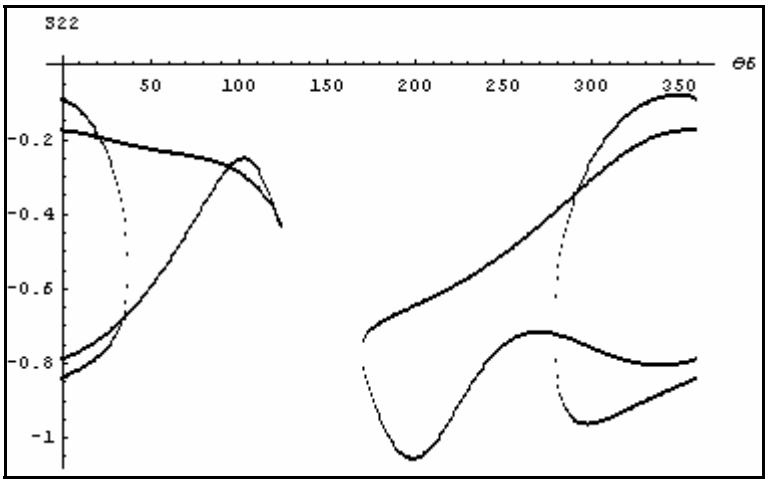

Figure 4.28 S_{22} versus θ_6 graph

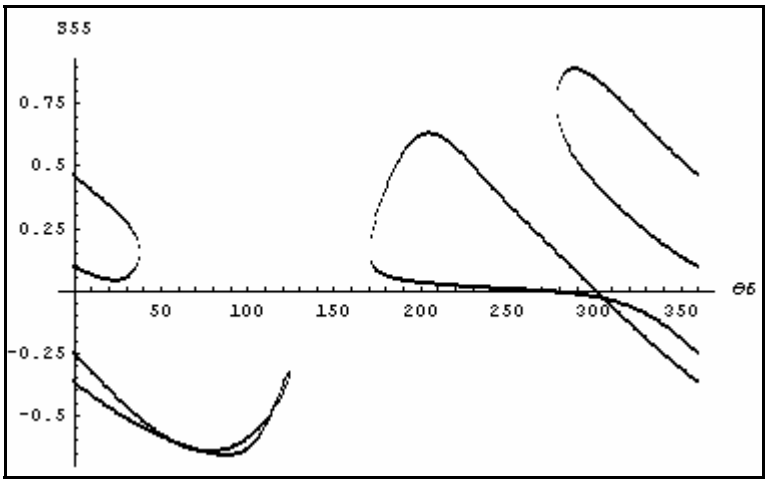

Figure 4.29 S_{55} versus θ_6 graph

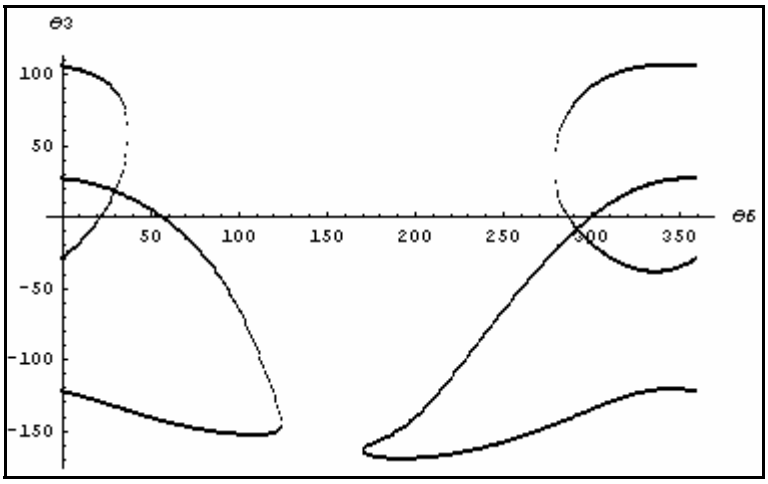

Figure 4.30 θ_3 versus θ_6 graph

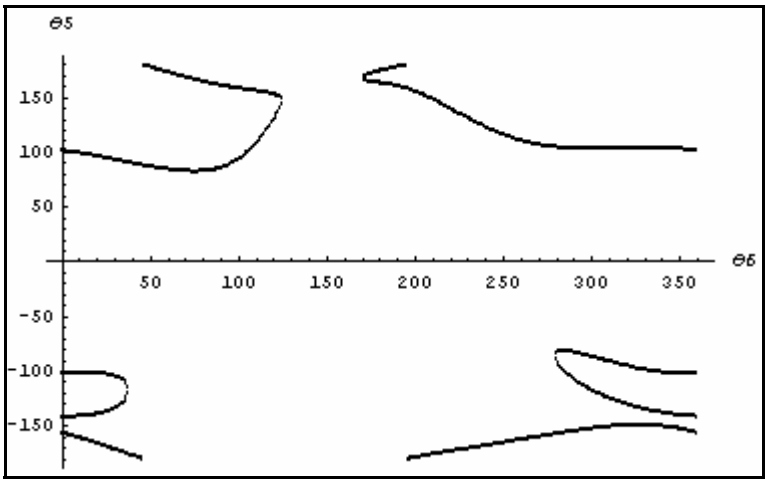

Figure 4.31 θ_5 versus θ_6 graph

4.4.2 Closure Identification

Closure identification has three steps. In the first step, the developed package displays all unknown joint variable plots on the screen. In the second step, the package asks the user to select a convenient joint variable plot on which the closures of the mechanism can be easily identified. After performing many case studies, it has been observed that the graphs of the rotational joint variables are always more convenient than the graphs of the translational joint variables. Therefore, the user is advised to select one graph of the rotational joint variable. The package then asks the user to specify a value for the joint variable that is displayed in order to make this graph continuous in the vertical direction. The graph shown in Figure 4.26 is not continuous in the vertical direction. If this plot is

selected for the second step, the user should enter nearly 50° to make the graph continuous. On the other hand, the graph shown in Figure 4.27 is continuous in the vertical direction. If this graph is selected for the second step, the user should enter 180° meaning that there is no change. After these inputs are given to the package, the package plots all graphs with sets. In the third step, the user specifies, the sets, which make a closure by using *Joinclo* function of the package.

Now, let's apply these steps to a RPRRCR mechanism. All plots are shown in Figures 4.26-4.31. The graph in Figure 4.27 is selected for the second step. Angle is specified as 180 because graph 2 (i.e. Figure 4.27) is already continuous in the vertical direction. Then the package plots all graphs shown in Figures 4.32-4.37.

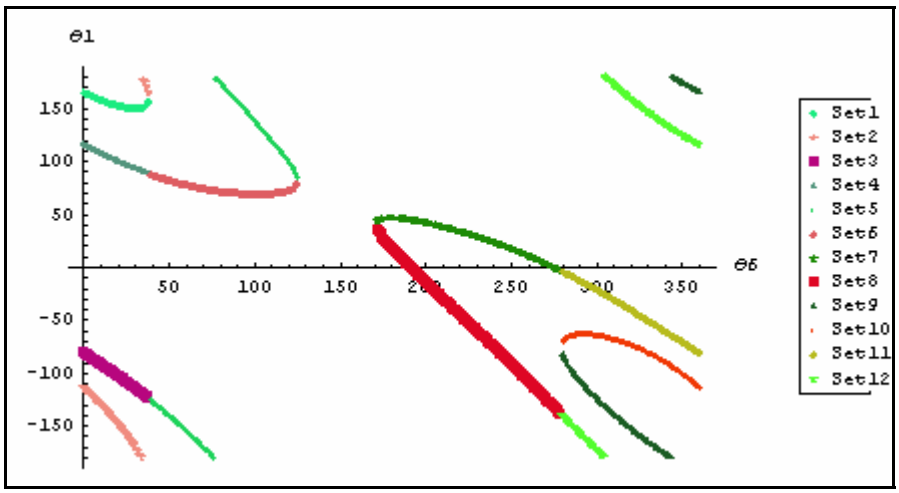

Figure 4.32 θ_1 versus θ_6 graph with sets

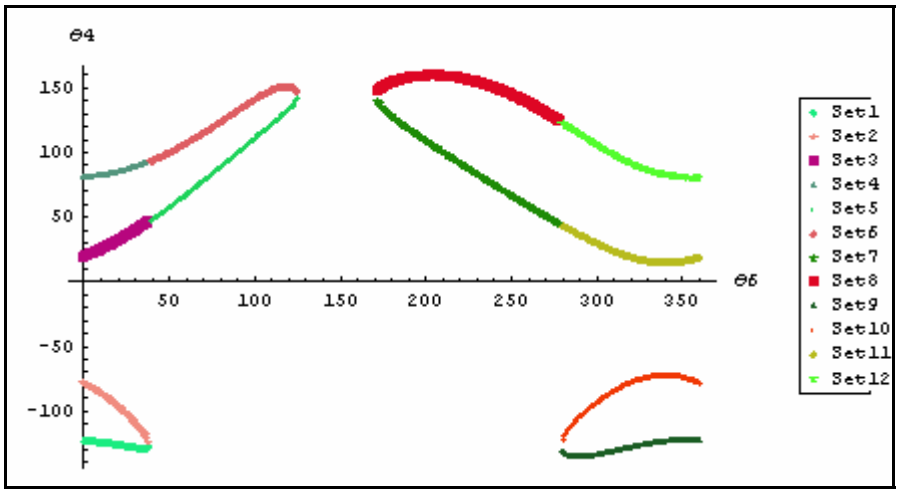

Figure 4.33 θ_4 versus θ_6 graph with sets

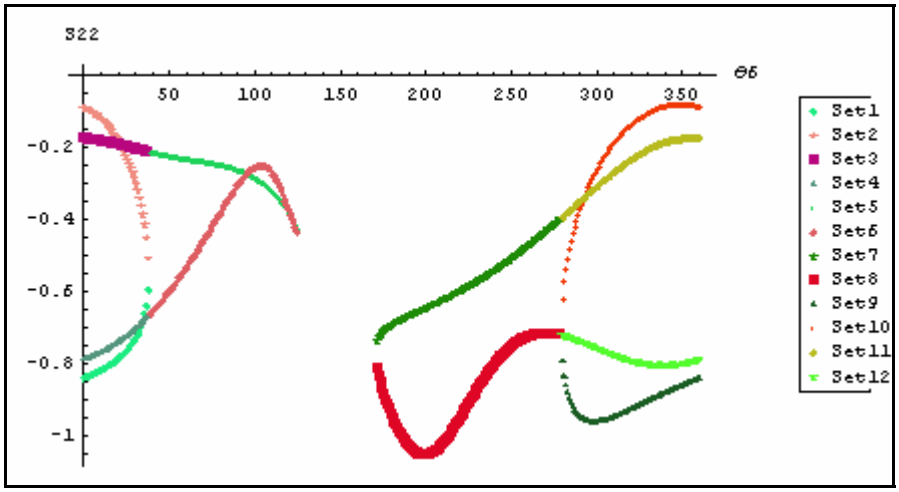

Figure 4.34 S_{22} versus θ_6 graph with sets

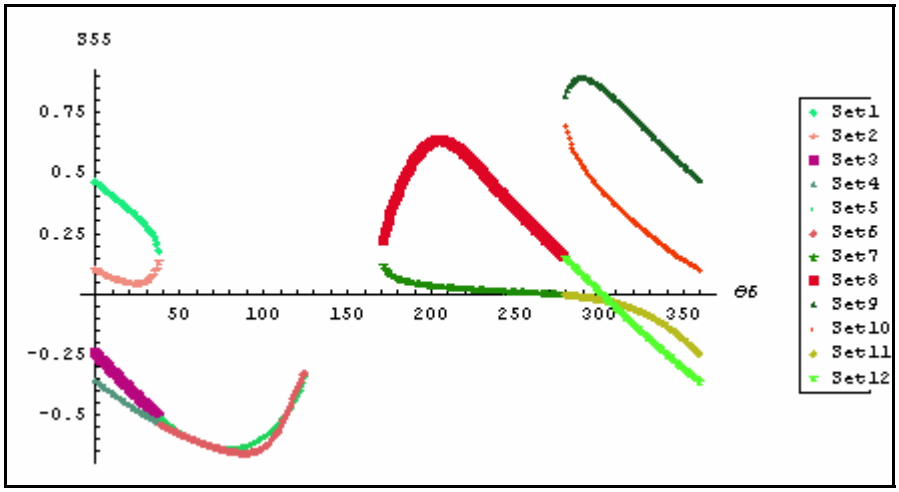

Figure 4.35 S_{55} versus θ_6 graph with sets

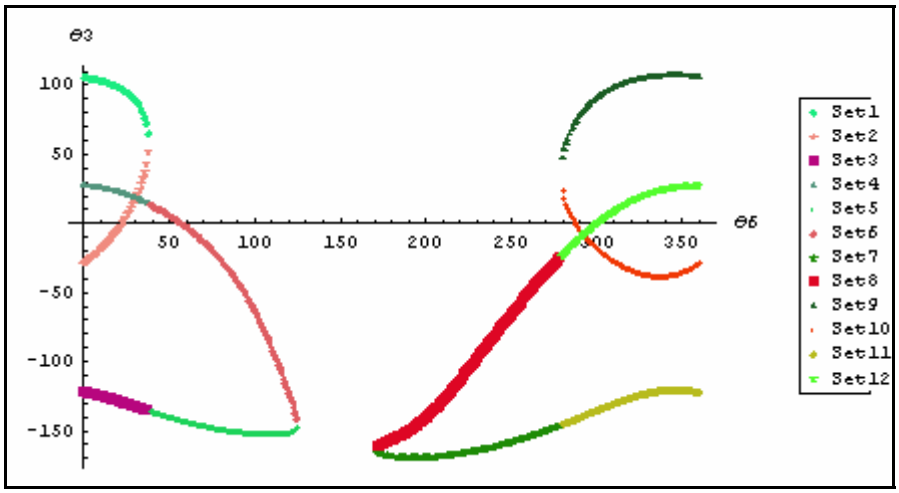

Figure 4.36 θ_4 versus θ_6 graph with sets

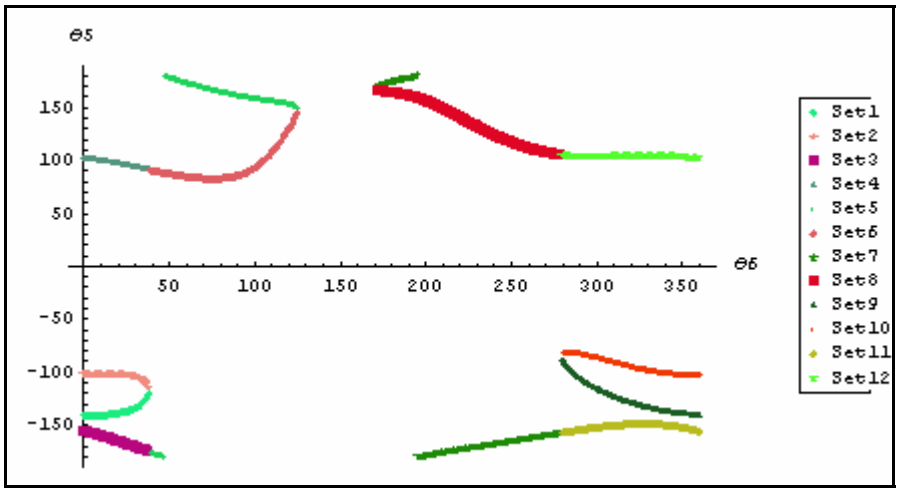

Figure 4.37 θ_5 versus θ_6 graph with sets

As seen in Figures 4.32-4.37, there are 12 sets for the entire position variables. Each set has a different color and point type to be distinguished. Sometimes it may be difficult to distinguish the sets because the package may generate nearly the same color and point type for different sets. In this case, the same colors are distinguished by set numbers. The set number increases from left below to right above in the selected graph for the second step. This is illustrated in Figure 4.38. Set1 and Set12 in the figure have nearly same green color. But Set1 is at the left below of the figure when Set12 is at the right above of the figure.

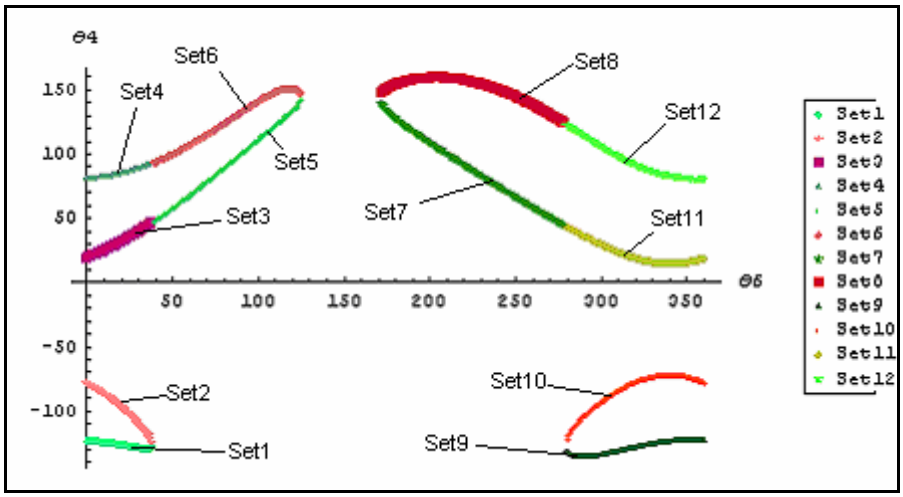

Figure 4.38 The order of sets on the graph

It can easily be seen that (Set1, Set9), (Set2, Set10), (Set3, Set5, Set7, Set11) and (Set4, Set6, Set8, Set12) make four different closures. The user writes *Joinclo[{{1,9},{2,10},{3,5,7,11},{4,6,8,12}}]* in mathematica . Then the package plots all graphs shown in Figure 4.39-4.44.

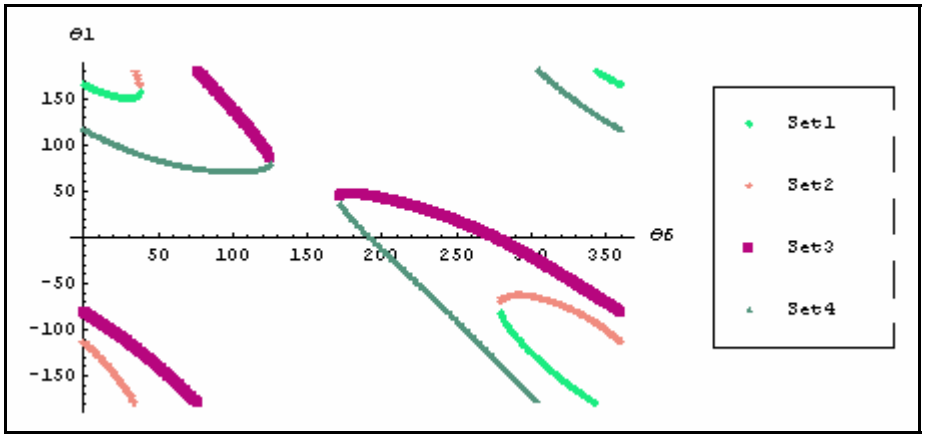

Figure 4.39 θ_1 versus θ_6 graph with closures (Set1 means closure1)

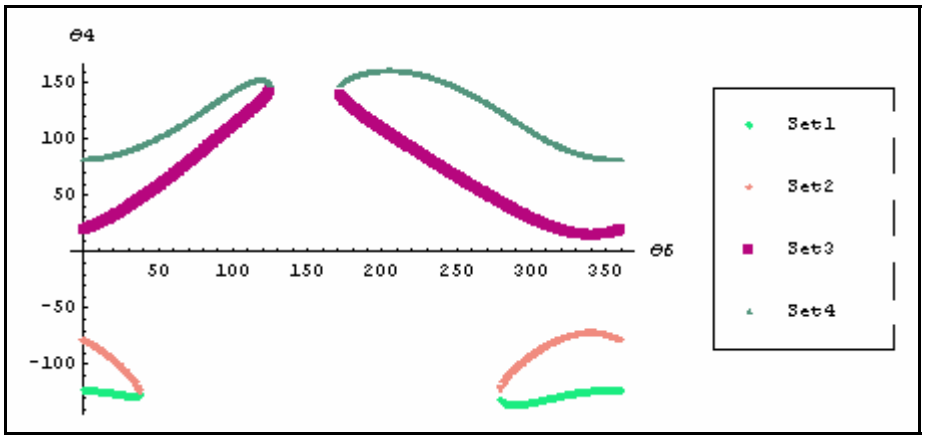

Figure 4.40 θ_4 versus θ_6 graph with closures

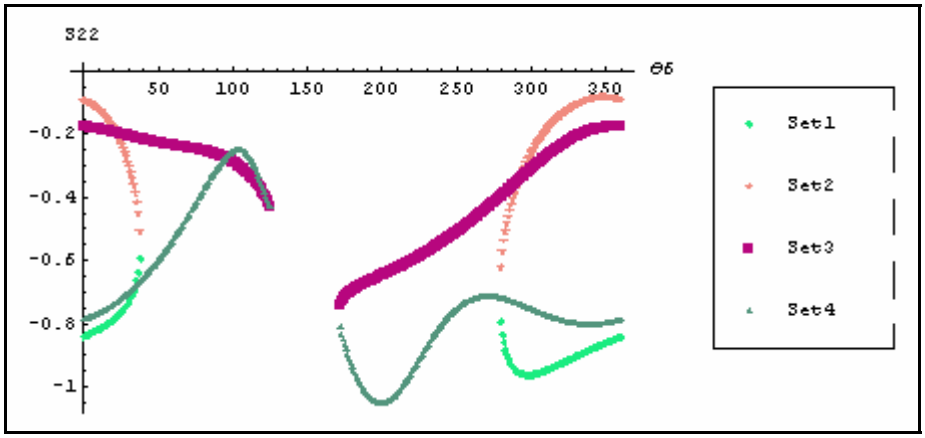

Figure 4.41 S_{22} versus θ_6 graph with closures

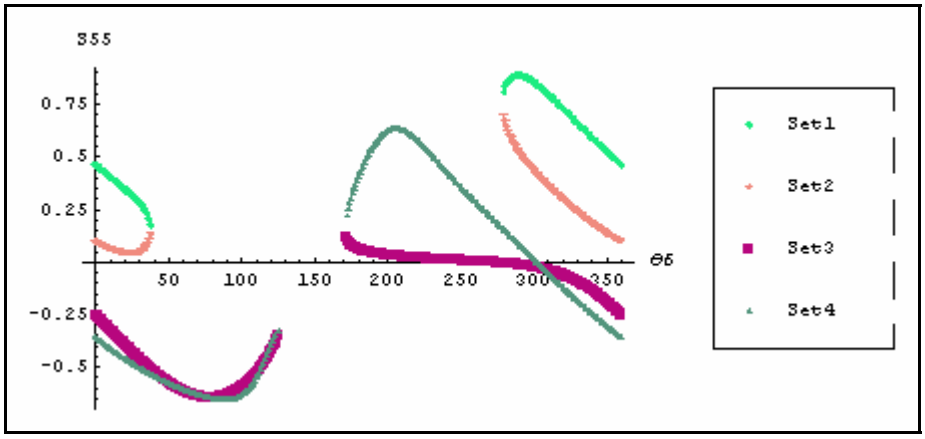

Figure 4.42 S_{55} versus θ_6 graph with closures

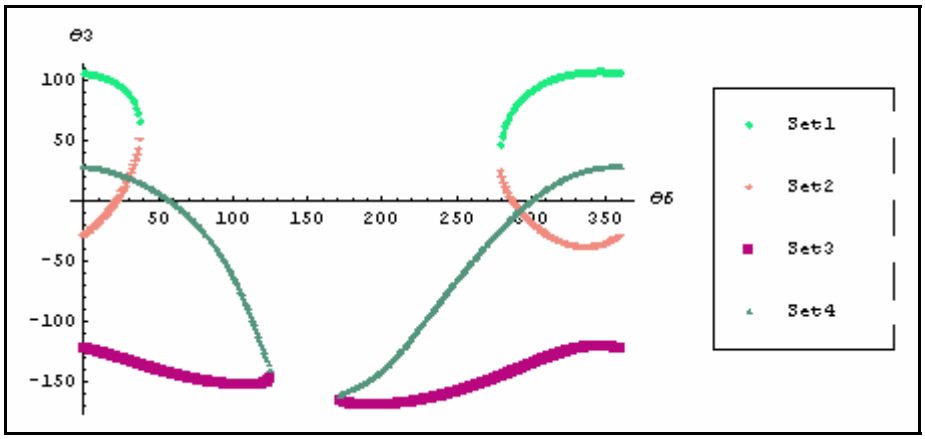

Figure 4.43 θ_3 versus θ_6 graph with closures

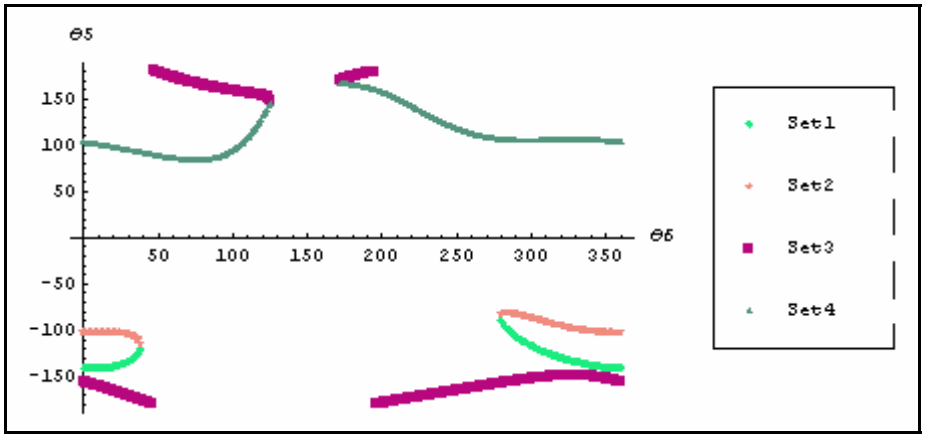

Figure 4.44 θ_5 versus θ_6 graph with closures

In figures 4.39-4.44, each set refers to a closure. The velocity, the acceleration or the dynamic analysis can be performed on any desired closure. However, one should be careful whether the input link can make a full cycle on the desired closure or not. If not, one should pay attention to the range in which the mechanism is running. This is important because the time range in the dynamic analysis should be selected conveniently for the desired closure.

4.3 Analysis of a RRRRCR Mechanism

This mechanism belongs to group (3) because it has only one sliding-joint. The schematic drawing of the mechanism is shown in the Figure 4.45. The

dimensions of the mechanism are given in the Table 4.3. This mechanism is similar to the mechanism in page 352 of Duffy [7].

Table 4.3 RRRRCR mechanism dimensions (link lengths and offsets in meters)

	Link 1	Link 2	Link 3	Link 4	Link 5	Link 6
Link lengths	a_{12}=0.2	a_{23}=0	A_{34}=0.8	a_{45}=0.2	a_{56}=0.2	a_{61}=0.3
Twist angles	α_{12}=90°	α_{23}=90°	α_{34}=90°	α_{45}=90°	α_{56}=90°	α_{61}=90°
Offsets	S_{11}=0.8	S_{22}=0.3	S_{33}=0	S_{44}=0	variable	S_{66}=0.2

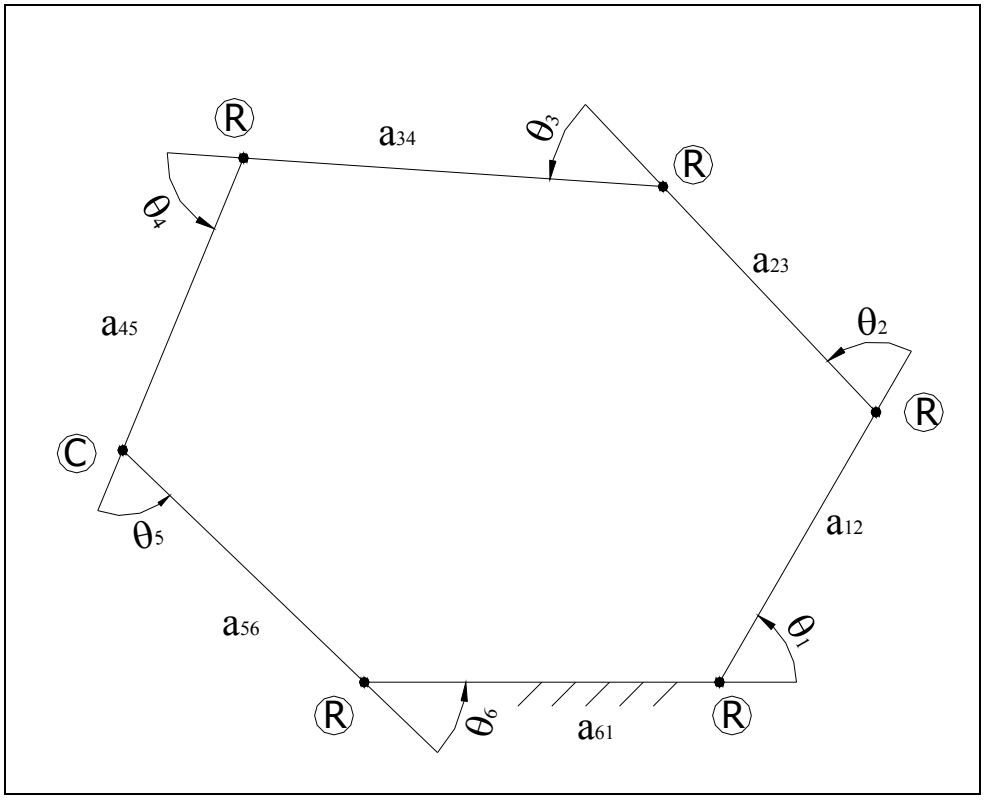

Figure 4.45 RRRRCR mechanism

Let's take θ_6 as the input variable of the mechanism and perform position analysis for $0 \le \theta_6 \le 360$.

For the position analysis, different pairs of θ_i's have been considered in the first step of the algorithm that yields the 4 nonlinear equations to be solved. The package has determined that if θ_1 and θ_4 are selected, the minimum

execution time is obtained. The other possible selections and their execution times are shown in Table 4.4. These data are obtained for the input angle $\theta_6 = 21°$.

Table 4.4 Possible selections in the first step of the algorithm and their execution times

Eliminated joint variables	Execution time for complete position analysis at $\theta_6 = 21°$
θ_1 , θ_4	12.979 second
θ_3 , θ_5	19.077 second
θ_4 , θ_5	19.088 second

As expected, if the joint variables to be eliminated are changed, equations required to be solved are also change. The following equations are obtained by using the developed package for two possible selections.

The equations obtained when θ_1 and θ_4 are selected are as follows:

ZZ law:

$$-Z_{23} + Z_{56} = 0 \tag{4.30}$$

$$\Rightarrow -\sin(\theta_2)\sin(\theta_3) + \sin(\theta_5)\sin(\theta_6) = 0 \tag{4.31}$$

Dual of ZZ law:

$$-Z_{023} + Z_{056} = 0 \tag{4.32}$$

$$\begin{aligned}\Rightarrow\ & 0.2\cos(\theta_3) + \cos(\theta_2)(-0.8 - 0.3\sin(\theta_3)) + 0.2\cos(\theta_6)(\sin(\theta_5) + 1) \\ & + \cos(\theta_5)(0.3 + 0.2\cos(\theta_6) + S_{55}\sin(\theta_6)) = 0\end{aligned} \tag{4.33}$$

For h=1, loop closure equation $r_{1,z}$:

$$\begin{aligned}& r_{1,z} = a_{23}R_2 + a_{34}R_{23} + a_{56}X_6 + a_{45}X_{56} + S_{11} + S_{22}\cos(\alpha_{12}) \\ & S_{33}Z_2 + S_{55}Z_6 + S_{66}\cos(\alpha_{61}) = 0\end{aligned} \tag{4.34}$$

$$\Rightarrow 0.8 - S_{55}\cos(\theta_6) + 0.8\cos(\theta_3)\sin(\theta_2) + 0.2\sin(\theta_6)(1 + \cos(\theta_5)) = 0 \tag{4.35}$$

For h=4, loop closure equation $r_{4,z}$:

$$r_{4,z} = a_{12}X_{23} + a_{23}X_3 + a_{56}R_5 + a_{61}R_{56} + S_{11}Z_{56} + S_{22}Z_3 + S_{33}\cos(\alpha_{34}) + S_{44} + S_{55}\cos(\alpha_{45}) + S_{66}Z_5 = 0 \tag{4.36}$$

$$\Rightarrow -0.3\cos(\theta_3) - 0.2\cos(\theta_5) + 0.2\cos(\theta_2)\sin(\theta_3) + \sin(\theta_5)(0.2 + 0.3\cos(\theta_6) + 0.8\sin(\theta_6)) = 0 \tag{4.37}$$

Equations (4.31), (4.33), (4.35) and (4.37) can be obtained by substituting the dimensions of the mechanism and the definitions of the DL terms into equations (4.30), (4.32), (4.34) and (4.36).

The equations obtained when θ_3 and θ_5 are selected are as follows:

ZZ law:

$$-Z_4 + Z_{612} = 0 \tag{4.38}$$

$$\Rightarrow \cos(\theta_4) + \cos(\theta_2)\cos(\theta_6) + \cos(\theta_1)\sin(\theta_2)\sin(\theta_6) = 0 \tag{4.39}$$

Dual of ZZ law:

$$-Z_{04} + Z_{0612} = 0 \tag{4.40}$$

$$\Rightarrow \cos(\theta_6)\sin(\theta_2)(-0.3 + 0.2\cos(\theta_1) - 0.3\sin(\theta_1)) + \cos(\theta_2)\sin(\theta_6)(-0.2 + 0.3\cos(\theta_1)) + \sin(\theta_1)(\sin(\theta_2)(-0.2 - 0.8\sin(\theta_6)) - 0.2\cos(\theta_2)\sin(\theta_6)) = 0 \tag{4.41}$$

For h=3, loop closure equation $r_{3,z}$:

$$r_{3,z} = a_{12}X_2 + a_{45}R_4 + a_{56}X_{612} + a_{61}X_{12} + S_{11}Z_2 + S_{22}\cos(\alpha_{23}) + S_{33} + S_{44}\cos(\alpha_{34}) + S_{55}Z_4 + S_{66}Z_{12} = 0 \tag{4.42}$$

$$\Rightarrow -S_{55}\cos(\theta_4) + \sin(\theta_2)(0.2 + \cos(\theta_1)(0.3 + 0.2\cos(\theta_6)) + 0.2\sin(\theta_1)) + 0.2\sin(\theta_4) + \cos(\theta_2)(-0.8 - 0.2\sin(\theta_6)) = 0 \tag{4.43}$$

For h=5, loop closure equation $r_{5,z}$:

$$r_{5,z} = a_{12}R_{61} + a_{23}R_{612} + a_{34}X_4 + a_{61}R_6 + S_{11}Z_6 + S_{22}Z_{61} + S_{33}Z_{612} + S_{44}\cos(\alpha_{45}) + S_{55} + S_{66}\cos(\alpha_{56}) = 0 \quad (4.44)$$

$$\Rightarrow S_{55} - 0.8\cos(\theta_6) + 0.8\sin(\theta_4) + \sin(\theta_6)(0.3 + 0.2\cos(\theta_1) + 0.3\sin(\theta_1)) = 0 \quad (4.45)$$

If the dimensions of the mechanism and definitions of the DL terms are substituted into equations (4.38), (4.40), (4.42) and (4.44), one can obtain equations (4.39), (4.41), (4.43) and (4.45).

If the equations of two possible selection are compared with each other, it is seen that the equations obtained by eliminating the variables θ_3 and θ_5 contain more trigonometrical expressions than the equations obtained by eliminating variables θ_1 and θ_4. This may be the reason for the difference in the execution time.

The graphs of the unknown joint variables versus the input joint variable are shown in Figures 4.46- 4.51. Closure identification of this mechanism is a very difficult problem as seen from the graphs. At the same time, it is very clear that the input link does not make a full cycle.

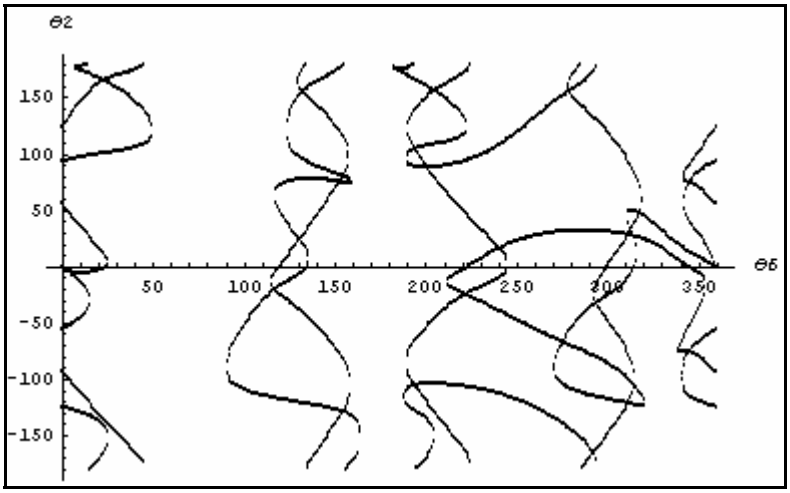

Figure 4.46 θ_2 versus θ_6 graph

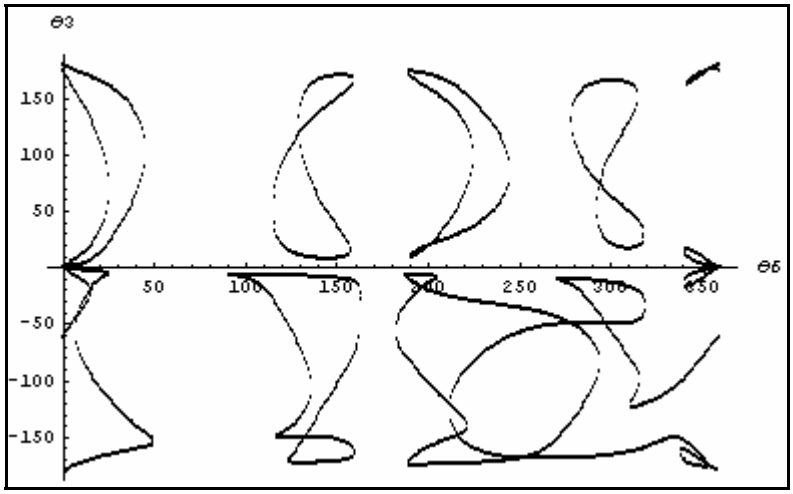

Figure 4.47 θ_3 versus θ_6 graph

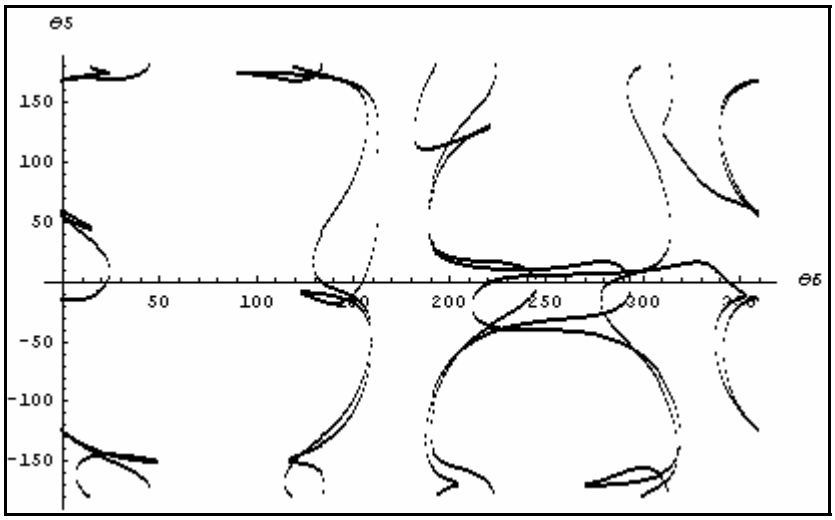

Figure 4.48 θ_5 versus θ_6 graph

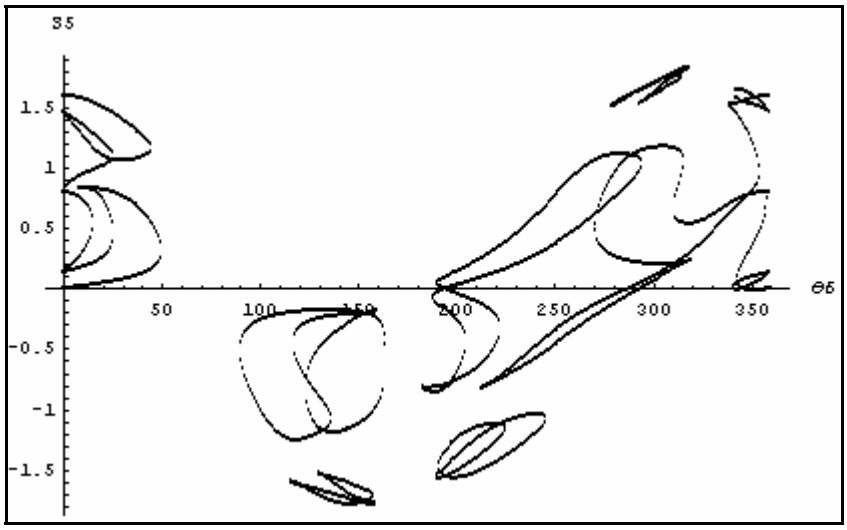

Figure 4.49 S_5 versus θ_6 graph

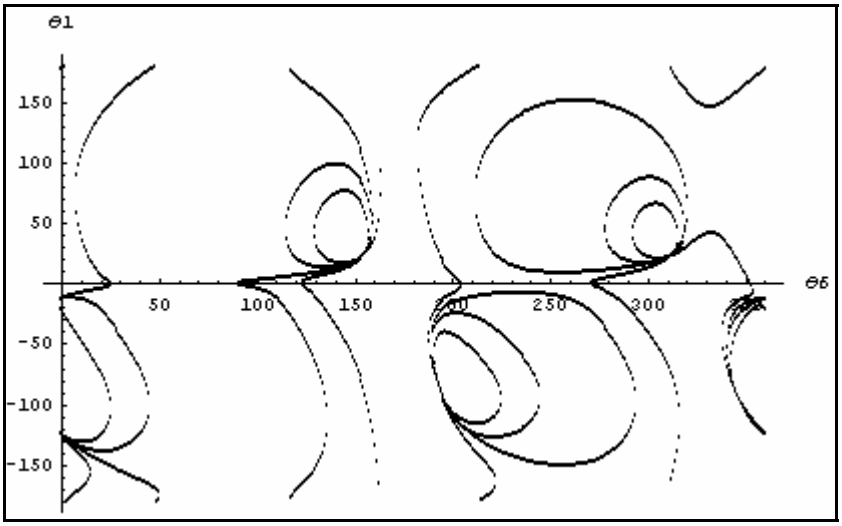

Figure 4.50 θ_1 versus θ_6 graph

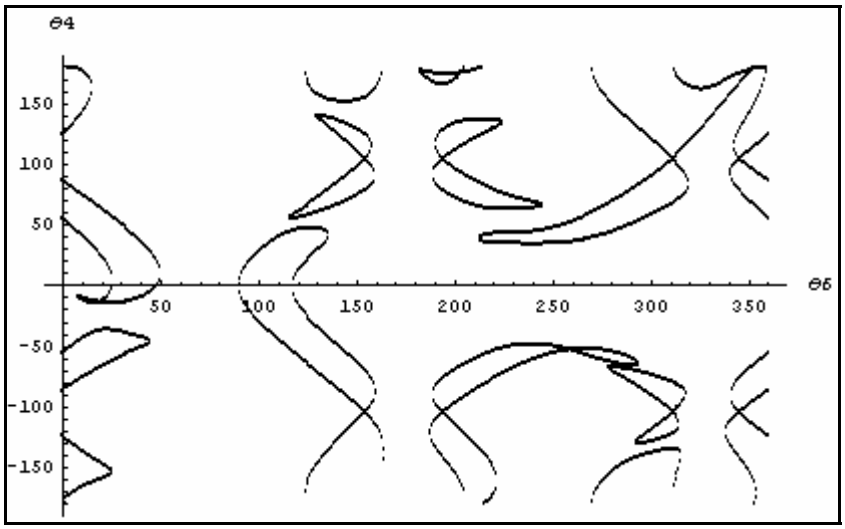

Figure 4.51 θ_4 versus θ_6 graph

Numerical values of the joint variables can also be obtained from the package. When θ_6=100°, for instance, the numerical values of the position variables are given in equation (4.46).

$\theta_1 = 2.862°$, $\theta_1 = -4.069°$

$\theta_2 = -108.379°$, $\theta_2 = -53.106°$

$\theta_3 = -5.913°$, $\theta_3 = -8.811°$

$\theta_4 = -28.5965°$, $\theta_4 = 27.1441°$

$\theta_5 = 174.303°$, $\theta_5 = 172.854°$

$S_{55} = -0.263$ meters, $S_{55} = -0.974$ meters. (4.46)

4.4 Analysis of a 7-R Mechanism

4.4.1 Kinematic Analysis

Table 4.5 7-R mechanism dimensions (link lengths and offsets in meters)

	Link 1	Link 2	Link 3	Link 4	Link 5	Link 6	Link 7
Link lengths	0.10	0.18	0.22	0.30	0.30	0.22	0.18
Twist angles	35°	80°	93°	120°	120°	93°	80°
Offsets	0.20	0.20	0.24	0.16	0.40	0.16	0.24

The 7-R mechanism, whose dimensions are given in Table 4.5, is the same mechanism that has been used in Chiou and Tsai [2]. Let's take Link1 as the input link and perform position analysis for $0 \leq \theta_1 \leq 2\pi$. The minimum execution time can be obtained when θ_2 and θ_5 are eliminated. The developed package spends nearly 320 seconds to solve for the complete position analysis for a given value of θ_1. A total of 120 points are used to find all joint variables in the full cycle. Therefore, full position analysis of this mechanism lasts nearly 10 hours. All graphs of the position variables are depicted in figure 4.52-4.57.

It should be noted that the mechanism has general dimensions (i.e., no zero link lengths or offsets and no twist angles which are 90° or 0°). It is expected that the execution time will decrease for a 7-R mechanism with special dimensions.

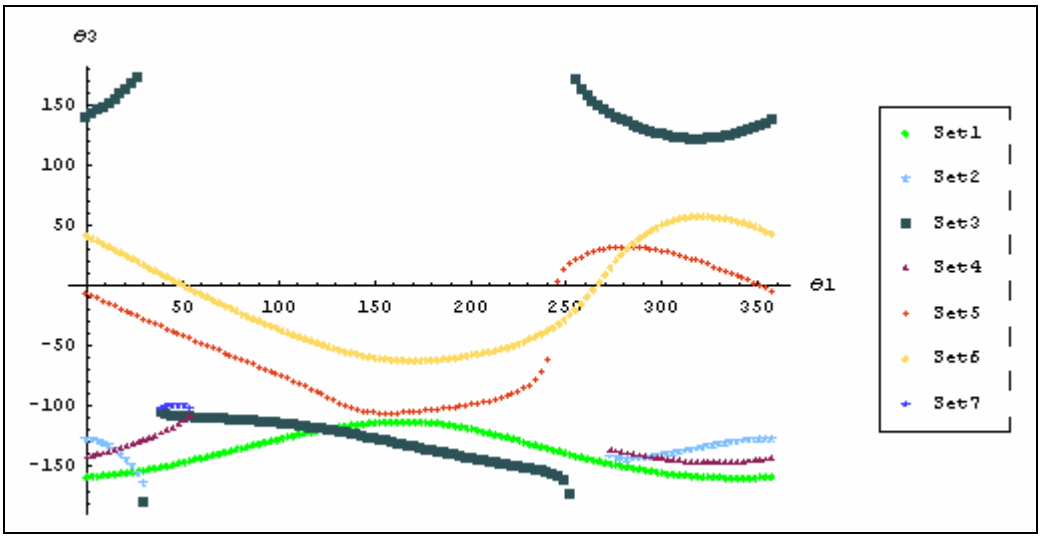

Figure 4.52 θ_3 versus θ_1 graph

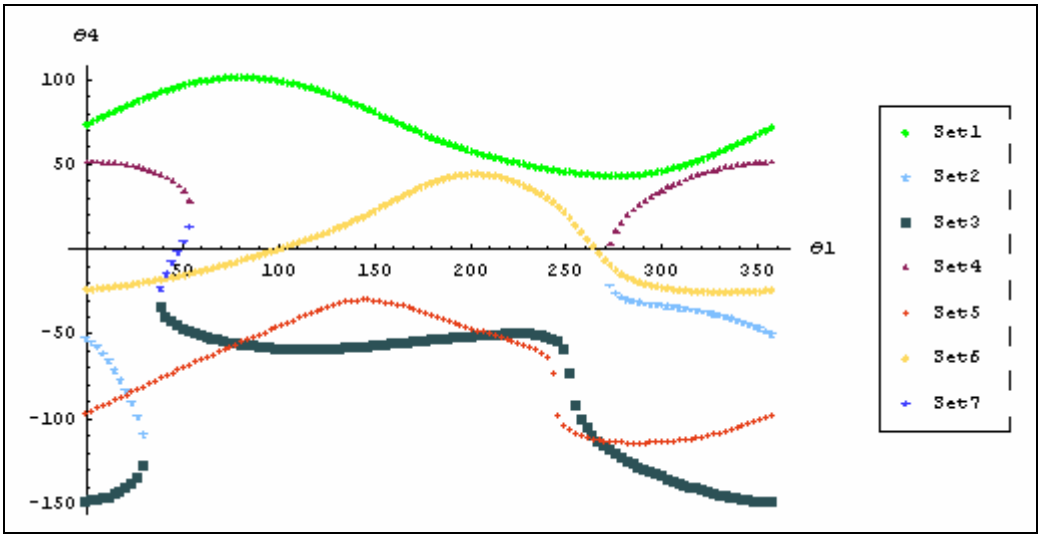

Figure 4.53 θ_4 versus θ_1 graph

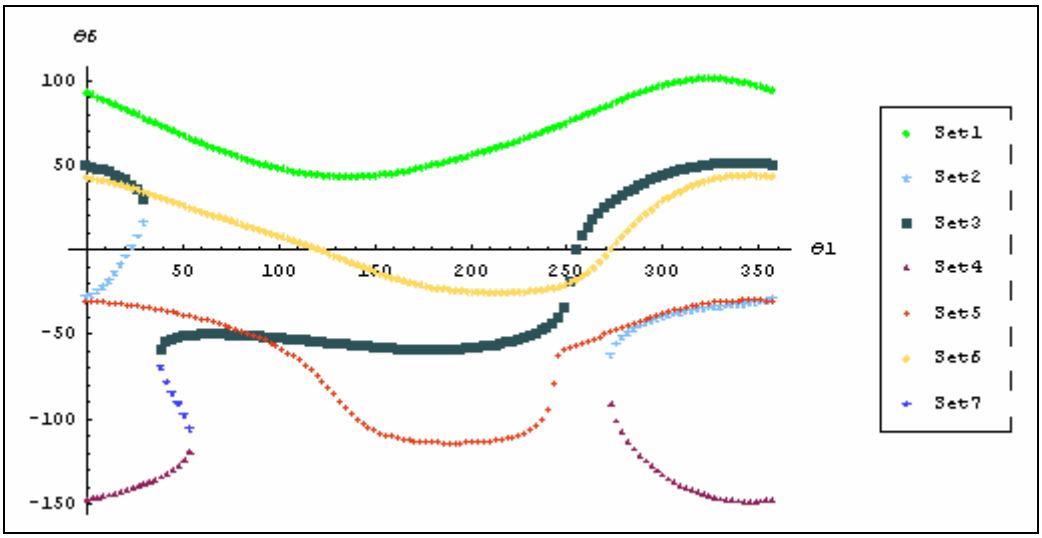

Figure 4.54 θ_6 versus θ_1 graph

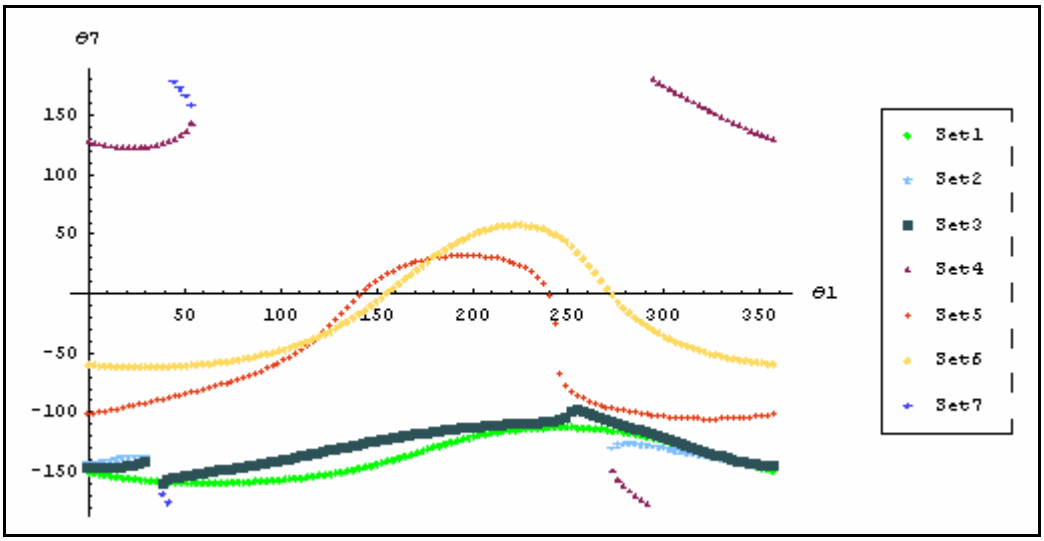

Figure 4.55 θ_7 versus θ_1 graph

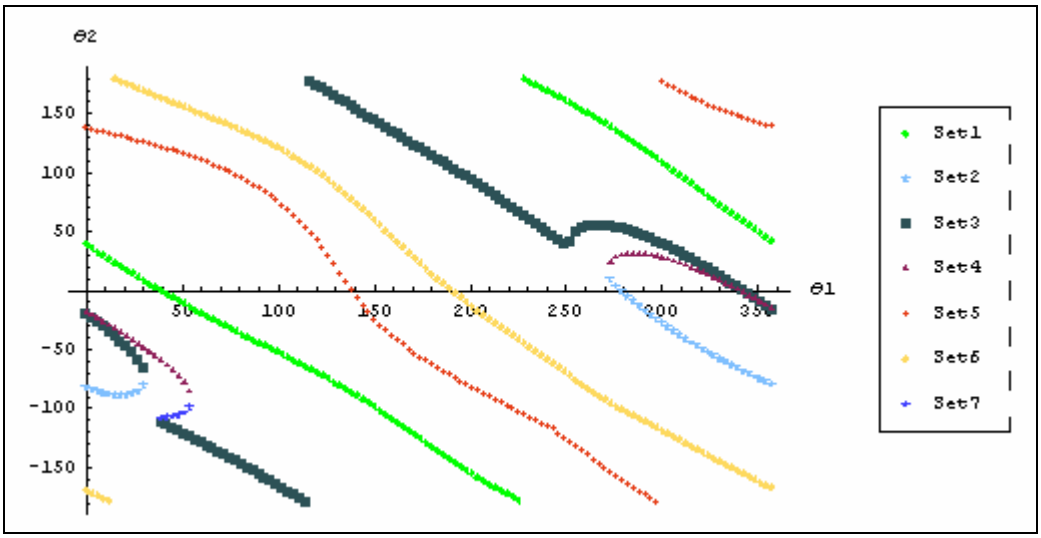

Figure 4.56 θ_2 versus θ_1 graph

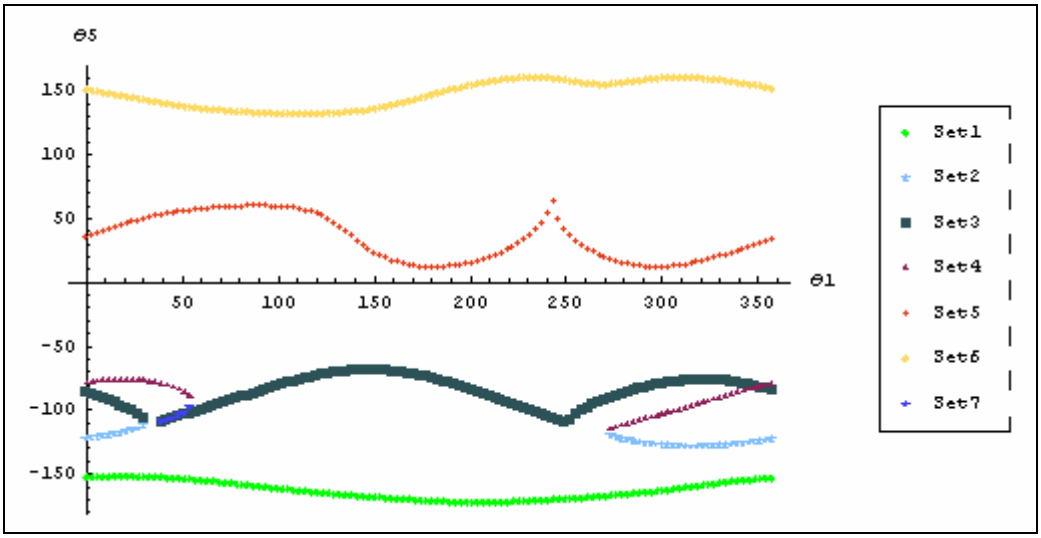

Figure 4.57 θ_5 versus θ_1 graph

4.4.2 Shaking Force Balancing of a 7-R mechanism

Consider closure 1 of a 7-R mechanism. If one takes into account only the shaking force in the X_7 (i.e. the first axis of the inertial frame) direction, FFN should be represented as:

$$FFN^2 = \int_R \left[(F_{x1,7} + F_{x6,7}) - (F_{x1,7} + F_{x6,7})_d \right]^2 dt$$

(4.47)

Here, the desired value of FFN, $(F_{x1,7} + F_{x6,7})_d$, is specified to be zero. The gravitational acceleration is neglected and the input motion is given by

$$\theta_1(t) = 20t \tag{4.48}$$

50 Gaussian Quadrature points have been used to find FFN^2.

One can obtain FFN^2 by taking $R = \{t : 0 \le t \le 0.1\pi\}$ and using the developed package. The result can be seen in Appendix B (see equation (B.10)).

Inertial parameters that affect *FFN* and the minimum value of FFN^2 can be obtained via the developed package as

$$\mathbf{I_f} = \begin{Bmatrix} m_2,\ m_3, m_4, m_5, m_6, MX_1, MX_2, MX_3, MX_4, MX_5, MX_6 \\ , MY_1, MY_2, MY_3, MY_4, MY_5, MY_6, MZ_1, MZ_2, MZ_3, MZ_4, MZ_5, MZ_6 \end{Bmatrix} \tag{4.49}$$

$$\begin{aligned} FFN_*^2 &= 1.13687\times10^{-12}c_1^2 + 5.68434\times10^{-12}c_1c_2 + 1.3074\times10^{-12}c_2^2 \\ &+1.31877\times10^{-11}c_1c_3 - 5.68434\times10^{-12}c_2c_3 - 2.95586\times10^{-12}c_3^2 \\ &-9.09495\times10^{-13}c_1c_4 - 1.36424\times10^{-12}c_2c_4 - 1.59162\times10^{-12}c_3c_4 \\ &-3.46745\times10^{-12}c_4^2 - 6.59384\times10^{-12}c_1c_5 - 5.11591\times10^{-12}c_2c_5 \\ &-6.82121\times10^{-12}c_4c_5 - 1.98952\times10^{-12}c_5^2 \end{aligned} \tag{4.50}$$

respectively. The optimal inertial parameters i.e., $\mathbf{I_f^*}$ of the mechanism are given in Appendix B. (see equation B.9)

The arbitrary constants c_1, c_2, c_3, c_4 and c_5 can be obtained in terms of m_2, m_3, m_4, m_5 and m_6 by using the first five elements of the $\mathbf{I_f^*}$ vector to yield

$$\begin{Bmatrix} c_1 \to 0.0360458\,m_2 + 0.301487\,m_3 + 0.459017\,m_4 + 0.771052\,m_5 + 1.18859\,m_6 \\ c_2 \to 0.757052\,m_2 + 0.454176\,m_3 - 0.363918\,m_4 - 0.337175\,m_5 + 0.133705\,m_6 \\ c_3 \to 0.346509\,m_2 - 0.0737685\,m_3 + 0.939717\,m_4 - 0.322969\,m_5 - 0.0977781\,m_6 \\ c_4 \to -0.563618\,m_2 + 0.645573\,m_3 + 0.123873\,m_4 - 0.539512\,m_5 + 0.0802759\,m_6 \\ c_5 \to 0.0890347\,m_2 + 0.623937\,m_3 + 0.219016\,m_4 + 0.622864\,m_5 - 0.530569\,m_6 \end{Bmatrix} \tag{4.51}$$

If c_1, c_2, c_3, c_4 and c_5 are substituted into the $\mathbf{I}_\mathbf{f}^*$ vector, all inertial parameters can be obtained in terms of m_2, m_3, m_4, m_5 and m_6. Therefore, the masses of the links may be arbitrarily selected by the user. For instance, assume that $m_2 = 0.5$, $m_3 = 0.6$, $m_4 = 0.5$, $m_5 = 0.4$ and $m_6 = 0.8$ (kg) are the selected values. Then, $\mathbf{I}_\mathbf{f}^*$ vector becomes

$$
\left\{\begin{array}{l}
m_2 \to 0.5 \\
m_3 \to 0.6 \\
m_4 \to 0.5 \\
m_5 \to 0.4 \\
m_6 \to 0.8 \\
MX_1 \to -0.279988 \\
MX_2 \to -0.413979 \\
MX_3 \to -0.373977 \\
MX_4 \to -0.359972 \\
MX_5 \to -0.239973 \\
MX_6 \to 0.0000214557
\end{array}\right\}
\left\{\begin{array}{l}
MY_1 \to 0.0922634 \\
MY_2 \to -0.180869 \\
MY_3 \to 0.371171 \\
MY_4 \to 0.0362792 \\
MY_5 \to -0.0371917 \\
MY_6 \to 0.0139036 \\
MZ_2 \to -0.367232 \\
MZ_3 \to -0.71618 \\
MZ_4 \to 0.120642 \\
MZ_5 \to -0.459536 \\
MZ_6 \to -0.170196
\end{array}\right\} \qquad (4.52)
$$

The inertial parameters that do not affect FFN, but affect the reaction force components can, for instance, be taken as

$$XX_2 = 0.34, YY_2 = 0.65, ZZ_2 = 0.41$$
$$XY_2 = -0.002, XZ_2 = -0.004, YZ_2 = -0.0014$$

$$XX_3 = 1.1, YY_3 = 1.1, ZZ_3 = 0.48$$
$$XY_3 = -0.003, XZ_3 = -0.005, YZ_3 = -0.0025$$

$$XX_4 = 0.1, YY_4 = 0.31, ZZ_4 = 0.29,$$
$$XY_4 = -0.004, XZ_4 = -0.003, YZ_4 = -0.05147$$

$$XX_5 = 0.55, YY_5 = 0.76, ZZ_5 = 0.53,$$
$$XY_5 = -0.002, XZ_5 = -0.006, YZ_5 = -0.006$$

$$XX_6 = 0.0813, YY_6 = 0.05, ZZ_6 = 0.07,$$
$$XY_6 = -0.0013, XZ_6 = 0.001, YZ_6 = 0.002 \quad (4.53)$$

so that all of the links are physically realizable.

Now, any component of the shaking force can be plotted. For instance, the X_7 components of the shaking force are shown in Figures 4.58 and 4.59.

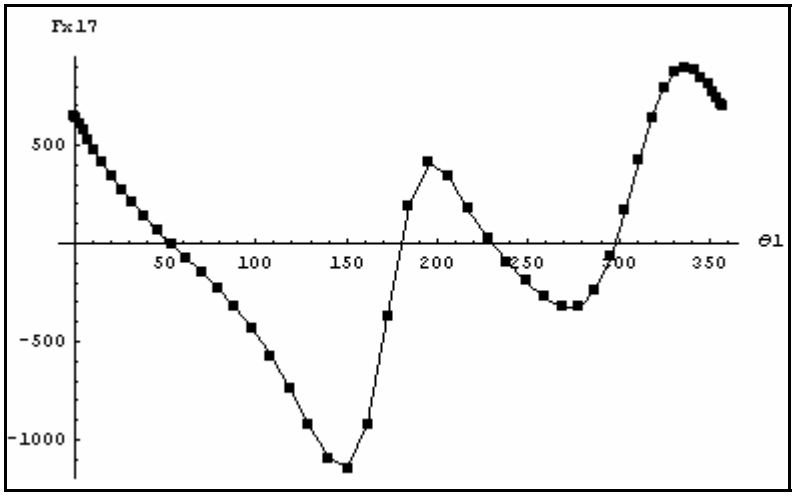

Figure 4.58 $F_{x\,1,7}$ versus θ_1 graph

From Figures 4.58, 4.59 and 4.60, it can be seen that the X_7 component of the shaking forces is fully balanced during the whole cycle because $F_{x\,1,7}$ and $F_{x\,6,7}$ have the same magnitude but opposite directions during the whole cycle.

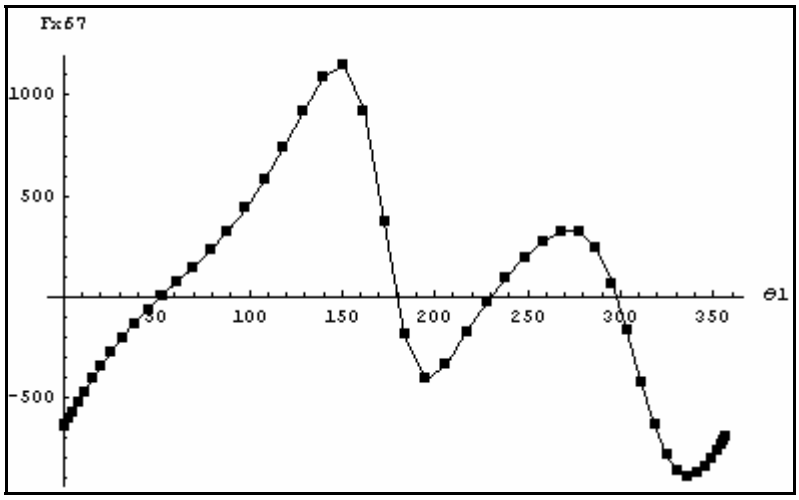

Figure 4.59 $F_{x\,6,7}$ versus θ_1 graph

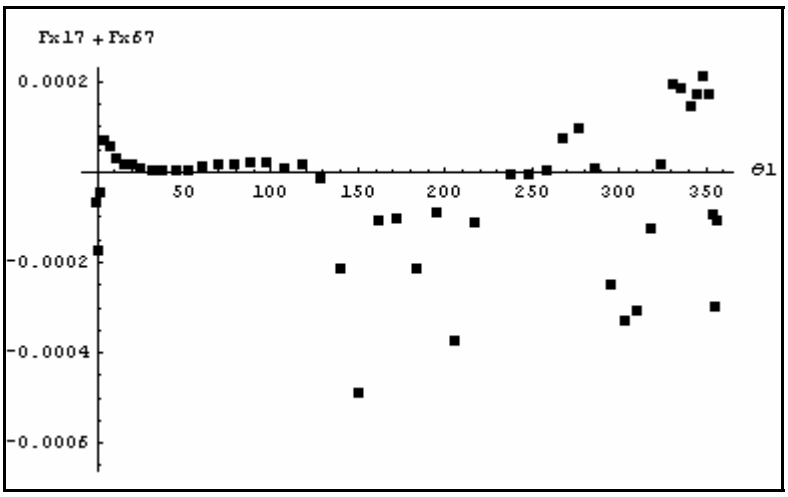

Figure 4.60 $F_{x\,6,7} + F_{x\,1,7}$ versus θ_1 graph

Note that the optimal inertial parameters that are found from the defined FFN^2 (to balance the X_7 component of the shaking forces only), lead to full balancing of the Y_7 and Z_7 components of the shaking forces during the whole cycle (See Figures 4.61-4.66).

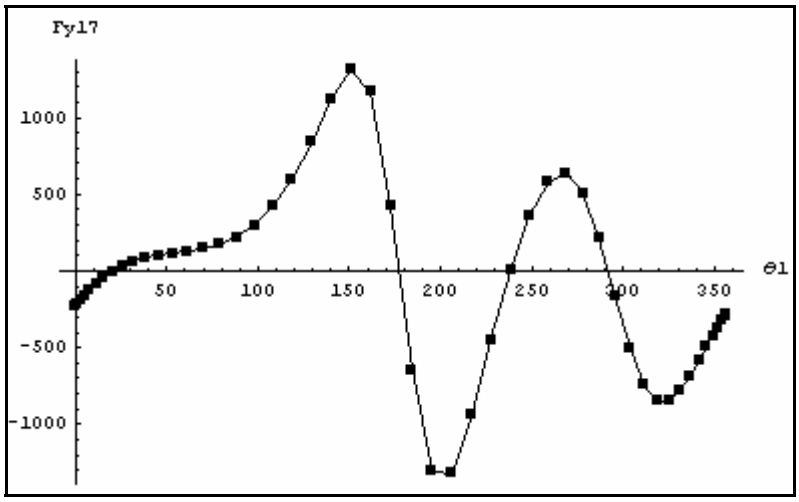

Figure 4.61 $F_{y\,1,7}$ versus θ_1 graph

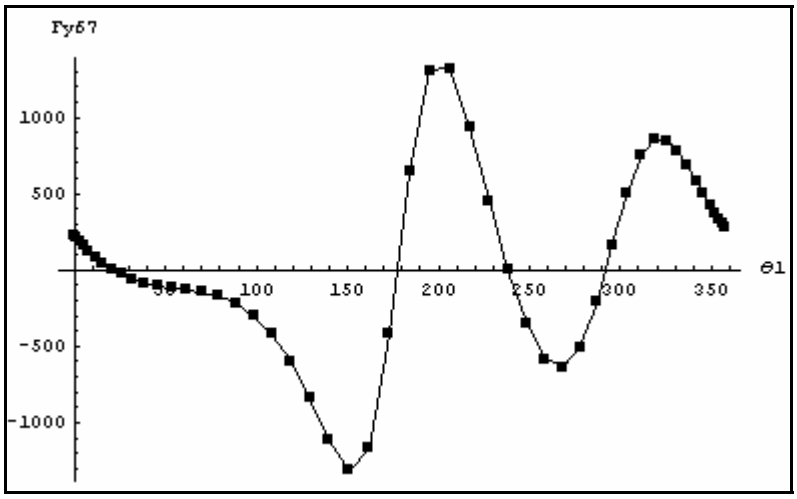

Figure 4.62 $F_{y\,6,7}$ versus θ_1 graph

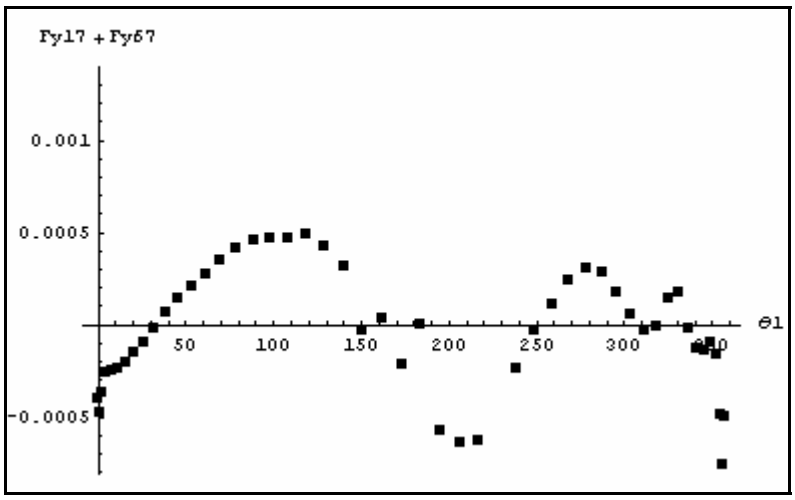

Figure 4.63 $F_{y\,6,7} + F_{y\,1,7}$ versus θ_1 graph

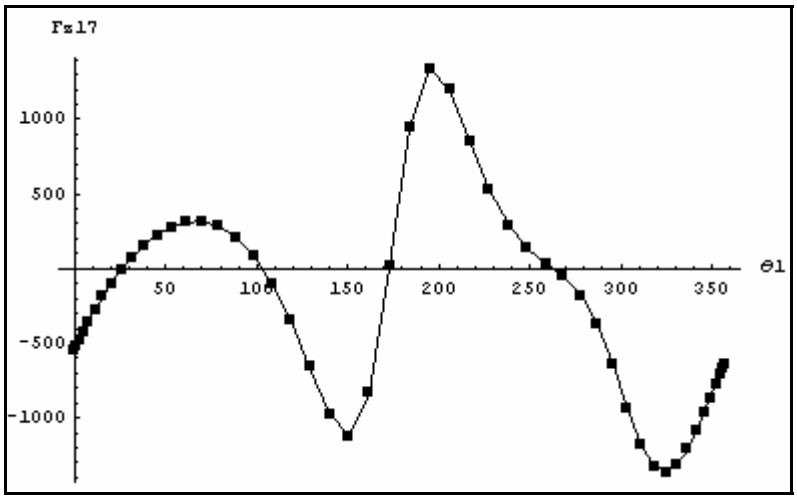

Figure 4.64 $F_{z\,1,7}$ versus θ_1 graph

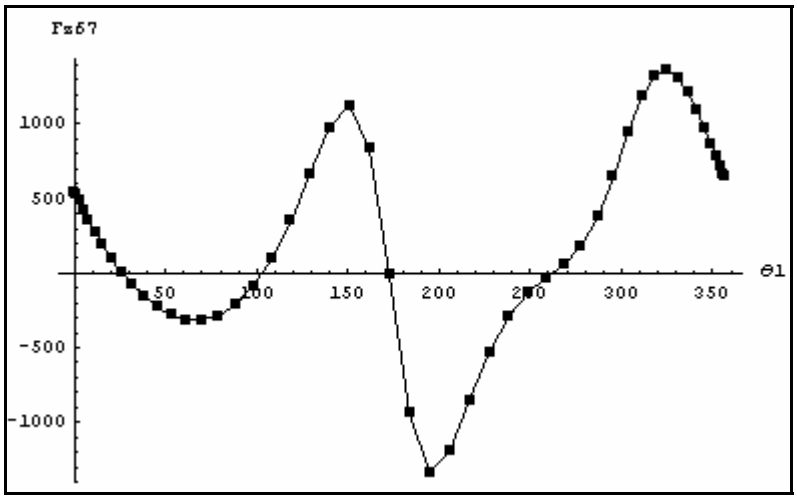

Figure 4.65 $F_{z\,6,7}$ versus θ_1 graph

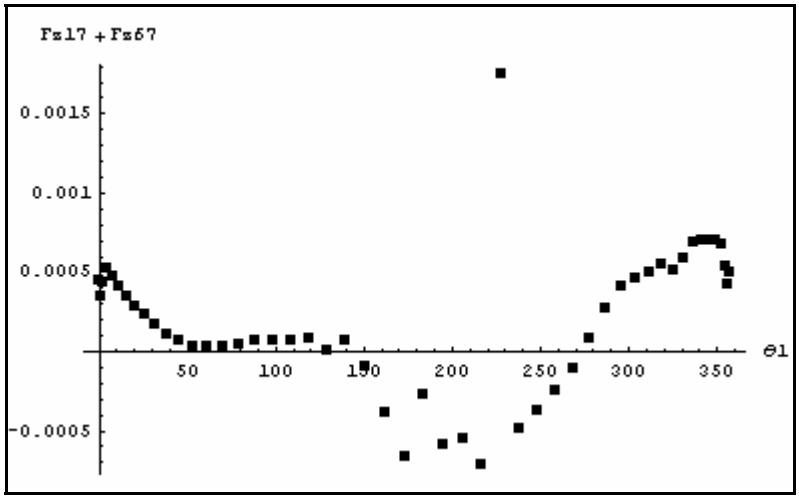

Figure 4.66 $F_{z\,6,7} + F_{z\,1,7}$ versus θ_1 graph

From Figures 4.58-4.66, it appears that this mechanism can be fully balanced by using mass distribution. To check this assertion, the location of the total mass center of the moving links is computed. In Figure 4.67, the x component of the total mass center in the inertial frame, P_{cx} , is shown. As can be seen from the figure , P_{cx} is almost constant at 0.18 m.

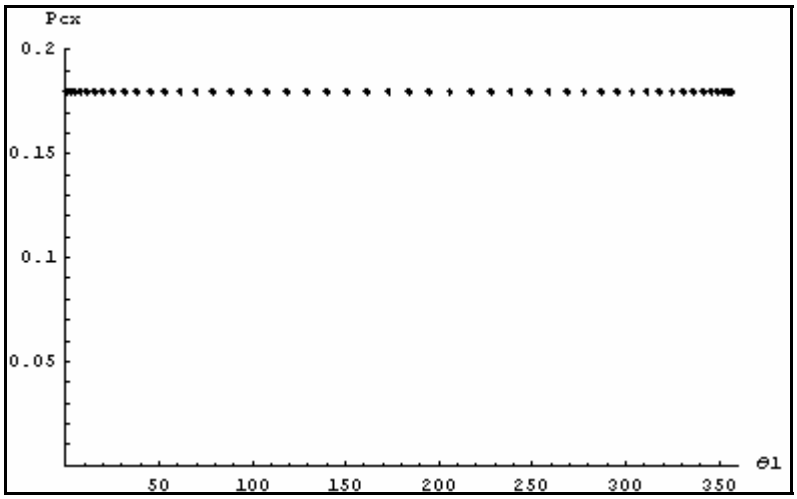

Figure 4.67 P_{cx} versus θ_1 graph

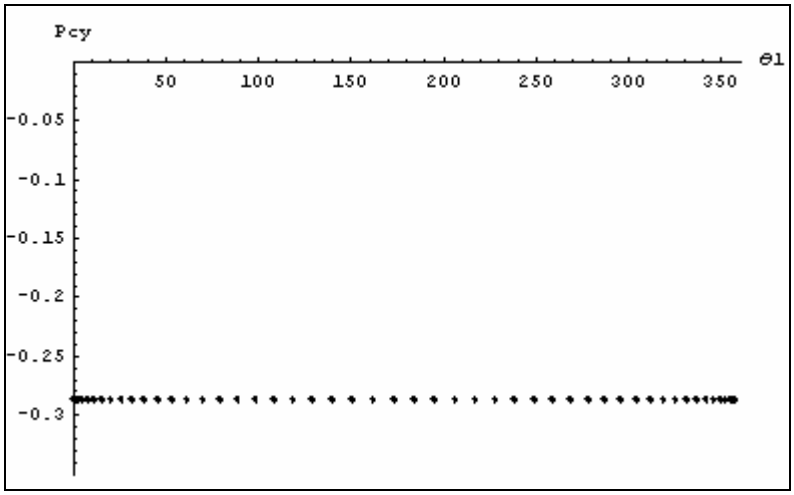

Figure 4.68 P_{cy} versus θ_1 graph

In Figure 4.68 and Figure 4.69, the y and z components of the total mass center of the whole mechanism in the inertial frame are shown .From Figures 4.67-4.69, it can be concluded that total center of mass of the mechanism is stationary. Therefore, the mechanism has been fully shaking force balanced, which is an expected result in view of the contour theorem.

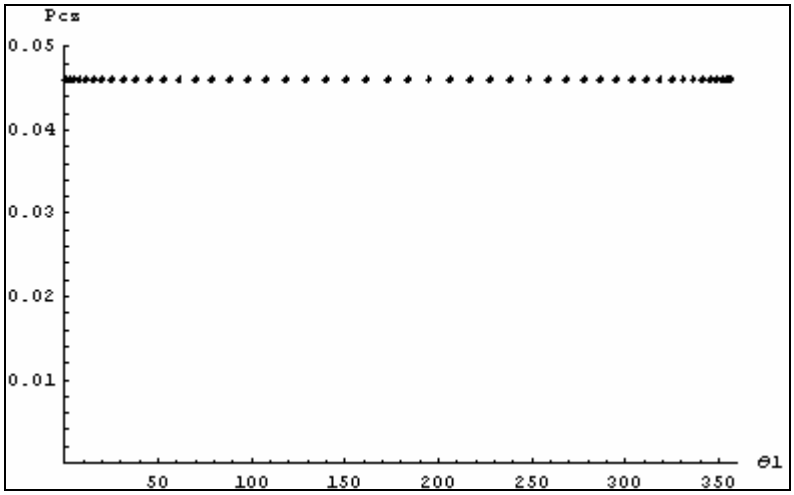

Figure 4.69 P_{cz} versus θ_1 graph

Let's, now, consider all components of the shaking force in the X_7, Y_7 and Z_7 directions. Therefore, FFN is defined via the equation

$$FFN^2 = \int_R \left\{ \left[(F_{x1,7} + F_{x6,7}) \right]^2 + \left[(F_{y1,7} + F_{y6,7}) \right]^2 + \left[(F_{z1,7} + F_{z6,7}) \right]^2 \right\} dt \qquad (4.54)$$

From the above definition, FFN^2 can be found by using the developed package. (see Appendix B, equation (B.11))

Inertial parameters that affect *FFN* are the same as in equation (4.49). Furthermore, the minimum value of FFN^2 is given by

$$
\begin{aligned}
FFN_*^2 &= 1.20508\times10^{-11}c_1^2 + 6.25278\times10^{-13}c_1c_2 - 3.24007\times10^{-12}c_2^2 \\
&+1.11413\times10^{-11}c_1c_3 + 2.27374\times10^{-12}c_2c_3 + 2.04636\times10^{-12}c_3^2 \\
&-1.59162\times10^{-11}c_1c_4 - 3.75167\times10^{-12}c_2c_4 + 6.13909\times10^{-12}c_3c_4 \\
&+3.63798\times10^{-12}c_4^2 + 2.27374\times10^{-12}c_1c_5 - 1.27898\times10^{-12}c_2c_5 \\
&+6.13909\times10^{-13}c_3c_5 - 6.82121\times10^{-12}c_4c_5 - 9.09495\times10^{-13}c_5^2
\end{aligned}
\tag{4.55}
$$

Using the Nullspace command, the optimal inertial parameters (or $\mathbf{I}_\mathbf{f}^*$ vector) can be obtained in terms of five arbitrary coefficients (see Appendix B equation (B.12)). Therefore, the arbitrary constants can be obtained in terms of m_2, m_3, m_4, m_5 and m_6 as given bellow.

$$
\left\{
\begin{array}{l}
c_1 \to 0.0638975\,m_2 + 1.71083\,m_3 + 1.88825\,m_4 + 3.98396\,m_5 + 2.29123\,m_6 \\
c_2 \to -0.434223\,m_2 - 0.653703\,m_3 - 0.583192\,m_4 - 0.190835\,m_5 - 1.13037\,m_6 \\
c_3 \to -0.252506\,m_2 - 2.99145\,m_3 - 2.63473\,m_4 + 9.21752\,m_5 + 7.19762m_6 \\
c_4 \to 0.638685\,m_2 + 1.436\,m_3 + 0.288013\,m_4 + 3.17634m_5 + 2.05627\,m_6 \\
c_5 \to -0.631522\,m_2 + 0.818084\,m_3 - 0.200094\,m_4 + 0.0962777\,m_5 + 0.197692\,m_6
\end{array}
\right\}
\tag{4.56}
$$

The balancing of the mechanism can be realized by arbitrarily selecting the masses m_2, m_3, m_4, m_5 and m_6. For instance, again, assume that $m_2 = 0.5$, $m_3 = 0.6$, $m_4 = 0.5$, $m_5 = 0.4$ and $m_6 = 0.8$ (kg). Then, $\mathbf{I}_\mathbf{f}^*$ vector becomes

$$\left\{\begin{array}{l} m_2 \to 0.5 \\ m_3 \to 0.6 \\ m_4 \to 0.5 \\ m_5 \to 0.4 \\ m_6 \to 0.8 \\ MX_1 \to -0.240001 \\ MX_2 \to -0.342002 \\ MX_3 \to -0.286003 \\ MX_4 \to -0.240003 \\ MX_5 \to -0.120003 \\ MX_6 \to 0.0879974 \end{array}\right\}$$
$$\left\{\begin{array}{l} MY_1 \to -0.0280094 \\ MY_2 \to -0.0145551 \\ MY_3 \to 0.205155 \\ MY_4 \to -0.0182451 \\ MY_5 \to 0.0554265 \\ MY_6 \to 15.3908 \\ MZ_2 \to -0.526269 \\ MZ_3 \to -0.460031 \\ MZ_4 \to -0.0130988 \\ MZ_5 \to -0.309072 \\ MZ_6 \to 0.806597 \end{array}\right\} \quad (4.57)$$

The inertial parameters that do not affect FFN, but affect the reaction force components can, for instance, be taken as in equation (4.58).

$$\begin{array}{l} XX_2 = 3.4, YY_2 = 6.5, ZZ_2 = 4.1 \\ XY_2 = -0.002, XZ_2 = -0.004, YZ_2 = -0.0014 \\ \\ XX_3 = 1.1, YY_3 = 1.1, ZZ_3 = 0.48 \\ XY_3 = -0.003, XZ_3 = -0.005, YZ_3 = -0.0025 \\ \\ XX_4 = 0.1, YY_4 = 0.31, ZZ_4 = 0.29, \\ XY_4 = -0.004, XZ_4 = -0.003, YZ_4 = -0.05147 \\ \\ XX_5 = 0.55, YY_5 = 0.76, ZZ_5 = 0.53, \\ XY_5 = -0.002, XZ_5 = -0.006, YZ_5 = -0.006 \\ \\ XX_6 = 300, YY_6 = 4, ZZ_6 = 300, \\ XY_6 = 1, XZ_6 = 1, YZ_6 = 2 \end{array} \quad (4.58)$$

Now, any component of the shaking forces can be plotted. For instance, the X_7 component of the shaking forces are shown in Figure 4.70 and 4.71.

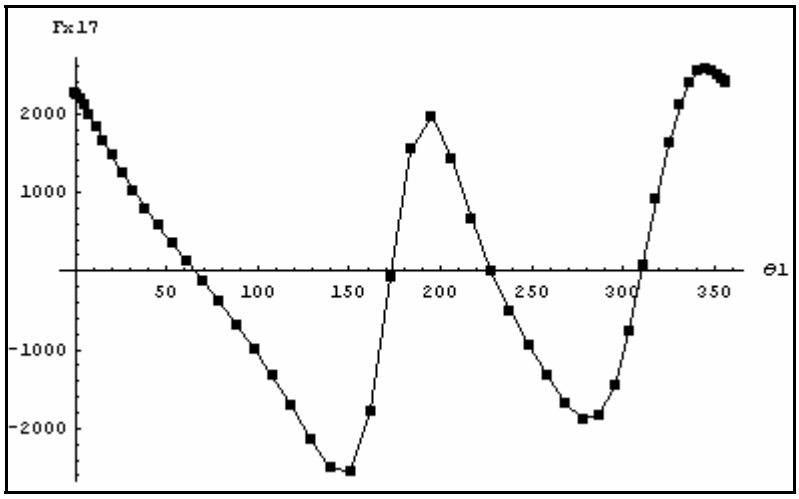

Figure 4.70 $F_{x\,1,7}$ versus θ_1 graph

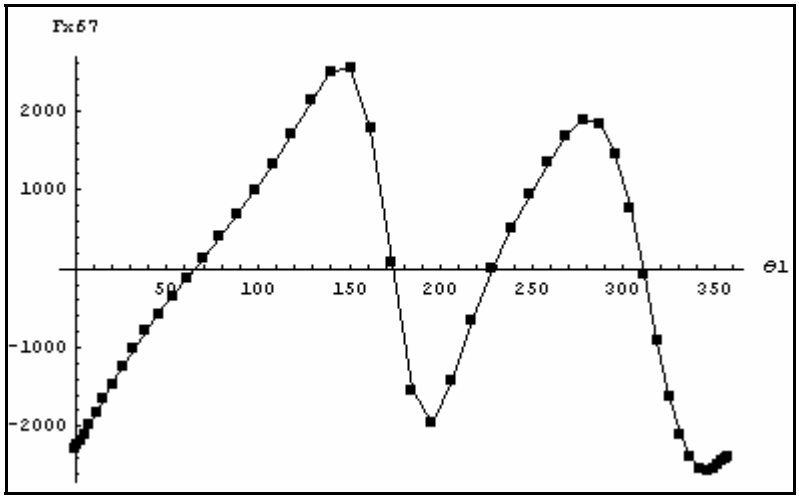

Figure 4.71 $F_{x\,6,7}$ versus θ_1 graph

From Figure 4.70 and Figure 4.71, it is clear that the X_7 component of the shaking force is fully balanced during the full cycle because they have the same magnitude but opposite direction.

The Y_7 and Z_7 components of the shaking force (not shown here for the sake of brevity) are also balanced. The x, y, z coordinates of the total mass center of the moving links have been computed as well. It has been observed that the x, y, z coordinates of the total mass center are 0.156, -0.206, -4.966 respectively in the inertial frame during the full cycle of the link (i.e. for $0° \leq \theta_1 \leq 360°$). Note that the coordinates of center of mass found here are different than the ones obtained in the previous case, where the definition of FFN was based upon the X_7 components of the shaking force only. Note also that the previous case leads to inertial parameters which are more practical to implement. (MY_6=15.3908 and m_6=0.8 in equation (4.57), leading to y_6=19.25). Therefore, for fully shaking force balanceable mechanisms, one might consider only the x, y or z component of the shaking force in the definition of FFN to obtain alternative optimal inertial parameters, which may lead to more practical solutions.

4.4.3 External load on a 7-R mechanism

Consider, again, closure 1 of a 7-R mechanism. But, this time, let the effects of the gravitational acceleration and the load force and moment, $F_{ext,6}$ and $M_{ext,6}$, be also taken into account i.e.,

$$\mathbf{g} = \{9.81, \{0, 0, -1\}\}$$

$$F_{ext,6} = \begin{cases} \{0, 0, -1000\}\, N \text{ if } 65° \leq \theta_1 \leq 244° \,(i.e. \text{if } \dot{\theta}_7 > 0) \\ 0 \quad \text{otherwise} \end{cases}$$

$$M_{ext,6} = \begin{cases} \{0, 110, 0\}\, N.m \text{ if } 65° \leq \theta_1 \leq 244° \,(i.e. \text{if } \dot{\theta}_7 > 0) \\ 0 \quad \text{otherwise} \end{cases} \tag{4.59}$$

$F_{ext,6}$ and $M_{ext,6}$ are given in the body fixed frame. Note that $F_{ext,6}$ and $M_{ext,6}$ is applied to the origin of the body fixed frame [B_6]. Let the input motion be $\theta_1 = 20t$ and consider the *FFN* defined by

$$FFN^2 = \int_R \left\{ \begin{array}{l} \left[(F_{x1,7} + F_{x6,7}) - \overline{(F_{x1,7} + F_{x6,7})} \right]^2 + \left[(F_{y1,7} + F_{y6,7}) - \overline{(F_{y1,7} + F_{y6,7})} \right]^2 \\ + \left[(F_{z1,7} + F_{z6,7}) - \overline{(F_{z1,7} + F_{z6,7})} \right]^2 \end{array} \right\} dt \tag{4.60}$$

which takes into account the deviation of all components of the shaking force from their average (desired) values. For the integration in (4.60), 100 Gaussian Quadrature points have been selected. The components of the shaking force have been determined for each selected point by using the developed package. Then the average value of the components of the shaking force has been found by using the definition.

$$\overline{F}_i = \frac{\sum_{k=1}^{100} F_{i,k}}{100} \tag{4.61}$$

FFN^2 has been obtained by using the developed package. Using the NMinimize command of MATHEMATICA with the physical realizability constraints given by equations (3.3), (3.4) and (3.7), one obtains the optimal inertial parameters, which are given by equation (4.62).

$$
\left\{\begin{array}{l}
m_2 \to 1.555 \\
m_3 \to 0.881 \\
m_4 \to 0.542 \\
m_5 \to 0.899 \\
m_6 \to 1.017 \\
MX_1 \to -0.215 \\
MX_2 \to 0.409 \\
MX_3 \to -0.27 \\
MX_4 \to -0.37 \\
MX_5 \to -0.266 \\
MX_6 \to -0.201
\end{array}\right\}
\left\{\begin{array}{l}
MY_1 \to 0.126 \\
MY_2 \to -0.024 \\
MY_3 \to 0.064 \\
MY_4 \to -0.092 \\
MY_5 \to -0.254 \\
MY_6 \to 0.112 \\
MZ_2 \to -0.137 \\
MZ_3 \to -0.310 \\
MZ_4 \to -0.142 \\
MZ_5 \to 0.329 \\
MZ_6 \to 0.338
\end{array}\right\}
$$

$$
\begin{array}{l}
XX_2 = 0.296, YY_2 = 0.415, ZZ_2 = 0.694 \\
XY_2 = -0.0106, XZ_2 = -0.330, YZ_2 = -0.375 \\
\\
XX_3 = 1.334, YY_3 = 0.505, ZZ_3 = 0.222 \\
XY_3 = 0.118, XZ_3 = 0.22, YZ_3 = 0.045 \\
\\
XX_4 = 1.011, YY_4 = 0.626, ZZ_4 = 0.319, \\
XY_4 = 0.287, XZ_4 = 0.021, YZ_4 = -0.121 \\
\\
XX_5 = 0.761, YY_5 = 0.561, ZZ_5 = 0.862, \\
XY_5 = 0.0203, XZ_5 = 0.306, YZ_5 = 0.0915 \\
\\
XX_6 = 0.774, YY_6 = 0.473, ZZ_6 = 0.321, \\
XY_6 = -0.227, XZ_6 = 0.265, YZ_6 = -0.018
\end{array}
\qquad (4.62)
$$

The shaking force, F_s, defined by equation

$$F_s = \sqrt{\left(F_{x1,7} + F_{x6,7}\right)^2 + \left(F_{y1,7} + F_{y6,7}\right)^2 + \left(F_{z1,7} + F_{z6,7}\right)^2} \tag{4.63}$$

is shown in Figure (4.72). In the figure, the box symbol (curve 1) indicates the shaking force which has been found by using inertial parameters in equation (4.62). On the other hand, the diamond symbol (curve 2) indicates the shaking force which has been found by using inertial parameters in equation (4.52) and equation (4.53). (i.e. the optimal inertial parameters obtained by disregarding the exrternal force and moment). As expected, the deviation of curve 1 from its average is much less the deviation of curve 2 from its average.

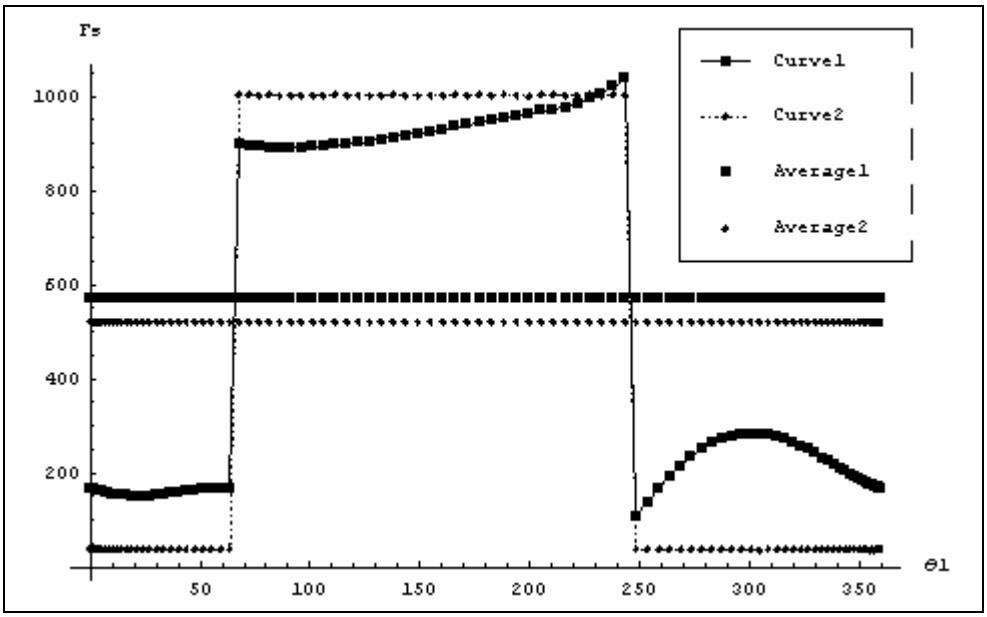

Figure 4.72 F_s versus θ_1 graph

The x, y and z components of the shaking have also been plotted. (see Figure (4.73)-(4.75)).

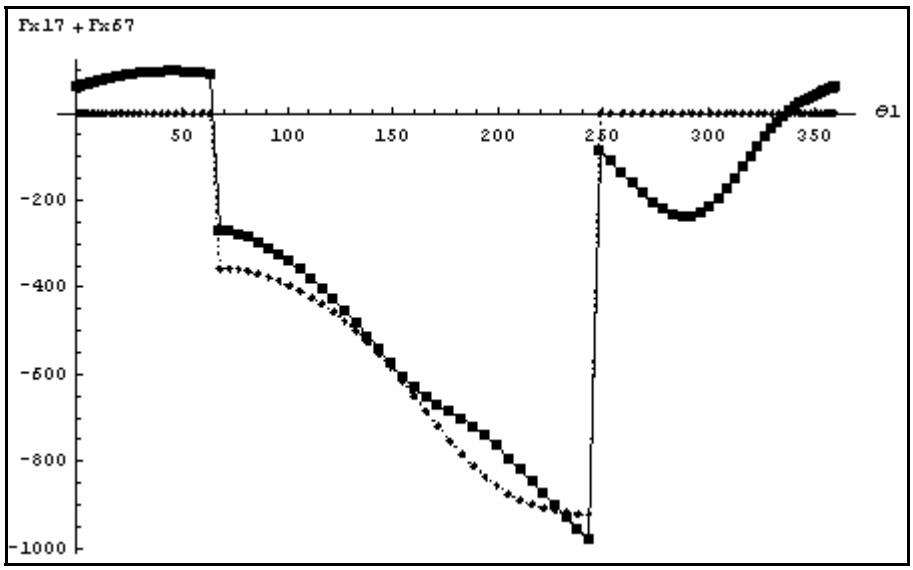

Figure 4.73 $F_{x\,6,7} + F_{x\,1,7}$ versus θ_1 graph

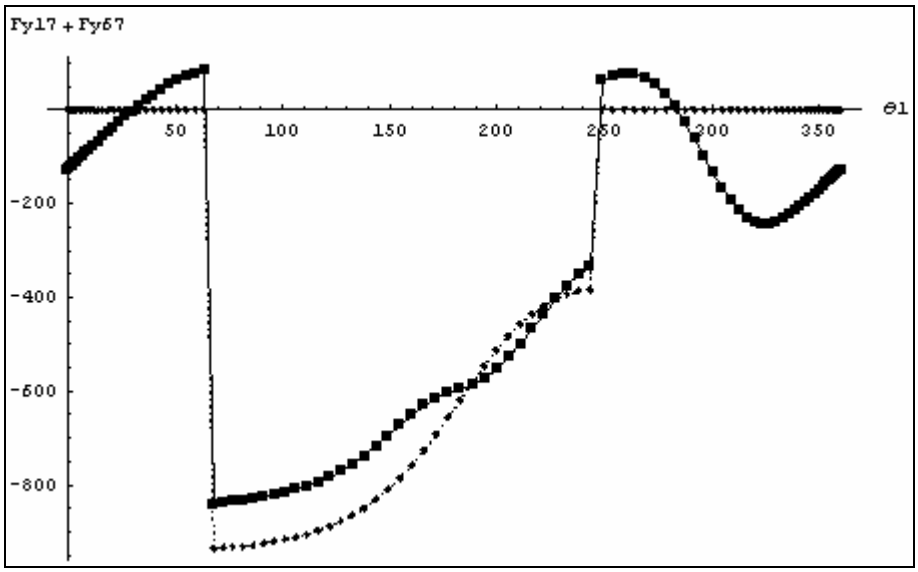

Figure 4.74 $F_{y\,6,7} + F_{y\,1,7}$ versus θ_1 graph

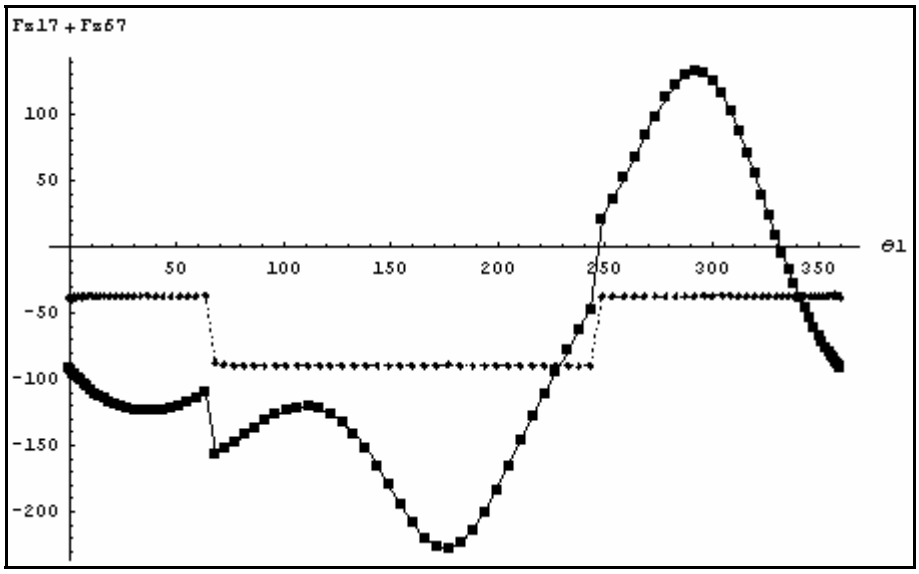

Figure 4.75 $F_{z\,6,7} + F_{z\,1,7}$ versus θ_1 graph

CHAPTER V

CONCLUSIONS

In this study, the concept of FFN has been used to optimize various aspects of the dynamic behaviour of a spatial mechanism. It has been observed that FFN possesses the following useful properties.

- Definition of FFN is flexible such that various aspects of dynamic behaviour can be considered even in a combined fashion.
- FFN is analytically minimizable, leading to linear constraints to be satisfied by the optimal inertial parameters.
- FFN can be used to analyze the transient or steady state parts of the motion of the mechanism.

The kinematic and dynamic force analysis packages (that have been developed to compute FFN) may be used on their own as well. These packages possess the following useful properties.

- Any one degree of freedom, single loop spatial mechanisms with revolute, prismatic and cylindrical joints can be solved.
- The execution time for the kinematic analysis has been optimized by using different algorithms for different group of spatial mechanisms.
- The 4 nonlinear equations required to be solved in the position analysis can be obtained symbolically.
- Closure identification of the mechanism can be performed. Therefore, the mechanism can be analyzed in any desired closure.

- The developed packages are user-friendly. The loop closure equations are obtained automatically in the position analysis.

Currently, the developed package is restricted to one degree of freedom and single loop spatial mechanisms. In the future, the package can be extended to multi degree of freedom, multi-loop spatial mechanisms.

REFERENCES

[1] V.Arekelian and M. Dahan, "Partial Shaking Moment Balancing of Fully Force Balanced Linkages", *Mechanism and Machine Theory*, Vol. 36, pp. 1241-1252, 2001

[2] S.T. Chiou and R.J.Tsai, "The ideal shaft locations of three-rotating-mass balancers for spatial mechanisms", *Mechanism and Machine Theory*, Vol. 30, No. 3, pp. 405-416, 1994

[3] N.X. Chen, "Partial balancing of the shaking force of a spatial 4-bar RCCC Linkage by the Optimization Method", *Mechanism and Machine Theory*, Vol. 19, No. 2, pp. 257-265, 1984

[4] Y.Q. Yu, "Complete Shaking Force and Shaking Moment Balancing of Spatial Irregular Force Transmission Mechanisms using Additional Links", *Mechanism and Machine Theory*, Vol. 23, No. 4, pp. 279-285, 1988

[5] J. Wawrzecki, "A Method of the Balancing of Spatial Mechanisms", *Mechanism and Machine Theory*, Vol. 33, pp. 1195-1209, 1997

[6] R. Soylu and M. B. Akbulut, "Extraneous Roots and Kinematic Analysis of Spatial Mechanisms and Robots", *Mechanism and Machine Theory*, Vol. 32, No. 7, pp.775-788, 1997

[7] J. Duffy, *Analysis of Mechanisms and Robot Manipulators*, New York: John Wiley&Sons ,1980

[8] H. Lipkin and J. Duffy, *A Vector Analysis of Robot Manipulators. Recent Advances in Robotics*, New York: John Wiley&Sons, 1985

[9] R. Soylu and J. Duffy, "Hypersurfaces of Special Configurations of Serial Manipulators and related concepts. Part1: Theory and Development of the Hypersurfaces of Special Configurations", *Journal of Robotic Systems*, Vol. 5, No: 1, 1988

[10] M. Tursun, *Inertial Parameter Design of Planar Mechanisms*, MS thesis, Middle East Technical University, 2000

[11] R. Soylu and M. Çetin, “Linerization of Hybrid Robots and Input Torque Balancing of Mechanisms”, *Mechanism and Machine Theory*, Vol. 33, No. 5, pp. 611-624, 1998

[12] F.R. Tepper and G.G. Lowen, “General theorems concerning full force balancing of planar linkages by inertial mass distributions”, Trans. ASME Jl Engng Ind., Vol. 94, pp.789-796, 1972

[13] R. Soylu , Classnotes for ME 525, Middle East Technical University, 1998

APPENDIX A

In the definitions given below, h, i, j, k, l, m and n denote a consecutive integer number set, in an increasing order. Furthermore, $\sin(\theta_i)$, $\cos(\theta_i)$, $\sin(\alpha_{hi})$, $\cos(\alpha_{hi})$ are denoted by s_i, c_i, s_{hi} and c_{hi}.

Ascending order single-subscripted elements

$$\begin{aligned} &P_i \equiv c_i \qquad U_i \equiv -s_i \qquad X_i \equiv s_{ij}s_i \\ &Q_i \equiv c_{hi}s_i \quad V_i \equiv c_{hi}c_i \qquad Y_i \equiv -(s_{hi}c_{ij} + c_{hi}s_{ij}c_i) \\ &R_i \equiv s_{hi}s_i \quad W_i \equiv s_{hi}c_i \qquad Z_i \equiv (c_{hi}c_{ij} - s_{hi}s_{ij}c_i) \end{aligned} \tag{A.1}$$

Ascending order multiple-subscripted elements

$$\begin{aligned} &E_{ij\ldots n} \equiv c_i E_{j\ldots n} - s_i F_{j\ldots n} \\ &F_{ij\ldots n} \equiv c_{hi}(s_i E_{j\ldots n} + c_i F_{j\ldots n}) - s_{hi} G_{j\ldots n} \\ &G_{ij\ldots n} \equiv s_{hi}(s_i E_{j\ldots n} + c_i F_{j\ldots n}) + c_{hi} G_{j\ldots n} \end{aligned} \tag{A.2}$$

where, $(E,F,G) \equiv (P,Q,R)\, or\, (U,V,W)\, or\, (X,Y,Z)$

Descending order single-subscripted elements

$$\begin{aligned} &\overline{P}_i \equiv c_i \qquad \overline{U}_i \equiv -s_i \quad \overline{X}_i \equiv s_{hi}s_i \\ &\overline{Q}_i \equiv c_{ij}s_i \quad \overline{V}_i \equiv c_{ij}c_i \quad \overline{Y}_i \equiv -(s_{ij}c_{hi} + c_{ij}s_{hi}c_i) \\ &\overline{R}_i \equiv s_{ij}s_i \quad \overline{W}_i \equiv s_{hi}c_i \quad \overline{Z}_i \equiv (c_{hi}c_{ij} - s_{hi}s_{ij}c_i) \end{aligned} \tag{A.3}$$

Descending order multi-subscripted elements

$$
\begin{aligned}
E_{ij\ldots n} &\equiv c_i E_{j\ldots n} - s_i F_{j\ldots n} \\
F_{ij\ldots n} &\equiv c_{hi}(s_i E_{j\ldots n} + c_i F_{j\ldots n}) - s_{hi} G_{j\ldots n} \\
G_{ij\ldots n} &\equiv s_{hi}(s_i E_{j\ldots n} + c_i F_{j\ldots n}) + c_{hi} G_{j\ldots n}
\end{aligned}
\tag{A.4}
$$

where, $(E,F,G) \equiv (P,Q,R)\, or\, (U,V,W)\, or\, (X,Y,Z)$. In equation (A.4), if the E, F and G terms on the right hand side have a single subscript they will be replaced by $\overline{E}$, $\overline{F}$ and $\overline{G}$.

Definition of dual elements

If the dual of $A_{\alpha\beta\ldots\gamma}$ is denoted by $A_{o\alpha\beta\ldots\gamma}$ then,

$$
A_{o\alpha\beta\ldots\gamma} = \sum_{IJ=fe}^{jk} a_{ij} \frac{\partial A_{\alpha\beta\ldots\gamma}}{\partial \alpha_{ij}} + \sum_{K=e}^{k} S_{kk} \frac{\partial A_{\alpha\beta\ldots\gamma}}{\partial \theta_k} \tag{A.5}
$$

where A denotes any of the elements P, Q, R, U, V, W, Y and Z.

APPENDIX B

Mathematica outputs in Chapter II.

$\mathbf{F_{in,i}}$ =

$$\begin{pmatrix} -\text{aox}\,\text{m} + \text{MY}\,(\alpha\text{z} - \Omega\text{x}\,\Omega\text{y}) + \text{MZ}\,(-\alpha\text{y} - \Omega\text{x}\,\Omega\text{z}) + \text{MX}\,(\Omega\text{y}^2 + \Omega\text{z}^2) \\ -\text{aoy}\,\text{m} + \text{MX}\,(-\alpha\text{z} - \Omega\text{x}\,\Omega\text{y}) + \text{MZ}\,(\alpha\text{x} - \Omega\text{y}\,\Omega\text{z}) + \text{MY}\,(\Omega\text{x}^2 + \Omega\text{z}^2) \\ -\text{aoz}\,\text{m} + \text{MZ}\,(\Omega\text{x}^2 + \Omega\text{y}^2) + \text{MX}\,(\alpha\text{y} - \Omega\text{x}\,\Omega\text{z}) + \text{MY}\,(-\alpha\text{x} - \Omega\text{y}\,\Omega\text{z}) \end{pmatrix} \quad \text{(B.1)}$$

$(\mathbf{T_{in,i}})_{o_i}$ =

$$\begin{pmatrix} -\text{aoz}\,\text{MY} + \text{aoy}\,\text{MZ} - \text{XX}\,\alpha\text{x} + \text{XZ}\,(\alpha\text{z} + \Omega\text{x}\,\Omega\text{y}) + \text{YY}\,\Omega\text{y}\,\Omega\text{z} - \text{ZZ}\,\Omega\text{y}\,\Omega\text{z} + \text{XY}\,(\alpha\text{y} - \Omega\text{x}\,\Omega\text{z}) + \text{YZ}\,(\Omega\text{y}^2 - \Omega\text{z}^2) \\ \text{aoz}\,\text{MX} - \text{aox}\,\text{MZ} - \text{YY}\,\alpha\text{y} + \text{YZ}\,(\alpha\text{z} - \Omega\text{x}\,\Omega\text{y}) - \text{XX}\,\Omega\text{x}\,\Omega\text{z} + \text{ZZ}\,\Omega\text{x}\,\Omega\text{z} + \text{XY}\,(\alpha\text{x} + \Omega\text{y}\,\Omega\text{z}) + \text{XZ}\,(-\Omega\text{x}^2 + \Omega\text{z}^2) \\ -\text{aoy}\,\text{MX} + \text{aox}\,\text{MY} - \text{ZZ}\,\alpha\text{z} + \text{XX}\,\Omega\text{x}\,\Omega\text{y} - \text{YY}\,\Omega\text{x}\,\Omega\text{y} + \text{XY}\,(\Omega\text{x}^2 - \Omega\text{y}^2) + \text{YZ}\,(\alpha\text{y} + \Omega\text{x}\,\Omega\text{z}) + \text{XZ}\,(\alpha\text{x} - \Omega\text{y}\,\Omega\text{z}) \end{pmatrix}$$

(B.2)

Mathematica outputs in Chapter IV.

Angular acceleration in equation (4.6)

α_1 =

$$\text{Csc}[\theta 2]\,(-0.394931\,\text{w3}\,\text{w4}\,\text{Cos}[\theta 3] + (-0.394931\,\alpha 4 + 0.394931\,\text{w2}\,\text{w4}\,\text{Cot}[\theta 2])\,\text{Sin}[\theta 3]) \quad \text{(B.3)}$$

FFN^2 in equation (4.12)

$$\begin{aligned} &2.934\times10^{-16}\,\text{m1}^2 + 1.29512\,\text{m2}^2 + 1.94818\,\text{m3}^2 + 5.17692\,\text{m3}\,\text{MX1} + \\ &100.695\,\text{MX1}^2 + 43.8095\,\text{m3}\,\text{MX2} - 118.553\,\text{MX1}\,\text{MX2} + 384.853\,\text{MX2}^2 - \\ &77.9273\,\text{m3}\,\text{MX3} - 103.538\,\text{MX1}\,\text{MX3} - 876.191\,\text{MX2}\,\text{MX3} + 779.273\,\text{MX3}^2 + \\ &8.89279\,\text{m3}\,\text{MY1} + 174.068\,\text{MX1}\,\text{MY1} - 21.6443\,\text{MX2}\,\text{MY1} - 177.856\,\text{MX3}\,\text{MY1} + \\ &132.857\,\text{MY1}^2 - 13.3392\,\text{m3}\,\text{MY2} - 48.7083\,\text{MX1}\,\text{MY2} - 124.472\,\text{MX2}\,\text{MY2} + \\ &266.784\,\text{MX3}\,\text{MY2} - 52.5357\,\text{MY1}\,\text{MY2} + 144.504\,\text{MY2}^2 + 8.44028\times10^{-9}\,\text{m3}\,\text{MY3} - \\ &291.774\,\text{MX1}\,\text{MY3} + 215.593\,\text{MX2}\,\text{MY3} + 2.61404\times10^{-9}\,\text{MX3}\,\text{MY3} - \\ &475.363\,\text{MY1}\,\text{MY3} - 288.767\,\text{MY2}\,\text{MY3} + 688.115\,\text{MY3}^2 - 7.70138\,\text{m3}\,\text{MZ2} - \\ &150.747\,\text{MX1}\,\text{MZ2} + 18.7445\,\text{MX2}\,\text{MZ2} + 154.028\,\text{MX3}\,\text{MZ2} - \\ &230.115\,\text{MY1}\,\text{MZ2} + 45.4972\,\text{MY2}\,\text{MZ2} + 411.676\,\text{MY3}\,\text{MZ2} + 99.6425\,\text{MZ2}^2 + \\ &\text{m1}\,(-1.43847\times10^{-8}\,\text{m2} - 4.23788\times10^{-10}\,\text{m3} - 3.42426\times10^{-8}\,\text{MX1} + 2.96461\times10^{-8} \\ &\quad \text{MX2} + 8.47577\times10^{-9}\,\text{MX3} + 6.02451\times10^{-8}\,\text{MY1} - 3.15558\times10^{-8}\,\text{MY2} - \\ &\quad 8.07925\times10^{-8}\,\text{MY3} - 5.21737\times10^{-8}\,\text{MZ2} - 2.94061\times10^{-8}\,\text{MZ3}) + \\ &3.07201\times10^{-9}\,\text{m3}\,\text{MZ3} - 106.197\,\text{MX1}\,\text{MZ3} + 78.4696\,\text{MX2}\,\text{MZ3} + \\ &9.51379\times10^{-10}\,\text{MX3}\,\text{MZ3} - 173.018\,\text{MY1}\,\text{MZ3} - 105.103\,\text{MY2}\,\text{MZ3} + \\ &500.907\,\text{MY3}\,\text{MZ3} + 149.838\,\text{MZ2}\,\text{MZ3} + 91.1576\,\text{MZ3}^2 + \\ &\text{m2}\,(-0.545522\,\text{m3} + 11.812\,\text{MX1} - 12.206\,\text{MX2} + 10.9104\,\text{MX3} - 0.94384\,\text{MY1} - \\ &\quad 2.02377\,\text{MY2} + 4.72496\,\text{MY3} + 0.817389\,\text{MZ2} + 1.71975\,\text{MZ3}) \end{aligned} \quad \text{(B.4)}$$

$\vec{I}_f^*$ in equation (4.15)

$$\begin{pmatrix} -0.000233489\,c1 - 0.000693356\,c2 + 0.0000286613\,c3 + 1.\,c4 \\ 3.56867\times10^{-6}\,c1 - 1.94215\times10^{-9}\,c2 + 8.72082\times10^{-10}\,c3 + 1.43334\times10^{-8}\,c4 \\ -0.000188898\,c1 - 0.0392707\,c2 + 0.99798\,c3 - 0.0000558787\,c4 \\ -1.12307\times10^{-6}\,c1 + 7.22026\times10^{-10}\,c2 - 2.94512\times10^{-10}\,c3 - 1.87935\times10^{-9}\,c4 \\ -0.739632\,c1 + 0.000402135\,c2 - 0.000115291\,c3 - 0.000129322\,c4 \\ 9.90277\times10^{-8}\,c1 - 3.78029\times10^{-11}\,c2 + 1.79259\times10^{-12}\,c3 - 7.40679\times10^{-10}\,c4 \\ -0.11259\,c1 + 0.0000886416\,c2 - 4.16159\times10^{-6}\,c3 + 0.0000400131\,c4 \\ -0.659042\,c1 + 0.000310814\,c2 - 0.000125919\,c3 - 0.000218633\,c4 \\ -9.3287\times10^{-6}\,c1 - 0.00196354\,c2 + 0.049899\,c3 - 2.79453\times10^{-6}\,c4 \\ -0.0721971\,c1 + 0.341813\,c2 + 0.0134455\,c3 + 0.000262331\,c4 \\ -0.02682\,c1 - 0.938945\,c2 - 0.0369496\,c3 - 0.000640724\,c4 \end{pmatrix}$$

(B.5)

FFN^2 in equation (4.19)

$$\begin{aligned} &4.23365\,m1^2 + 10.5192\,m2^2 + 3.89636\,m3^2 + 15.8664\,m3\,MX1 + 233.551\,MX1^2 + \\ &47.5989\,m3\,MX2 - 166.652\,MX1\,MX2 + 855.069\,MX2^2 - 155.855\,m3\,MX3 - \\ &317.329\,MX1\,MX3 - 951.979\,MX2\,MX3 + 1558.55\,MX3^2 + 2.33165\,m3\,MY1 - \\ &6.24854\times10^{-16}\,MX1\,MY1 + 64.4285\,MX2\,MY1 - 46.633\,MX3\,MY1 + 233.551\,MY1^2 - \\ &3.49746\,m3\,MY2 + 160.977\,MX1\,MY2 - 44.7223\,MX2\,MY2 + 69.9492\,MX3\,MY2 - \\ &324.687\,MY1\,MY2 + 690.797\,MY2^2 + 8.41721\times10^{-9}\,m3\,MY3 - 221.142\,MX1\,MY3 - \\ &71.3235\,MX2\,MY3 - 1.40076\times10^{-9}\,MX3\,MY3 - 516.481\,MY1\,MY3 - \\ &1228.9\,MY2\,MY3 + 1376.23\,MY3^2 - 2.01926\,m3\,MZ2 + 0.000569408\,MX1\,MZ2 - \\ &55.7962\,MX2\,MZ2 + 40.3852\,MX3\,MZ2 - 404.523\,MY1\,MZ2 + 281.188\,MY2\,MZ2 + \\ &447.285\,MY3\,MZ2 + 175.163\,MZ2^2 + 3.06361\times10^{-9}\,m3\,MZ3 - 80.4891\,MX1\,MZ3 - \\ &25.9596\,MX2\,MZ3 - 5.09843\times10^{-10}\,MX3\,MZ3 - 187.984\,MY1\,MZ3 - \\ &447.283\,MY2\,MZ3 + 1001.81\,MY3\,MZ3 + 162.798\,MZ2\,MZ3 + 182.315\,MZ3^2 + \\ &m1\,(8.10757\,m2 + 2.47969\,m3 - 0.000151995\,MX1 - 21.1041\,MX2 - 49.5939\,MX3 + \\ &\quad 0.000178817\,MY1 - 40.6809\,MY2 + 55.8849\,MY3 - 0.000177431\,MZ2 + \\ &\quad 20.3404\,MZ3) + m2\,(3.03279\,m3 + 51.8235\,MX1 - 20.1642\,MX2 - 60.6558\,MX3 - \\ &\quad 37.4675\,MY1 + 4.94832\,MY2 + 70.4083\,MY3 + 32.4479\,MZ2 + 25.6265\,MZ3) \end{aligned}$$

(B.6)

$\vec{I}_f^*$ in equation (4.22)

$$\begin{pmatrix} 2.13863\times10^{-12}\,c1 - 3.21998\times10^{-10}\,c2 \\ 1.74533\times10^{-10}\,c1 + 7.35142\times10^{-10}\,c2 \\ 0.844801\,c1 - 0.532746\,c2 \\ -8.21086\times10^{-11}\,c1 - 2.07009\times10^{-10}\,c2 \\ -4.83487\times10^{-6}\,c1 - 0.0000233361\,c2 \\ 2.291\times10^{-14}\,c1 - 1.47065\times10^{-11}\,c2 \\ -0.0000109456\,c1 - 0.0000326741\,c2 \\ 0.0000133755\,c1 + 0.0000296469\,c2 \\ 0.04224\,c1 - 0.0266373\,c2 \\ 0.18243\,c1 + 0.289279\,c2 \\ -0.501245\,c1 - 0.794852\,c2 \end{pmatrix}$$

(B.7)

FFN^2 in equation (4.27)

$$3.70668 + 4.42202\,mb3 + 3.89636\,mb3^2 - 88.4403\,MXb3 - 155.855\,mb3\,MXb3 + 1558.55\,MXb3^2 + 52.9847\,MYb3 + 8.41721\times10^{-9}\,mb3\,MYb3 - 1.40076\times10^{-9}\,MXb3\,MYb3 + 1376.23\,MYb3^2 + 19.2848\,MZb3 + 3.06361\times10^{-9}\,mb3\,MZb3 - 5.09843\times10^{-10}\,MXb3\,MZb3 + 1001.81\,MYb3\,MZb3 + 182.315\,MZb3^2 \quad \text{(B.8)}$$

Optimal inertial parameters of the 7-R mechanism.

$\mathbf{I}_\mathbf{f}^* =$

$$\begin{pmatrix} m2 \to 0.0145955\,c1 + 0.740847\,c2 + 0.336629\,c3 - 0.559776\,c4 + 0.0726576\,c5 \\ m3 \to 0.143774\,c1 + 0.444541\,c2 - 0.108545\,c3 + 0.626271\,c4 + 0.548843\,c5 \\ m4 \to 0.159752\,c1 - 0.319392\,c2 + 0.81525\,c3 + 0.105014\,c4 + 0.143031\,c5 \\ m5 \to 0.277224\,c1 - 0.289203\,c2 - 0.30883\,c3 - 0.476401\,c4 + 0.53297\,c5 \\ m6 \to 0.562888\,c1 + 0.175728\,c2 - 0.0971733\,c3 + 0.126614\,c4 - 0.542397\,c5 \\ MX1 \to -0.115818\,c1 - 0.0752482\,c2 - 0.0637318\,c3 + 0.0178257\,c4 - 0.0755097\,c5 \\ MX2 \to -0.205845\,c1 - 0.00209423\,c2 - 0.0541241\,c3 - 0.0686735\,c4 - 0.122839\,c5 \\ MX3 \to -0.21996\,c1 + 0.0952394\,c2 - 0.0900312\,c3 + 0.0538455\,c4 - 0.0293913\,c5 \\ MX4 \to -0.252021\,c1 + 0.0340543\,c2 + 0.121806\,c3 + 0.10493\,c4 + 0.00283025\,c5 \\ MX5 \to -0.168855\,c1 - 0.0527067\,c2 + 0.0291574\,c3 - 0.0379902\,c4 + 0.162721\,c5 \\ MX6 \to 9.30848\times10^{-6}\,c1 + 8.63157\times10^{-6}\,c2 + 3.69506\times10^{-6}\,c3 - 4.60705\times10^{-6}\,c4 + 1.59875\times10^{-6}\,c5 \\ MY1 \to 0.0145876\,c1 + 0.0667354\,c2 + 0.0899222\,c3 + 0.00107792\,c4 + 0.00845664\,c5 \\ MY2 \to -0.118017\,c1 + 0.0474935\,c2 - 0.0732218\,c3 + 0.0179074\,c4 + 0.0728935\,c5 \\ MY3 \to 0.212365\,c1 - 0.0739362\,c2 + 0.0925715\,c3 - 0.0163912\,c4 + 0.0266255\,c5 \\ MY4 \to 0.0220832\,c1 - 0.0178628\,c2 - 0.032968\,c3 - 0.0347917\,c4 + 0.0576316\,c5 \\ MY5 \to -0.0223556\,c1 - 0.0104032\,c2 + 0.0461263\,c3 + 0.011766\,c4 - 0.0371467\,c5 \\ MY6 \to 0.00908042\,c1 + 0.00192633\,c2 - 0.00362449\,c3 + 0.000244609\,c4 - 0.00242615\,c5 \\ MZ2 \to -0.185396\,c1 - 0.0425212\,c2 + 0.0422224\,c3 + 0.0343733\,c4 - 0.149129\,c5 \\ MZ3 \to -0.383169\,c1 + 0.041559\,c2 - 0.141665\,c3 - 0.0742399\,c4 - 0.0883722\,c5 \\ MZ4 \to 0.0654349\,c1 - 0.0150857\,c2 + 0.00818758\,c3 + 0.00265974\,c4 + 0.0385601\,c5 \\ MZ5 \to -0.323431\,c1 + 0.0187732\,c2 + 0.150969\,c3 + 0.106525\,c4 + 0.0488745\,c5 \\ MZ6 \to -0.11539\,c1 - 0.0400219\,c2 + 0.0686215\,c3 - 0.0066628\,c4 + 0.0437644\,c5 \end{pmatrix} \quad \text{(B.9)}$$

FFN^2 of the 7-R mechanism.

$$
\begin{aligned}
&578.126\,m2^2 + 1257.11\,m2\,m3 + 958.129\,m3^2 + 1017.39\,m2\,m4 + 1518.17\,m3\,m4 + \\
&655.865\,m4^2 + 252.872\,m2\,m5 + 167.159\,m3\,m5 + 407.051\,m4\,m5 + 521.611\,m5^2 + \\
&444.904\,m2\,m6 + 718.302\,m3\,m6 + 611.751\,m4\,m6 + 222.275\,m5\,m6 + 171.555\,m6^2 + \\
&4945.36\,m2\,MX1 + 4701.7\,m3\,MX1 + 3089.8\,m4\,MX1 - 2962.54\,m5\,MX1 + \\
&1199.93\,m6\,MX1 + 24714.2\,MX1^2 + 331.156\,m2\,MX2 + 1917.33\,m3\,MX2 + \\
&923.269\,m4\,MX2 - 2193.34\,m5\,MX2 - 74.0034\,m6\,MX2 + 2330.13\,MX1\,MX2 + \\
&8088.24\,MX2^2 - 3106.96\,m2\,MX3 - 3678.47\,m3\,MX3 - 2701.24\,m4\,MX3 - \\
&169.079\,m5\,MX3 - 1243.29\,m6\,MX3 - 12068.4\,MX1\,MX3 - 3511.32\,MX2\,MX3 + \\
&5035.15\,MX3^2 + 1080.67\,m2\,MX4 + 670.378\,m3\,MX4 + 1262.84\,m4\,MX4 + \\
&2649.05\,m5\,MX4 + 640.122\,m6\,MX4 - 4564.34\,MX1\,MX4 - 5807.63\,MX2\,MX4 - \\
&1863.02\,MX3\,MX4 + 3778.56\,MX4^2 - 517.726\,m2\,MX5 + 505.687\,m3\,MX5 - \\
&459.995\,m4\,MX5 - 3251.69\,m5\,MX5 - 158.354\,m6\,MX5 + 10723.5\,MX1\,MX5 + \\
&7117.4\,MX2\,MX5 - 26.4574\,MX3\,MX5 - 8757.73\,MX4\,MX5 + 5887.45\,MX5^2 - \\
&2022.29\,m2\,MX6 - 3265.01\,m3\,MX6 - 2780.68\,m4\,MX6 - 1010.34\,m5\,MX6 - \\
&1559.59\,m6\,MX6 - 5454.22\,MX1\,MX6 + 336.378\,MX2\,MX6 + 5651.31\,MX3\,MX6 - \\
&2909.65\,MX4\,MX6 + 719.79\,MX5\,MX6 + 3544.52\,MX6^2 - 5768.32\,m2\,MY1 - \\
&6859.91\,m3\,MY1 - 6175.38\,m4\,MY1 - 4786.86\,m5\,MY1 - 2832.33\,m6\,MY1 - \\
&21.9124\,MX1\,MY1 - 855.534\,MX2\,MY1 + 16563.8\,MX3\,MY1 - 13399.3\,MX4\,MY1 + \\
&13861.1\,MX5\,MY1 + 12874.2\,MX6\,MY1 + 25132.4\,MY1^2 + 408.876\,m2\,MY2 - \\
&634.862\,m3\,MY2 - 791.074\,m4\,MY2 - 823.607\,m5\,MY2 - 926.636\,m6\,MY2 + \\
&2807.69\,MX1\,MY2 + 5695.03\,MX2\,MY2 - 1931.27\,MX3\,MY2 - 1331.84\,MX4\,MY2 - \\
&311.473\,MX5\,MY2 + 4211.98\,MX6\,MY2 - 1116.75\,MY1\,MY2 + 4433.05\,MY2^2 - \\
&2786.66\,m2\,MY3 - 2641.95\,m3\,MY3 - 2500.34\,m4\,MY3 - 1801.68\,m5\,MY3 - \\
&1107.61\,m6\,MY3 - 6383.81\,MX1\,MY3 + 1676.19\,MX2\,MY3 + 7736.36\,MX3\,MY3 - \\
&6411.83\,MX4\,MY3 + 6063.64\,MX5\,MY3 + 5034.61\,MX6\,MY3 + 18727.\,MY1\,MY3 - \\
&1229.71\,MY2\,MY3 + 4900.05\,MY3^2 + 1541.39\,m2\,MY4 + 2996.9\,m3\,MY4 + \\
&2305.77\,m4\,MY4 - 542.182\,m5\,MY4 + 1076.18\,m6\,MY4 + 9754.65\,MX1\,MY4 + \\
&4766.85\,MX2\,MY4 - 4455.06\,MX3\,MY4 - 1073.82\,MX4\,MY4 + 3938.11\,MX5\,MY4 - \\
&4891.71\,MX6\,MY4 - 4933.26\,MY1\,MY4 - 2028.96\,MY2\,MY4 - 1939.11\,MY3\,MY4 + \\
&3124.3\,MY4^2 - 935.346\,m2\,MY5 - 642.385\,m3\,MY5 - 620.588\,m4\,MY5 - 886.593\,m5\,MY5 - \\
&375.554\,m6\,MY5 - 63.4459\,MX1\,MY5 + 2098.27\,MX2\,MY5 + 3233.57\,MX3\,MY5 - \\
&3191.33\,MX4\,MY5 + 3406.45\,MX5\,MY5 + 1707.06\,MX6\,MY5 + 8098.32\,MY1\,MY5 - \\
&460.563\,MY2\,MY5 + 4334.34\,MY3\,MY5 + 492.457\,MY4\,MY5 + 1344.56\,MY5^2 - \\
&113.774\,m2\,MY6 - 130.835\,m3\,MY6 - 112.25\,m4\,MY6 - 50.6255\,m5\,MY6 - \\
&55.1398\,m6\,MY6 - 309.664\,MX1\,MY6 + 5.20177\,MX2\,MY6 + 349.255\,MX3\,MY6 - \\
&202.552\,MX4\,MY6 + 143.838\,MX5\,MY6 + 250.635\,MX6\,MY6 + 721.851\,MY1\,MY6 + \\
&3.14006\,MY2\,MY6 + 368.501\,MY3\,MY6 - 143.114\,MY4\,MY6 + 167.343\,MY5\,MY6 + \\
&7.80643\,MY6^2 + 3308.57\,m2\,MZ2 + 3934.68\,m3\,MZ2 + 3542.06\,m4\,MZ2 + \\
&2745.63\,m5\,MZ2 + 1624.56\,m6\,MZ2 + 12.5684\,MX1\,MZ2 + 490.714\,MX2\,MZ2 - \\
&9500.59\,MX3\,MZ2 + 7685.51\,MX4\,MZ2 - 7950.4\,MX5\,MZ2 - 7384.35\,MX6\,MZ2 - \\
&28830.7\,MY1\,MZ2 + 640.54\,MY2\,MZ2 - 10741.4\,MY3\,MZ2 + 2829.6\,MY4\,MZ2 - \\
&4645.01\,MY5\,MZ2 - 414.037\,MY6\,MZ2 + 8268.29\,MZ2^2 + 171.863\,m2\,MZ3 + \\
&1308.47\,m3\,MZ3 + 1394.13\,m4\,MZ3 + 1287.87\,m5\,MZ3 + 1194.66\,m6\,MZ3 - \\
&2762.85\,MX1\,MZ3 - 5523.3\,MX2\,MZ3 + 252.167\,MX3\,MZ3 + 2646.18\,MX4\,MZ3 - \\
&1073.83\,MX5\,MZ3 - 5430.27\,MX6\,MZ3 - 3906.61\,MY1\,MZ3 - 8620.18\,MY2\,MZ3 - \\
&654.2\,MY3\,MZ3 + 2489.49\,MY4\,MZ3 - 353.031\,MY5\,MZ3 - 74.9891\,MY6\,MZ3 + \\
&2240.74\,MZ2\,MZ3 + 4439.16\,MZ3^2 + 2773.85\,m2\,MZ4 + 2569.85\,m3\,MZ4 + \\
&2423.95\,m4\,MZ4 + 1731.81\,m5\,MZ4 + 1043.57\,m6\,MZ4 + 6519.65\,MX1\,MZ4 - \\
&1384.82\,MX2\,MZ4 - 7738.96\,MX3\,MZ4 + 6264.55\,MX4\,MZ4 - 5999.13\,MX5\,MZ4 - \\
&4743.51\,MX6\,MZ4 - 18496.9\,MY1\,MZ4 + 1679.17\,MY2\,MZ4 - 9752.44\,MY3\,MZ4 + \\
&1806.16\,MY4\,MZ4 - 4309.93\,MY5\,MZ4 - 364.071\,MY6\,MZ4 + 10609.4\,MZ2\,MZ4 + \\
&188.646\,MZ3\,MZ4 + 4864.6\,MZ4^2 - 2721.8\,m2\,MZ5 - 3880.31\,m3\,MZ5 - 3208.83\,m4\,MZ5 - \\
&396.359\,m5\,MZ5 - 1453.78\,m6\,MZ5 - 11707.6\,MX1\,MZ5 - 3435.8\,MX2\,MZ5 + \\
&7727.67\,MX3\,MZ5 - 2202.32\,MX4\,MZ5 - 410.938\,MX5\,MZ5 + 6608.09\,MX6\,MZ5 + \\
&13520.8\,MY1\,MZ5 + 917.544\,MY2\,MZ5 + 6555.53\,MY3\,MZ5 - 6314.51\,MY4\,MZ5 + \\
&1728.48\,MY5\,MZ5 + 305.976\,MY6\,MZ5 - 7755.2\,MZ2\,MZ5 - 2250.28\,MZ3\,MZ5 - \\
&6428.78\,MZ4\,MZ5 + 4341.45\,MZ5^2 + 2170.93\,m2\,MZ6 + 2496.48\,m3\,MZ6 + \\
&2141.86\,m4\,MZ6 + 965.993\,m5\,MZ6 + 1052.13\,m6\,MZ6 + 5908.75\,MX1\,MZ6 - \\
&99.2556\,MX2\,MZ6 - 6664.19\,MX3\,MZ6 + 3864.93\,MX4\,MZ6 - 2744.6\,MX5\,MZ6 - \\
&4782.41\,MX6\,MZ6 - 13773.7\,MY1\,MZ6 - 59.9158\,MY2\,MZ6 - 7031.42\,MY3\,MZ6 + \\
&2730.78\,MY4\,MZ6 - 3193.09\,MY5\,MZ6 - 297.911\,MY6\,MZ6 + 7900.3\,MZ2\,MZ6 + \\
&1430.88\,MZ3\,MZ6 + 6946.9\,MZ4\,MZ6 - 5838.37\,MZ5\,MZ6 + 2842.24\,MZ6^2
\end{aligned}
\tag{B.10}
$$

FFN^2 of the 7-R mechanism.

$$
\begin{aligned}
&1154.43\,m2^2 + 2611.15\,m2\,m3 + 2894.59\,m3^2 + 2194.29\,m2\,m4 + 4228.16\,m3\,m4 + 1758.97\,m4^2 + 540.648\,m2\,m5 + \\
&1035.28\,m3\,m5 + 1436.13\,m4\,m5 + 1593.54\,m5^2 + 471.666\,m2\,m6 + 1392.74\,m3\,m6 + 1048.24\,m4\,m6 + \\
&668.571\,m5\,m6 + 309.497\,m6^2 + 9969.32\,m2\,MX1 + 9232.73\,m3\,MX1 + 7797.41\,m4\,MX1 - 780.294\,m5\,MX1 + \\
&1726.84\,m6\,MX1 + 49846.6\,MX1^2 + 472.329\,m2\,MX2 + 7221.77\,m3\,MX2 + 3226.73\,m4\,MX2 - 4302.96\,m5\,MX2 + \\
&771.738\,m6\,MX2 + 1304.83\,MX1\,MX2 + 21834.1\,MX2^2 - 4281.69\,m2\,MX3 - 7559.99\,m3\,MX3 - 3995.05\,m4\,MX3 + \\
&1905.84\,m5\,MX3 - 1577.8\,m6\,MX3 - 8906.32\,MX1\,MX3 - 14566.5\,MX2\,MX3 + 12043.9\,MX3^2 + 2116.89\,m2\,MX4 + \\
&1873.72\,m3\,MX4 + 3240.44\,m4\,MX4 + 7178.5\,m5\,MX4 + 1277.81\,m6\,MX4 + 4380.85\,MX1\,MX4 - 13913.6\,MX2\,MX4 + \\
&2857.2\,MX3\,MX4 + 9724.92\,MX4^2 - 1326.57\,m2\,MX5 + 1307.19\,m3\,MX5 - 1227.01\,m4\,MX5 - 7474.71\,m5\,MX5 - \\
&165.256\,m6\,MX5 + 6396.46\,MX1\,MX5 + 18158.\,MX2\,MX5 - 6703.91\,MX3\,MX5 - 19803.5\,MX4\,MX5 + 12462.4\,MX5^2 - \\
&2143.93\,m2\,MX6 - 6330.64\,m3\,MX6 - 4764.72\,m4\,MX6 - 3038.96\,m5\,MX6 - 2813.61\,m6\,MX6 - 7849.29\,MX1\,MX6 - \\
&3507.9\,MX2\,MX6 + 7171.84\,MX3\,MX6 - 5808.2\,MX4\,MX6 + 751.163\,MX5\,MX6 + 6394.57\,MX6^2 - 11436.3\,m2\,MY1 - \\
&14713.6\,m3\,MY1 - 12330.9\,m4\,MY1 - 5393.16\,m5\,MY1 - 2606.29\,m6\,MY1 - 2979.95\,MX2\,MY1 + 29560.6\,MX3\,MY1 - \\
&14634.5\,MX4\,MY1 + 17140.\,MX5\,MY1 + 11846.8\,MX6\,MY1 + 49846.6\,MY1^2 + 237.343\,m2\,MY2 - 6458.07\,m3\,MY2 - \\
&4900.71\,m4\,MY2 - 4824.3\,m5\,MY2 - 3045.69\,m6\,MY2 + 4110.2\,MX1\,MY2 + 5001.32\,MX2\,MY2 - 212.775\,MX3\,MY2 - \\
&8087.28\,MX4\,MY2 + 951.763\,MX5\,MY2 + 13844.1\,MX6\,MY2 + 1513.98\,MY1\,MY2 + 15991.8\,MY2^2 - 3333.85\,m2\,MY3 - \\
&1049.6\,m3\,MY3 - 1373.06\,m4\,MY3 - 161.799\,m5\,MY3 - 187.164\,m6\,MY3 - 3067.77\,MX1\,MY3 + 5189.46\,MX2\,MY3 + \\
&10998.2\,MX3\,MY3 - 5113.5\,MX4\,MY3 + 6768.54\,MX5\,MY3 + 850.744\,MX6\,MY3 + 26387.7\,MY1\,MY3 - \\
&8381.2\,MY2\,MY3 + 8436.42\,MY3^2 + 4712.11\,m2\,MY4 + 10471.\,m3\,MY4 + 8207.26\,m4\,MY4 + 1228.7\,m5\,MY4 + \\
&2193.18\,m6\,MY4 + 26664.6\,MX1\,MY4 + 12538.9\,MX2\,MY4 - 8301.52\,MX3\,MY4 + 2812.32\,MX4\,MY4 + \\
&4707.79\,MX5\,MY4 - 9969.02\,MX6\,MY4 - 17832.4\,MY1\,MY4 - 13012.9\,MY2\,MY4 + 1973.15\,MY3\,MY4 + \\
&12079.7\,MY4^2 + 929.185\,m2\,MY5 + 5670.25\,m3\,MY5 + 4550.81\,m4\,MY5 + 2573.69\,m5\,MY5 + 1101.31\,m6\,MY5 + \\
&10032.9\,MX1\,MY5 + 7533.05\,MX2\,MY5 + 3346.65\,MX3\,MY5 + 2446.74\,MX4\,MY5 + 1655.15\,MX5\,MY5 - \\
&5005.95\,MX6\,MY5 + 645.965\,MY1\,MY5 - 14387.6\,MY2\,MY5 + 10874.9\,MY3\,MY5 + 14522.6\,MY4\,MY5 + 9061.34\,MY5^2 - \\
&107.76\,m2\,MY6 + 11.3638\,m3\,MY6 + 6.48254\,m4\,MY6 + 90.4367\,m5\,MY6 - 192.663\,MX1\,MY6 + 122.075\,MX2\,MY6 + \\
&482.306\,MX3\,MY6 - 13.216\,MX4\,MY6 + 55.0324\,MX5\,MY6 + 771.42\,MY1\,MY6 - 489.056\,MY2\,MY6 + 673.416\,MY3\,MY6 + \\
&146.695\,MY4\,MY6 + 644.919\,MY5\,MY6 + 17.5151\,MY6^2 + 6559.61\,m2\,MZ2 + 8439.4\,m3\,MZ2 + 7072.72\,m4\,MZ2 + \\
&3093.39\,m5\,MZ2 + 1494.91\,m6\,MZ2 + 1709.23\,MX2\,MZ2 - 16955.3\,MX3\,MZ2 + 8394.\,MX4\,MZ2 - 9831.1\,MX5\,MZ2 - \\
&6795.03\,MX6\,MZ2 - 57181.7\,MY1\,MZ2 - 868.384\,MY2\,MZ2 - 15135.4\,MY3\,MZ2 + 10228.3\,MY4\,MZ2 - \\
&370.51\,MY5\,MZ2 - 442.468\,MY6\,MZ2 + 16399.\,MZ2^2 + 905.328\,m2\,MZ3 + 7825.45\,m3\,MZ3 + 6054.42\,m4\,MZ3 + \\
&5288.17\,m5\,MZ3 + 3259.01\,m6\,MZ3 - 4047.75\,MX1\,MZ3 - 4628.54\,MX2\,MZ3 - 2734.71\,MX3\,MZ3 + 9422.02\,MX4\,MZ3 - \\
&2644.46\,MX5\,MZ3 - 14813.7\,MX6\,MZ3 - 11420.5\,MY1\,MZ3 - 31648.6\,MY2\,MZ3 + 5625.64\,MY3\,MZ3 + \\
&14591.4\,MY4\,MZ3 + 14104.6\,MY5\,MZ3 + 404.793\,MY6\,MZ3 + 6550.51\,MZ2\,MZ3 + 16152.6\,MZ3^2 + 3281.9\,m2\,MZ4 + \\
&638.606\,m3\,MZ4 + 1054.31\,m4\,MZ4 - 115.186\,m5\,MZ4 + 16.3433\,m6\,MZ4 + 3275.4\,MX1\,MZ4 - 4940.11\,MX2\,MZ4 - \\
&10840.\,MX3\,MZ4 + 4613.38\,MX4\,MZ4 - 6620.86\,MX5\,MZ4 - 74.2884\,MX6\,MZ4 - 25753.9\,MY1\,MZ4 + 10026.1\,MY2\,MZ4 - \\
&17144.1\,MY3\,MZ4 - 2734.1\,MY4\,MZ4 - 11598.1\,MY5\,MZ4 - 693.678\,MY6\,MZ4 + 14771.8\,MZ2\,MZ4 - \\
&7308.66\,MZ3\,MZ4 + 8751.58\,MZ4^2 - 5721.76\,m2\,MZ5 - 9387.49\,m3\,MZ5 - 7634.84\,m4\,MZ5 - 1006.49\,m5\,MZ5 - \\
&1907.52\,m6\,MZ5 - 24729.9\,MX1\,MZ5 - 8388.99\,MX2\,MZ5 + 12609.3\,MX3\,MZ5 - 4742.22\,MX4\,MZ5 - \\
&766.636\,MX5\,MZ5 + 8670.56\,MX6\,MZ5 + 28320.3\,MY1\,MZ5 + 6256.49\,MY2\,MZ5 + 6863.27\,MY3\,MZ5 - \\
&19555.6\,MY4\,MZ5 - 6777.85\,MY5\,MZ5 + 219.797\,MY6\,MZ5 - 16243.8\,MZ2\,MZ5 - 8982.15\,MZ3\,MZ5 - \\
&6383.78\,MZ4\,MZ5 + 10063.8\,MZ5^2 + 2056.18\,m2\,MZ6 - 216.833\,m3\,MZ6 - 123.694\,m4\,MZ6 - 1725.63\,m5\,MZ6 + \\
&3676.23\,MX1\,MZ6 - 2329.32\,MX2\,MZ6 - 9202.95\,MX3\,MZ6 + 252.176\,MX4\,MZ6 - 1050.08\,MX5\,MZ6 - \\
&14719.6\,MY1\,MZ6 + 9331.75\,MY2\,MZ6 - 12849.5\,MY3\,MZ6 - 2799.11\,MY4\,MZ6 - 12305.8\,MY5\,MZ6 - \\
&668.415\,MY6\,MZ6 + 8442.79\,MZ2\,MZ6 - 7723.9\,MZ3\,MZ6 + 13236.2\,MZ4\,MZ6 - 4193.98\,MZ5\,MZ6 + 6377.06\,MZ6^2
\end{aligned}
\tag{B.11}
$$

Optimal inertial parameters.

$$\mathbf{I}_\mathbf{f}^* =$$

$$\left\{\begin{array}{r}
m2 \to 0.0262884\,c1 + 0.072281\,c2 + 0.0122169\,c3 - 0.239842\,c4 + 0.944358\,c5 \\
m3 \to 0.175302\,c1 + 0.00187275\,c2 - 0.421037\,c3 - 0.767984\,c4 - 0.230726\,c5 \\
m4 \to 0.608328\,c1 - 0.132083\,c2 + 0.639306\,c3 - 0.0543129\,c4 - 0.043448\,c5 \\
m5 \to 0.162887\,c1 + 0.291845\,c2 - 0.344475\,c3 + 0.437681\,c4 + 0.0975919\,c5 \\
m6 \to -0.597758\,c1 - 0.436509\,c2 + 0.31017\,c3 - 0.135314\,c4 + 0.0151654\,c5 \\
MX1 \to -0.0673918\,c1 - 0.0015655\,c2 - 0.00411006\,c3 + 0.0692117\,c4 - 0.0775359\,c5 \\
MX2 \to -0.116573\,c1 + 0.0101927\,c2 - 0.00519908\,c3 + 0.0814096\,c4 + 0.0304198\,c5 \\
MX3 \to -0.103912\,c1 + 0.0128697\,c2 - 0.0989825\,c3 - 0.0694559\,c4 - 0.0135799\,c5 \\
MX4 \to 0.0408\,c1 - 0.0220754\,c2 + 0.0568157\,c3 - 0.111007\,c4 - 0.0315524\,c5 \\
MX5 \to 0.0896662\,c1 + 0.0654781\,c2 - 0.0465268\,c3 + 0.0202977\,c4 - 0.00227488\,c5 \\
MX6 \to -0.0657515\,c1 - 0.0480146\,c2 + 0.0341179\,c3 - 0.0148842\,c4 + 0.00166814\,c5 \\
MY1 \to 0.0228171\,c1 + 0.0131315\,c2 + 0.00932201\,c3 + 0.0279957\,c4 + 0.00717031\,c5 \\
MY2 \to -0.0698912\,c1 + 0.000544964\,c2 - 0.0796641\,c3 - 0.0484531\,c4 - 0.00949434\,c5 \\
MY3 \to 0.122612\,c1 - 0.00414621\,c2 + 0.0751095\,c3 + 0.0139028\,c4 - 0.00334135\,c5 \\
MY4 \to 0.0437239\,c1 + 0.0388254\,c2 - 0.0333156\,c3 + 0.0300319\,c4 + 0.00406187\,c5 \\
MY5 \to -0.0414151\,c1 - 0.030243\,c2 + 0.0214898\,c3 - 0.0093751\,c4 + 0.00105072\,c5 \\
MY6 \to 0.283538\,c1 - 0.829705\,c2 - 0.397828\,c3 + 0.223148\,c4 + 0.112758\,c5 \\
MZ2 \to -0.0826794\,c1 + 0.019667\,c2 + 0.0220792\,c3 + 0.195776\,c4 - 0.140897\,c5 \\
MZ3 \to -0.219975\,c1 + 0.0139263\,c2 - 0.0838888\,c3 + 0.0600741\,c4 + 0.0307438\,c5 \\
MZ4 \to 0.0724517\,c1 + 0.0276237\,c2 - 0.0160096\,c3 - 0.0192526\,c4 - 0.0108771\,c5 \\
MZ5 \to 0.080977\,c1 - 0.00206298\,c2 + 0.0496919\,c3 - 0.118744\,c4 - 0.0367731\,c5 \\
MZ6 \to 0.0148595\,c1 - 0.0434829\,c2 - 0.0208493\,c3 + 0.0116947\,c4 + 0.00590941\,c5
\end{array}\right\} \quad \text{(B.12)}$$

APPENDIX C

1) Rotation package is prepared to obtain the DL terms symbolically. Firstly A new folder, namely Packages, must be opened into "*Program Files/Wolfram Research/Mathematica /version number/*". Then this package must be copied into this folder.

In order to run package, "<<*Package`Rotation`* " should be written in MATHEMATICA.

Rot ,a command of this package, is used to obtain all DL terms.

Rot[n_]

n= link number of the mechanism.

After the Rot command is executed, any of DL terms can be seen on the screen symbolically. For example, lets consider a 5-link mechanism and let's try to find the $P_{1,2,3,4}$ DL term. In Figure C.1, firstly the package has been run and the Rot command has been executed. P[{1,2,3,4},0] means that $P_{1,2,3,4}$ DL term is fully expanded. Therefore, this term involves only trigonometrical expressions. On the other hand, P[{1,2,3,4},1] means that the DL terms with the last subscript only in $P_{1,2,3,4}$ DL term are not expanded.

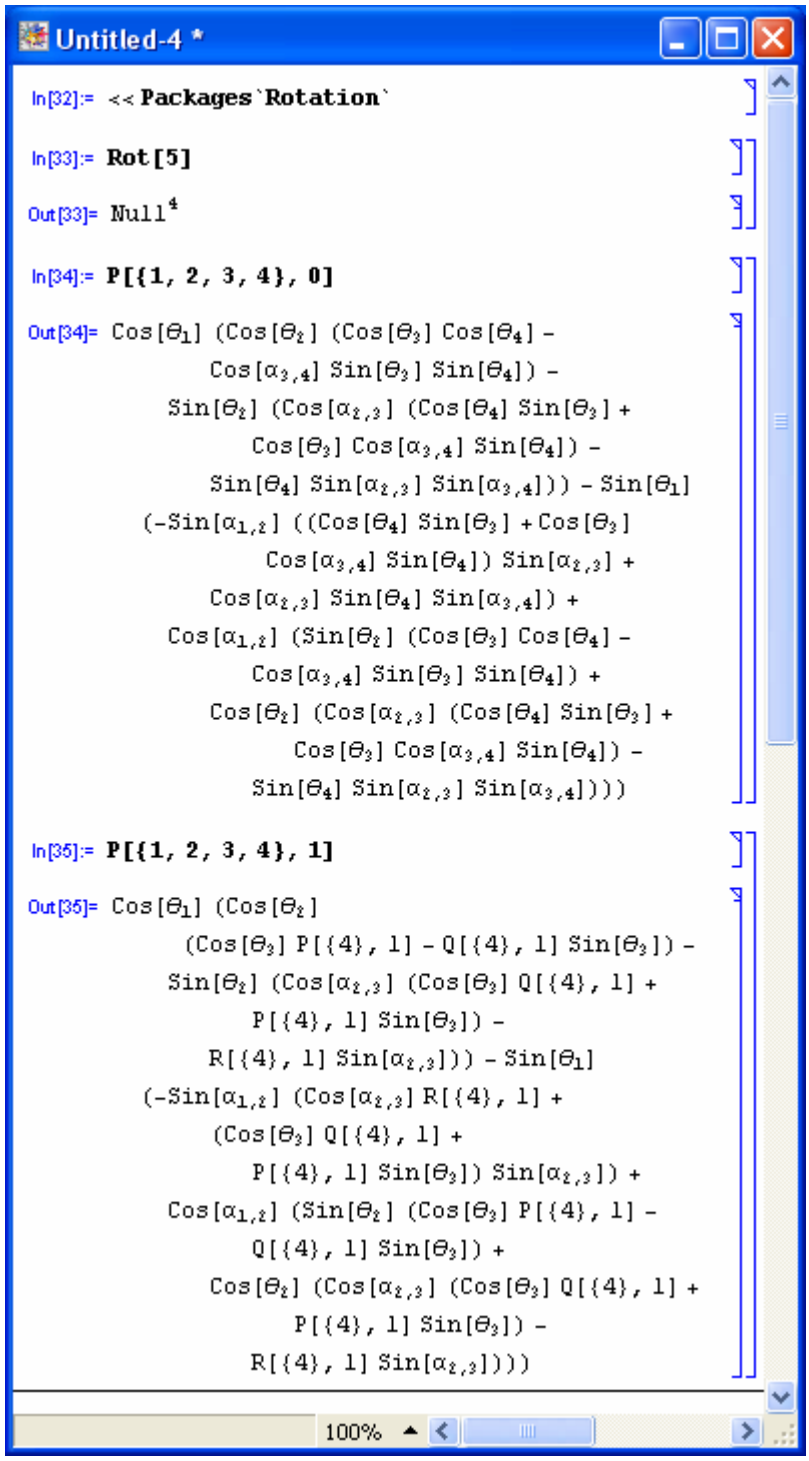

Figure C.1 Mathematica output for Rot command

2) Symboequations command is used to obtain the four nonlinear equations in the position analysis symbolically.

Symboequations[Nlnk_,jv1_,jv2_]

Nlnk: number of links in the mechanism.

jv1: number of the first joint variable to be eliminated.

jv2: number of the second joint variable to be eliminated.

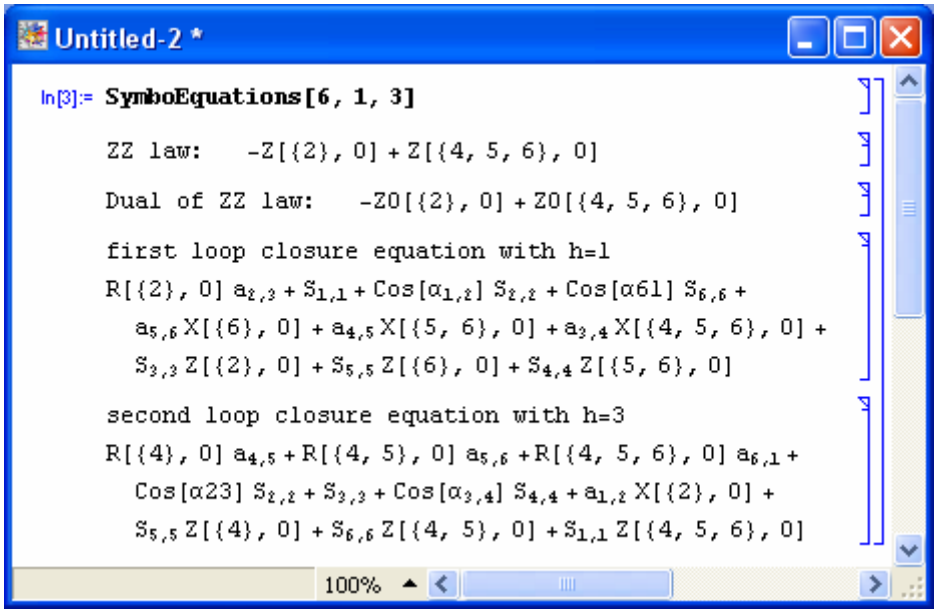

Figure C.2 Mathematica output for Symboequations command

3) getOuput command is used to analyze any position, velocity and acceleration variable.

getOutput [varname_, closureno_, vvsub_, ppsub_, inputsub_, inputfunc_, indepvar_, indepvarmin_, indepvarmax_, deltaindepvar_, listplotdesire_]

{varname : Which variable (position, velocity or acceleration variable) will be analyzed,

closureno : On which closure analysis will be done,

vvsub_ : Will the velocity analysis be substituted (If yes write 1; else, write 0),

ppsub_ : Will the position analysis be substituted (If yes write 1; else, write 0),

inputsub_ : Will the input variable be substituted (If yes write 1; else, write 0),

inputfunc_ : the input variable function of the independent variable,

indepvar_ : What is the independent variable,

indepvarmin : What is the minimum value of the independent variable,

indepvarmax: What is the maximum value of the independent variable,

listplotdesire: Is the plot of the variable versus the input position desired (If yes write 1; else, write 0)}

An example is shown in Figure C.3 for this command.

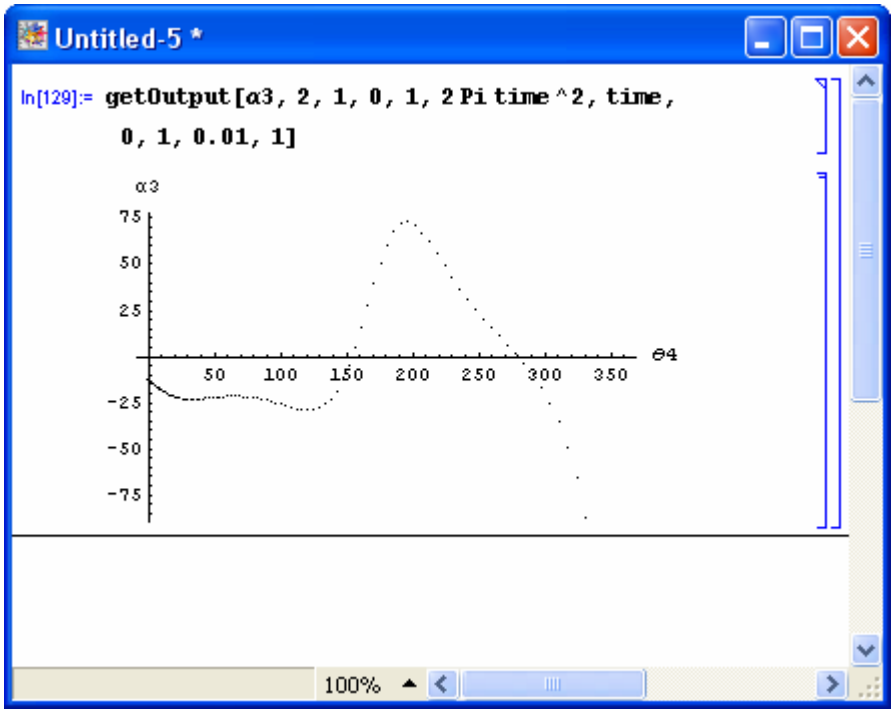

Figure C.3 Mathematica output for getOutput command

4) getOutput1 command is used to perform force analysis.

getOutput1[closureno_, noofpoints_, inputfunc_, indepvar_, tmin_, tmax_, precisionweights_]

{closureno_: On which closure the analysis will be done,

noofpoints_: What is the number of points of the Gaussian Quadrature,

inputfunc_: What does the input function correspond to in terms of the independent variable,

indepvar_: What is the independent variable,

precisionweights_: What is the precision value}

The result of this command can be seen on the screen by using Forceres.

Forceres [i] gives all forces and moments in terms of inertial parameters at the *i*th point. (i=1, 2,…, noofpoints)

For getOutput1 command , an example is given in Figure C.4.

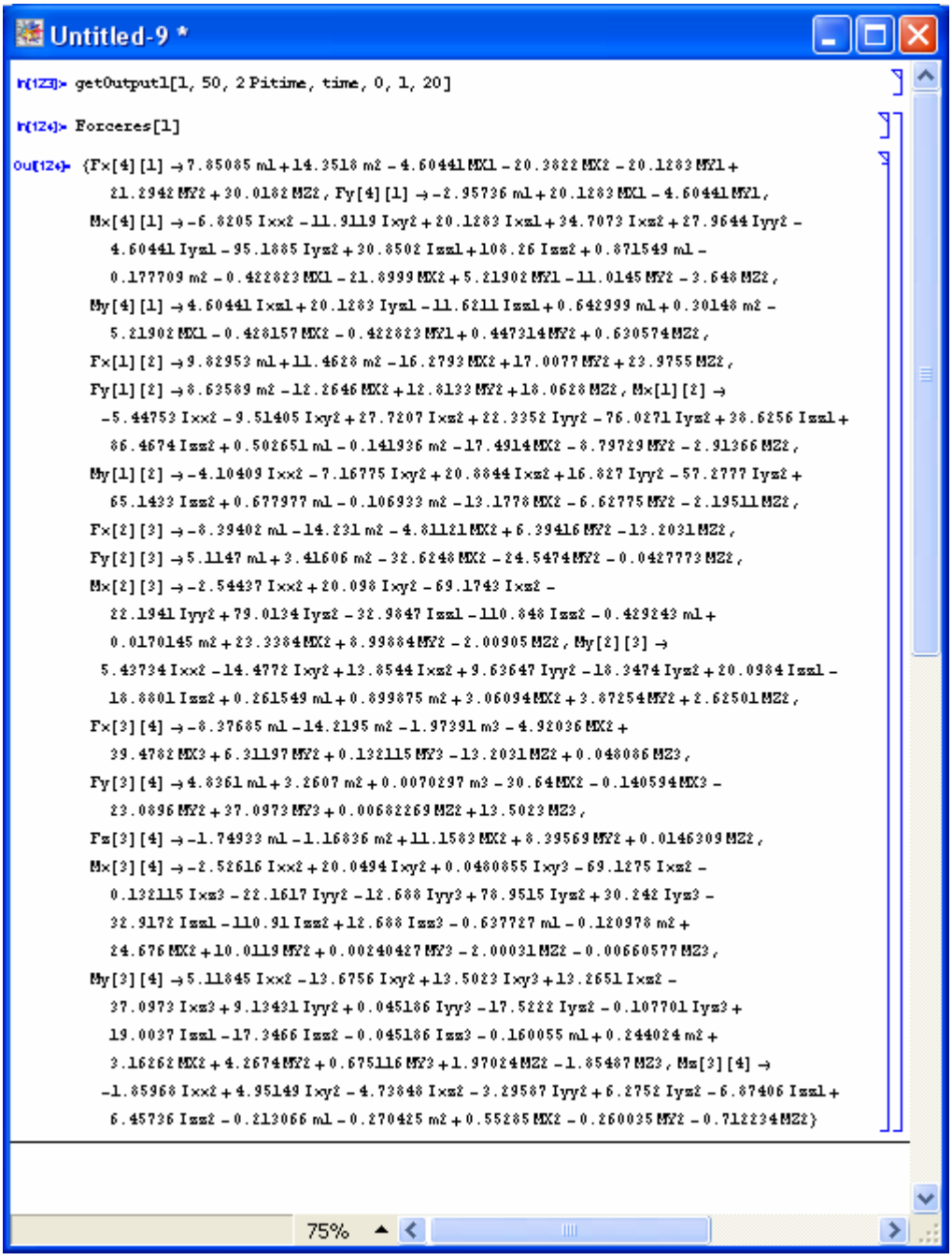

Figure C.4 Mathematica output for the getOutput1 command

APPENDIX D

Let Link i of the mechanism be divided into three parts as shown in Figure D.1. Part 1 and Part 2 are a solid cylinders. Part 3 is also a solid cylinder but there is a hole along its length. When the diameters and lengths of these cylinders are known, the inertial parameters of link i can be obtained in closed-form by using basic statics as seen in the following section. For this section, all derivation will be done with respect to the body fixed reference frame.(i.e. $[B_i]$)

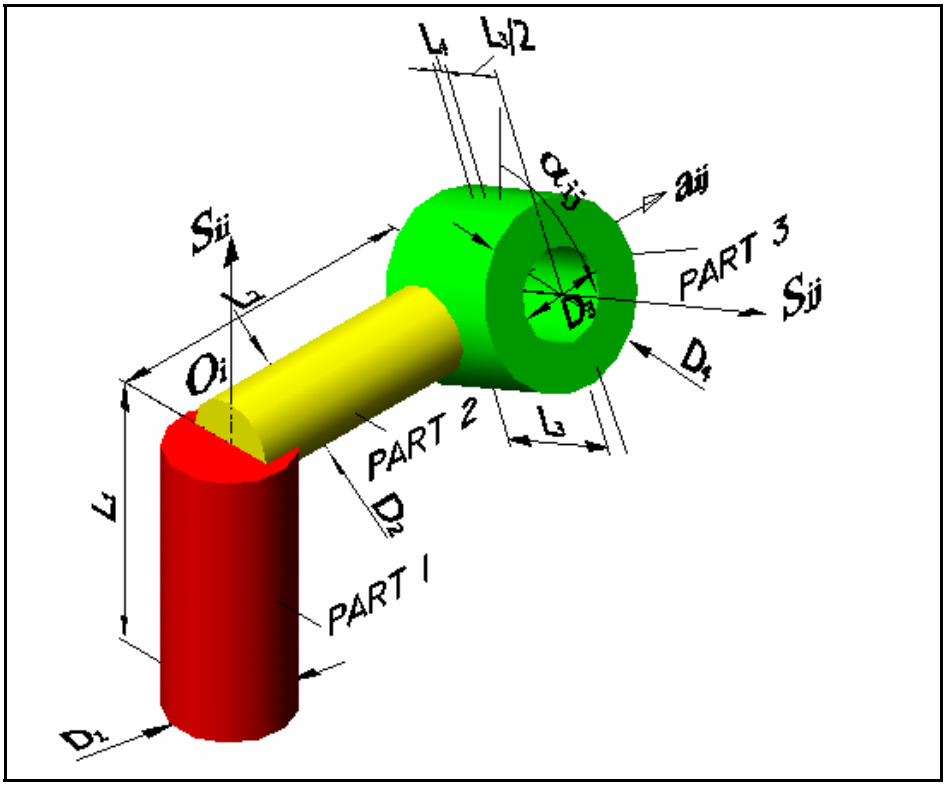

Figure D.1 Link i of the mechanism

Volumes and masses of the parts

In order to compute masses of the parts, the densities of the parts must be known. Let Part 1, Part 2 and Part 3 have densities ρ_1, ρ_2 and ρ_3 respectively. The masses of the parts can then be obtained as in Table D.1.

Table D.1 Volumes and masses of the parts

	Volumes	Masses
Part 1	$v_1 = \frac{\pi D_1^2 L_1}{4}$	$m_1 = \rho_1 v_1$
Part 2	$v_2 = \frac{\pi D_2^2 (L_2 - \frac{D_4}{2})}{4}$	$m_2 = \rho_2 v_2$
Part 3	$v_3 = \frac{\pi (D_4^2 - D_3^2) L_3}{4}$	$m_3 = \rho_3 v_3$

Center of masses

The coordinates of the center of masses of the parts (with respect to the body fixed frame) can be obtained via the formula given in Table D.2.

Table D.2 Center of masses of the parts

	x component	y component	z component
Part 1	$x_{p1} = 0$	$y_{p1} = 0$	$z_{p1} = -L_1 / 2$
Part 2	$x_{p2} = (L_2 - \frac{D_4}{2}) / 2$	$y_{p2} = 0$	$z_{p2} = 0$
Part 3	$x_{p3} = L_2$	$y_{p3} = -L_4 \sin(\alpha_{12})$	$z_{p3} = L_4 \cos(\alpha_{12})$

The coordinates of the center of mass of the link can be computed by using the following equations.

$$x_i = \frac{\sum_{k=1}^{3} m_k x_{pk}}{\sum_{k=1}^{3} m_k} \qquad \text{(D.1)}$$

$$y_i = \frac{\sum_{k=1}^{3} m_k y_{pk}}{\sum_{k=1}^{3} m_k} \tag{D.2}$$

$$z_i = \frac{\sum_{k=1}^{3} m_k z_{pk}}{\sum_{k=1}^{3} m_k} \tag{D.3}$$

Using equations (D.1)-(D.3), the following equations can then be written.

$$MX_i = \sum_{k=1}^{3} m_k x_{pk} \tag{D.4}$$

$$MY_i = \sum_{k=1}^{3} m_k y_{pk} \tag{D.5}$$

$$MZ_i = \sum_{k=1}^{3} m_k z_{pk} \tag{D.6}$$

Moments of inertia

The elements of the inertia tensor of the link can be found via the following equations.

$$\begin{aligned} XX_{p1} &= \frac{1}{16} m_1 D_1^2 + \frac{1}{3} m_1 L_1^2 \\ YY_{p1} &= XX_{p1} \\ ZZ_{p1} &= \frac{1}{8} m_1 D_1^2 \\ XY_{p1} &= YZ_{p1} = XZ_{p1} = 0 \end{aligned} \tag{D.7}$$

$$\begin{aligned} XX_{p2} &= \frac{1}{8} m_2 D_2^2 \\ YY_{p2} &= \frac{1}{16} m_2 D_2^2 + \frac{1}{3} m_2 \left(L_2 - \frac{D_4}{2} \right)^2 \\ ZZ_{p2} &= YY_{p2} \\ XY_{p2} &= YZ_{p2} = XZ_{p2} = 0 \end{aligned} \tag{D.8}$$

$$XX_{p3} = \frac{1}{16} m_3 (D_3^2 + D_4^2) + \frac{1}{12} m_3 L_3^2 + m_3 L_4^2$$

$$YY_{p3} = \frac{1}{48} m_3 \left((3D_3^2 + 3D_4^2 + 4L_3^2 + 48L_4^2) \cos(\alpha_{ij})^2 + 6\left(8L_2^2 + (D_3^2 + D_4^2) \sin(\alpha_{ij})^2\right)\right)$$

$$ZZ_{p3} = \frac{1}{48} m_3 \left(48L_2^2 + 6(D_3^2 + D_4^2) \cos(\alpha_{ij})^2 + (3D_3^2 + 3D_4^2 + 4L_3^2 + 48L_4^2) \sin(\alpha_{ij})^2 \right)$$

$$XY_{p3} = -L_2 L_4 m_3 \sin(\alpha_{ij})$$

$$XZ_{p3} = L_2 L_4 m_3 \cos(\alpha_{ij})$$

$$YZ_{p3} = \frac{1}{96} m_3 (3D_3^2 + 3D_4^2 - 4(L_3^2 + 12L_4^2)) \sin(2\alpha_{ij}) \qquad \text{(D.9)}$$

The elements of moment of inertia of link i can be represented as in (D.10).

$$XX_i = \sum_{k=1}^{3} XX_{pk}$$

$$YY_i = \sum_{k=1}^{3} YY_{pk}$$

$$ZZ_i = \sum_{k=1}^{3} ZZ_{pk}$$

$$XY_i = \sum_{k=1}^{3} XY_{pk}$$

$$XZ_i = \sum_{k=1}^{3} XZ_{pk}$$

$$YZ_i = \sum_{k=1}^{3} YZ_{pk} \qquad \text{(D.10)}$$